Some New Classes of Solutions of the Einstein-Maxwell Equations

by

Rashida Bibi

A thesis
submitted in partial fulfillment of
the requirements for the degree of
Doctor of Philosophy
in
Mathematics

Supervised by

Prof. Azad A. Siddiqui

Department of Mathematics
School of Natural Sciences (SNS),
National University of Sciences and Technology (NUST),
Sector H-12, Islamabad, Pakistan.

2020

.

Dedication

This thesis is dedicated to

my lovely parents

Muhammad Jahangir and **Tazeem Akther**

my lovely grandmother

Late Noor Jahan

and my supervisor

Prof. Azad A. Siddiqui

Acknowledgments

I am really thankful to all might ALLAH, WHO gave me strength to write this thesis and blessed me in every aspect of my life.

I am very grateful to my father **Muhammad Jahangir**, my mother **Tazeem Akther** and my grandmother **Late Noor Jahan** who always encouraged and helped me in all possible way. Without their support I could not go through the journey of my PhD. I am also very thankful to my family and friends who encouraged and motivated me to write this thesis.

I am very in debt of my supervisor **Prof. Azad A. Siddiqui** who helped me, guided me, encouraged me, and motivated me with his patience. He was always very affectionate towards me and I am very thankful to him.

I am thankful to **Dr. Timothy Clifton**, **Queen Marry University of London**, for his kind support and motivation and gaudiness. I have learnt a lot from him. I am also thankful to **Jessie Durk**, **Queen marry university of London**.

I am also thankful to **Higher Education Commission of Pakistan (HEC)** for giving me an opportunity to go to **Queen marry university of London** for six months research under the scholarship,"**International Research Support Initiative Program (IRSIP)**".

I am also thankful to **Pakistan Science Foundation (PSF)** and **Higher Education Commission of Pakistan (HEC)** for giving me travel grants for presenting my work in international conferences.

Rashida

Abstract

Finding new exact and numerical solutions of the Einstein-Maxwell field equations (EMFEs) is one of the fundamental area of research. The exact solutions which satisfy the physical criteria of compact objects can be considered as models for the compact object like neutron stars, and dark energy objects. The exact form of the equation of state satisfied by the compact objects is unknown. In order to obtain new models for compact objects, one generally chooses some equation of state, for example, linear equation of state, quadratic equation of state, or some other form. We obtain a new model for the dark energy star with linear equation of state, $p_r = -\rho$, where p_r is the radial pressure and ρ is the density. The physical criteria and stability of the model are investigated. A new solution with linear equation of state for ordinary matter object is obtained and the physical criteria and stability are discussed. By adding the initial conditions to the EFEs we get the Cauchy-Einstein field equations (CEFEs). In literature many solutions have been obtained for the CEFEs. An extension is done by adding charge into CEFEs. The constraints and evolution equations for the Cauchy Einstein-Maxwell field equations (CEMFEs) are given which can be solved for the cosmological universe which contains N discrete electrically charged black holes. For the simplicity, only regularly arranged charged masses in a

3-sphere are considered. The cosmological universe with N charged masses consists of linearly superposed Reissner-Nordstrom masses which represent the universe with discrete charged masses. In particular, a solution for 8-mass charged cosmological universe is obtained. These solutions generalize the Majumdar-Papapetrou solutions away from the extremal limit of charged black holes, and provide what we believe to be some of the first relativistic calculations of the effects of electric charge on cosmological backreaction.

Contents

****

List of Tables

List of Figures

List of publications

1. On Spherically Symmetric Solutions of the Einstein-Maxwell Field Equations, R. Bibi, T. Feroze, and Azad A. Siddiqui, General Letters on Mathematics, 3: 164-168, (2017), https://doi.org/DOI:10.31559/glm2016.3.3.3. (Chapter 1 is based on this paper.)

2. A New Solution of the Einstein-Maxwell Equations with Linear Equation of State, R. Bibi, T. Feroze, and Azad A. Siddiqui, (to be submitted) (Chapter 2 is based on this paper.)

3. Solution of the Einstein-Maxwell Equations with Anisotropic Negative Pressure as a Potential Model of a Dark Energy Star, R. Bibi, T. Feroze, and Azad A. Siddiqui, Canadian Journal of Physics, 94: 758-762, (2016), https://dx.doi.org/10.1139/cjp-2016-0069. (Chapter 3 is based on this paper.)

4. Cosmological Solutions with Charged Black Holes, R. Bibi, T. Clifton, and J. Durk, General Relativity and Gravitation, 49:98, (2017), https://doi.org/10.1007/s10714-017-2261-4. (Chapter 5 is based on this paper.)

Chapter 1

Introduction

Newton gave a comprehensive view of the universe through his famous theory, Newtons theory of gravity, more than three hundred years ago. It describes the motion of the heavenly bodies and the objects on the earth with the same principles and laws. In this theory the universe is considered as an unbounded flat space which is a 3-dimensional Euclidean geometry. Any event in this geometry is described by time, t, and three spatial coordinates, x^1, x^2, and x^3. In this theory time, t, is absolute. This means that all observers have same clock. In 1905, Einstein gave his Special Theory of Relativity in his famous paper, "*On the Electrodynamics of Moving Bodies*" [1]. Einstein based this theory on the following two postulates.

1. All laws of physics are valid in all inertial frames which are moving relative to each other with constant speed.

2. In all inertial frames, the speed of light, c, is same.

The first postulate implies that all physical laws are same for all coordinate systems in inertial frames. This means there is no preferred set of time and space coordinates. For example, if an observer is sitting at rest in a train moving at constant

speed and looks straight out of the train, everything outside appear to be moving in opposite direction. However, another observer sitting outside the train will observe that the first observer is moving with train's speed while other things (outside the train) are at rest. Now the question is, how to define coordinates of the observer in the train and the observer outside the train? Both observers measure the time and distance according to their frame of references. Special theory of Relativity holds only for frames of reference moving with constant velocity, v, relative to each other i.e. the acceleration is zero. The second postulate states that the speed of light, c, is constant in all internal frames. The time is different for different observers i.e. time is not absolute for all observers, or we can say that each observer has its own clock. Einstein generalized his Special theory of Relativity and gave a new theory called, General theory of Relativity but mathematical form of the theory would not be possible without the mathematical formulation given by Hermann Minkowski in 1907. Minkowski expressed the Special theory of Relativity in terms of 4-dimensional manifold which locally looks like Euclidean geometry. In this spacetime, events occurring in a universe can be described with a non-Euclidean geometry known as Minkowski space.

General theory of Relativity gives a well defined geometric description of one of the 4 fundamental forces in physics, the gravity. The gravity is an attractive force and on large scales it is dominant because other forces i.e. nuclear forces are short ranged. General theory of Relativity is based on a few simple principles and it is considered as one of the most beautiful theories in the natural sciences because of its geometric simplicity.

In this theory all objects are accelerated in the same manner by gravity. In Newtonian mechanics gravity is considered as a force while the equivalence principle in General theory of Relativity allows it to be considered as purely geometric effect rather than a force. The properties of the gravitational field can be ascribed by the curvature of the spacetime. Under the gravity all test bodies move along straight paths which is also postulated in Newtonian Mechanics. In the relativistic approach, this means that they will move on geodesics which is the generalization of straight lines in a curved geometry. As a consequence we can say that the earth orbits around the sun because mass of the sun curves the spacetime and creates curvature due to which the earth revolves around the sun.

1.1 The Einstein Field Equations

General theory of Relativity explains the interaction of gravity as a consequence of spacetime being curved by energy and matter. Einstein gave the Einstein field equations (EFEs) in 1916, which are in fact a set of tensor equations. EFEs are nonlinear partial differential equations (PDEs) which relate the energy and momentum present within a spacetime with the curvature of the spacetime.

The curvature of spacetime is expressed as the Einstein tensor, $E_{\gamma\beta}$, which is defined as

$$E_{\gamma\beta} = R_{\gamma\beta} - \frac{1}{2} g_{\gamma\beta} R. \tag{1.1}$$

The Einstein tensor, $E_{\gamma\beta}$, satisfies the symmetry condition, $E_{\gamma\beta} = E_{\beta\gamma}$ like the metric, $g_{\gamma\beta}$, and the Ricci tensor, $R_{\gamma\beta}$. It is a function of coefficients of the metric,

$g_{\gamma\beta}$. The energy and momentum of the spacetime are expressed as the stress-energy tensor, $T_{\gamma\beta}$. Here, $\gamma, \beta = 0, 1, 2, 3$.

The EFEs are used to find out the geometry of the spacetime due to the energy, mass and linear momentum present in a given spacetime. These equations describe how the spacetime is curved in the presence of matter and how the motion of the matter is influenced by the curvature of spacetime. In result they form a set of nonlinear system of PDEs for the gravitational field. The gravitational field is represented as a pseudo-Riemannian metric, $g_{\gamma\beta}$, with signature $(+,-,-,-)$ or $(-,+,+,+)$.

For a given stress-energy tensor one can determine the metric, $g_{\gamma\beta}$, of the spacetime using the EFEs. The mathematical form of the EFEs is [2, 3]

$$R_{\gamma\beta} - \frac{1}{2} g_{\gamma\beta} R = \frac{8\pi G}{c^4} T_{\gamma\beta}, \tag{1.2}$$

where G is the Newton gravitational constant and c is the speed of light. In this thesis we take the geometric units i.e. we take $c = 1$ and $G = 1$. The Ricci tensor, $R_{\gamma\beta}$, is given as

$$R_{\gamma\beta} = \Gamma^{\alpha}_{\beta\gamma,\alpha} - \Gamma^{\alpha}_{\alpha\gamma,\beta} + \Gamma^{\alpha}_{\alpha\delta}\Gamma^{\delta}_{\beta\gamma} - \Gamma^{\delta}_{\beta\alpha}\Gamma^{\alpha}_{\gamma\delta}, \tag{1.3}$$

where $\Gamma^{\alpha}_{\gamma\beta}$ are the Christoffel symbols defined by

$$\Gamma^{\alpha}_{\gamma\beta} = \frac{1}{2} g^{\alpha\delta} \left(\frac{\partial g_{\delta\gamma}}{\partial x^{\beta}} + \frac{\partial g_{\delta\beta}}{\partial x^{\gamma}} - \frac{\partial g_{\gamma\beta}}{\partial x^{\delta}} \right). \tag{1.4}$$

The Ricci scalar, R, is given by

$$R^{\delta}_{\delta} = g^{\alpha\beta} (\Gamma^{\gamma}_{\beta\alpha,\gamma} - \Gamma^{\gamma}_{\gamma\alpha,\beta} + \Gamma^{\gamma}_{\gamma\delta}\Gamma^{\delta}_{\beta\alpha} - \Gamma^{\gamma}_{\beta\delta}\Gamma^{\delta}_{\gamma\alpha}) \ . \tag{1.5}$$

The EFEs are tensor equations which give a relation between different 4×4 symmetric tensors. Each symmetric tensor has 10 independent components. Due to the freedom of choice of the coordinates, (t, x^1, x^2, x^3), these ten independent equations reduce to six equations. Although the EFEs were initially formulated for a four-dimensional theory but many people explored the EFEs in lower and higher dimensions as well. The relationship between the Einstein tensor, $E_{\gamma\beta}$, and metric tensor, $g_{\gamma\beta}$, is expressed as a set of nonlinear PDEs and solutions of these equations give coefficients of the metric tensor, $g_{\gamma\beta}$. The EFEs in geometric units are

$$E_{\gamma\beta} = 8\pi T_{\gamma\beta}. \tag{1.6}$$

The EFEs are coupled nonlinear PDEs. If the distribution of matter and energy is given in term of the stress-energy tensor, $T_{\gamma\beta}$, then the EFEs are solved for metric tensor, $g_{\gamma\beta}$. The Ricci tensor, $R_{\gamma\beta}$, and scalar curvature, R, are functions of coefficients of the metric [4]. It is very difficult to find the exact solutions of the EFEs, even in the vacuum case these turn out to be fairly complicated to analyze. There is a huge variety of exact solutions of the EFEs, describing gravitational waves, black holes, singularities, and etc.

The nonlinearity of the EFEs makes General theory of Relativity different from other physical theories. For example, the Maxwell equation are linear in the charge, electric field, magnetic field, and current distributions. Also in Quantum Mechanics, the Schrödinger equation is linear in the wave function.

1.2 The Maxwell Field Equations

The Maxwell field equations deal with the electric field and magnetic field in a given space. There are two types of electric fields [5]:

1. Electrostatic Field

2. Induced Electric Field.

If we have the electric charge in a space then the electrostatic field is produced around the source while if we vary the magnetic field with respect to time then the induced electric field is produced. For electrostatic fields, there is "*Gauss's law*". Mathematically, the law is

$$\nabla.\mathbf{E} = \frac{\rho}{\varepsilon_0}, \tag{1.7}$$

where $\mathbf{E}$ is the electric field, ρ is the charge density and ε_0 is the permittivity of free space [5]. If the charge is positive then the divergence of the electric field is positive and flow of the electric field lines is away from the source while in the presence of the negative charge the divergence of the electric field is negative and flow of the electric field lines is towards the source. The electric field for a point charge having charge, Q, is given as

$$\mathbf{E} = \frac{Q}{4\pi\varepsilon_0 r}\mathbf{r}, \tag{1.8}$$

where $\mathbf{r}$ is the distance of the object from the point charge. In magnetic field, there are poles called south and north poles. Positive and negative charges can be isolated but the magnetic poles can not be isolated. However, the north pole behaves similar to positive charge and the south pole behaves like the negative charge. The total magnetic charge and the total magnetic flux within a surface which is closed

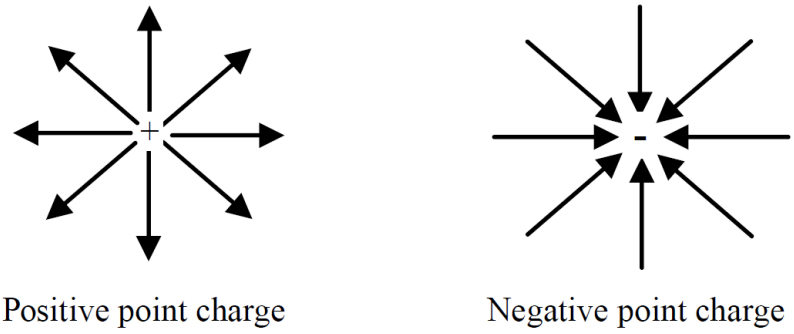

Figure 1.1: The Electric Field Lines for Positive and Negative Charges [5].

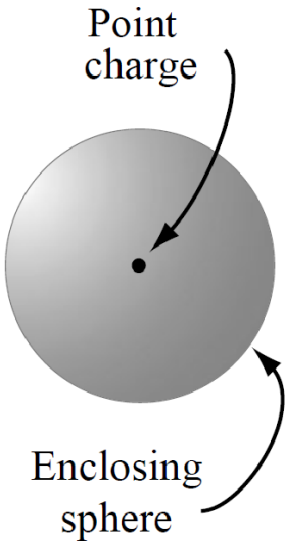

Figure 1.2: The Electric Field in enclosing sphere of a Point Charge [5].

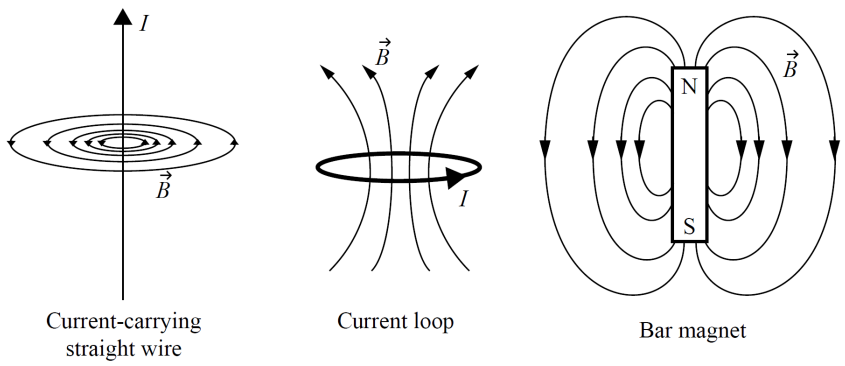

Figure 1.3: The lines of Magnetic Field [5].

are always zero, which means that the divergence of the magnetic field, **B**, is zero. Mathematically, "*Gauss's law for magnetic field*", is expressed as [5]

$$\nabla.\mathbf{B} = 0. \tag{1.9}$$

The lines of the magnetic field, **B**, start from the north pole and end at the south pole and form continuous loops and hence do not intersect each other.

"*Farady's law*" states that the electric field is produced by the time variation of the magnetic field [5]. Mathematically,

$$\nabla \times \mathbf{E} = -\frac{\partial \mathbf{B}}{\partial t}. \tag{1.10}$$

The induced electric field produced by the time varying magnetic field is a bit different from the electrostatic electric field. The field lines of induced electric field form loops.

Ampere showed that the magnetic field is produced by the electric current along a path which bounds the surface. Later, Maxwell showed that the time varying

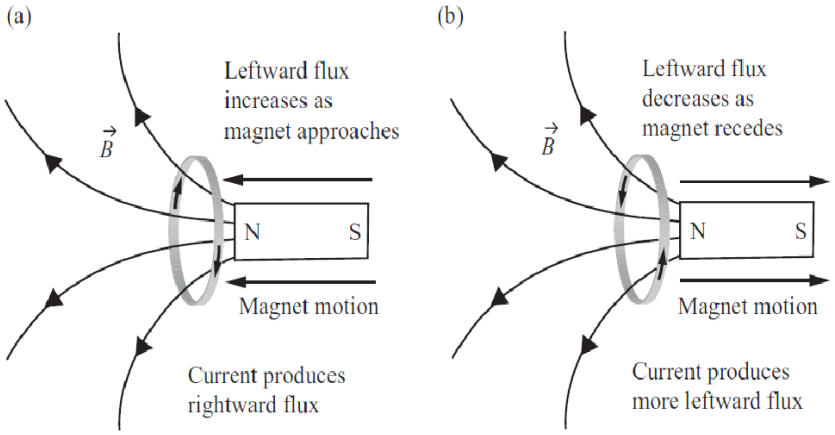

Figure 1.4: The Electric Field due to the Time Varying Magnetic Field [5].

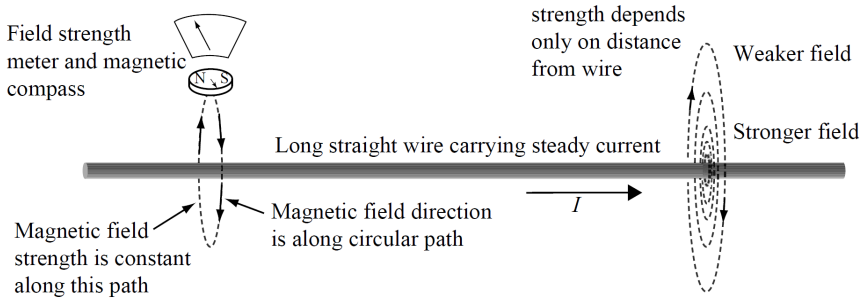

Figure 1.5: The Induced Magnetic Field due to the Time Varying Electric Field [5].

electric flux also produces the magnetic field. *Ampere's law* states that the magnetic field is produced by the electric current and the time varying electric flux [5]. Mathematically,

$$\nabla \times \mathbf{B} = \upsilon_0(\mathbf{j} + \varepsilon_0 \frac{\partial\, \mathbf{E}}{\partial t}), \tag{1.11}$$

where υ_0 is magnetic permeability of free space and $\mathbf{j}$ is the electric current density. Maxwell later worked on this and found the light travels in the form of electromagnetic waves and gave a comprehensive theory on the electromagnetism, known as the Maxwell field equations. The Maxwell equations are coupled linear PDEs in $\mathbf{E}$

and **B**. For region where charge density and current density are zero, we can rewrite the Maxwell field equations as

$$\nabla^2 \mathbf{E} = \upsilon_0 \varepsilon_0 \frac{\partial^2 \mathbf{E}}{\partial t}, \tag{1.12}$$

$$\nabla^2 \mathbf{B} = \upsilon_0 \varepsilon_0 \frac{\partial^2 \mathbf{B}}{\partial t}, \tag{1.13}$$

where $\frac{1}{\upsilon_0 \varepsilon_0} = c^2$. Eqs. (1.12) and (1.13) show that the electric and magnetic fields satisfy the wave equation and these travel with the speed $\frac{1}{\sqrt{\upsilon_0 \varepsilon_0}}$ which is the speed of light, hence, light travels as electromagnetic waves.

The electric field, **E**, can be expressed in terms of a scalar potential, ϕ, and a vector potential, **A**, while the magnetic field, **B**, is expressed in terms of a vector potential, **A**, mathematically we have

$$\mathbf{E} = -\nabla \phi - \frac{\partial \mathbf{A}}{\partial t}, \tag{1.14}$$

$$\mathbf{B} = \nabla \times \mathbf{A}. \tag{1.15}$$

1.2.1 The Maxwell Equations in Relativity

In Relativity the Maxwell equations can be written in terms of the Maxwell electromagnetic tensor, $F_{\gamma\beta}$,

$$F_{\gamma\beta} = \frac{\partial A_\beta}{\partial x^\gamma} - \frac{\partial A_\gamma}{\partial x^\beta}, \tag{1.16}$$

where the four-vector potential, $\boldsymbol{A}$, is given as

$$\boldsymbol{A} = (\frac{\phi}{c}, -\mathbf{A}). \tag{1.17}$$

In terms of the Maxwell tensor, $F_{\gamma\beta}$, the electric field, $\mathbf{E}$, and magnetic field, $\mathbf{B}$ are expressed as

$$\mathbf{E}_i = cF_{0i}, \tag{1.18}$$

$$\mathbf{B}_i = \frac{-1}{2}\varepsilon_{ijl}F^{jl}, \tag{1.19}$$

where ε_{ijl} is the Levi Civita symbol $(i, j, l = 1, 2, 3)$. Components of the Maxwell tensor, $F_{\gamma\beta}$, are

$$F_{\gamma\beta} = \begin{bmatrix} 0 & \frac{E_1}{c} & \frac{E_2}{c} & \frac{E_3}{c} \\ -\frac{E_1}{c} & 0 & -B_3 & B_2 \\ -\frac{E_2}{c} & B_3 & 0 & -B_1 \\ -\frac{E_3}{c} & -B_2 & B_1 & 0 \end{bmatrix}. \tag{1.20}$$

The Maxwell tensor, $F_{\gamma\beta}$, is anti symmetric tensor i.e. $F_{\gamma\beta} = -F_{\beta\gamma}$. The inner product $F_{\gamma\beta}F^{\gamma\beta} = 2(\mathbf{B}^2 - \frac{\mathbf{E}^2}{c})$ gives the Lorentz invariant i.e. it is independent of the coordinates. It has six independent components. The Maxwell equations can be written in 2 tensor equations as

$$F^{\gamma\beta}_{;\beta} = \upsilon_0 j^{\gamma}, \tag{1.21}$$

$$F_{[\gamma\beta,\delta]} = 0, \tag{1.22}$$

where j^{γ} is the four vector current density and $\gamma, \beta, \delta = 0, 1, 2, 3$.

1.3 The Stress-Energy Tensor

The stress-energy tensor, $T_{\gamma\beta}$, is also known stress-energy-momentum tensor. In physics, it describes the flux and density of energy and momentum in a given space-time, in fact it gives a generalization to the stress tensor, $\sigma_{\gamma\beta}$, of the Newtonian Physics. In Relativity, it is the source of the gravitational field in the EFEs. The flux of the γ^{th} component of the momentum vector across the surface with constant x^{β} coordinate is given by the component, $T_{\gamma\beta}$, of stress-energy tensor. It is given by [4]

$$T_{\gamma\beta} = \begin{bmatrix} \rho & q_x & q_y & q_z \\ q_x & \Pi_{11} & \Pi_{12} & \Pi_{13} \\ q_y & \Pi_{21} & \Pi_{22} & \Pi_{23} \\ q_z & \Pi_{31} & \Pi_{32} & \Pi_{33} \end{bmatrix}, \tag{1.23}$$

where $T_{00} = \rho$ is the time-time component which gives relativistic energy density which is the density of the relativistic mass. The flux of energy across a surface perpendicular to the α-direction is given by $T_{0\beta} = q_{\beta}$, and it is also equal to the β-component of momentum density i.e.

$$T_{0\beta} = T_{\beta 0}, \tag{1.24}$$

and the ij-th component of symmetric stress tensor, Π_{ij}, represents the i-component of stress, or flux of momentum, across a surface perpendicular to j-direction. The normal stress component, Π_{ii}, (not summed over i) is called pressure in i-th direction. Whereas, Π_{ij}, $i \neq j$, represents shear stress. The stress-energy tensor satisfies the

symmetry condition and it is also conserved i.e.

$$T_{\gamma\beta} = T_{\beta\gamma}, \tag{1.25}$$

$$T^{\gamma\beta}_{;\beta} = 0. \tag{1.26}$$

Stress-energy tensor has 6 independent components and its trace, T, is an invariant quantity which is given as

$$T = T^{\alpha\alpha} = -\rho + 3p, \tag{1.27}$$

where $p = \frac{\Pi_{ii}}{3}$ is the isotropic pressure. Isotropic pressure is same in all directions. In fact the stress-energy-momentum tensor is the source of curvature in the spacetime.

1.3.1 Different Forms of the Stress-Energy Tensor

Some well known forms of the stress-energy-momentum tensor are:

Isolated Particle

The stress-energy-momentum tensor for an isolated particle that has mass m and is moving on the trajectory, $\mathbf{y}_q(t)$, is given as

$$T_{\gamma\beta}(\mathbf{y}, t) = \frac{m u_\gamma(t) u_\beta(t)}{\sqrt{1-u^2}\delta(\mathbf{y} - \mathbf{y_q})(t)}, \tag{1.28}$$

where $\mathbf{u}$ is four vector velocity given as

$$\mathbf{u} = (1, \frac{d\mathbf{y}_p}{dt}(t)), \tag{1.29}$$

and $u = \sqrt{\mathbf{u}.\mathbf{u}}$ is the speed of the particle [6].

Fluid in Thermodynamic Equilibrium

For the fluid which is in thermodynamic equilibrium, the stress-energy-momentum tensor is given as

$$T_{\gamma\beta} = (p + \varrho)\mathrm{v}_\gamma \mathrm{v}_\beta + p g_{\gamma\beta}, \tag{1.30}$$

where p is the hydrostatic pressure, ϱ is the mass energy density, and $\mathbf{v}$ gives the 4-vector velocity of fluid [6]. The 4-vector velocity, v_μ, of fluid satisfies the following condition

$$\mathrm{v}_\gamma \mathrm{v}_\beta g^{\gamma\beta} = -1. \tag{1.31}$$

In special case, if we take the pressure of fluid to be zero then the stress-energy-momentum tensor becomes

$$T_{\gamma\beta} = \varrho \mathrm{v}_\gamma \mathrm{v}_\beta. \tag{1.32}$$

If the fluid is at rest then we only have one component, $T^{00} = \varrho$, of the stress-energy tensor, rest all others are zero.

The Electromagnetic Stress-Energy-Momentum Tensor

For the electromagnetic field the stress-energy-momentum tensor is given as [6]

$$T_{\gamma\beta} = F_{\gamma\delta} g^{\delta\alpha} F_{\beta\alpha} - \frac{1}{4} g_{\gamma\beta} F_{\alpha\delta} F^{\alpha\delta}. \tag{1.33}$$

Using Eq. (1.16) in Eq. (1.33) we have

$$T_{\gamma\beta} = \begin{bmatrix} \varepsilon_0 E^2 + \frac{1}{\upsilon_0} B^2 & \frac{S_x}{c} & \frac{S_y}{c} & \frac{S_z}{c} \\ -\frac{S_x}{c} & \Pi_{xx} & \Pi_{xy} & \Pi_{xz} \\ -\frac{S_y}{c} & \Pi_{yx} & \Pi_{yy} & \Pi_{yz} \\ -\frac{S_z}{c} & \Pi_{zx} & \Pi_{zy} & \Pi_{zz} \end{bmatrix}, \tag{1.34}$$

where $\mathbf{S}$ and space components T_{ij} are given as

$$\mathbf{S} = \frac{1}{\mu_0}\mathbf{E} \times \mathbf{B}, \tag{1.35}$$

$$T_{ij} = \varepsilon_0 E_i E_j + \frac{1}{\upsilon_0} B_i B_j - \frac{1}{2}(\varepsilon_0 E^2 - \frac{B^2}{2\upsilon_0})\delta_{ij}. \tag{1.36}$$

1.4 The Cosmological Constant

Including a cosmological term which is proportional to the metric tensor, $g_{\gamma\beta}$, Einstein modified his field equations as

$$R_{\gamma\beta} - \frac{1}{2} g_{\gamma\beta} R + g_{\gamma\beta}\Lambda = 8\pi T_{\gamma\beta}, \tag{1.37}$$

where Λ is cosmological constant with dimension $(\text{length})^{-2}$. It is remarkable that by adding the cosmological constant term the law of conservation of energy is not affected. Originally this term was introduced by Einstein to restrict the universe to be static i.e., the universe is not contracting or expanding [7]. This attempt was unsuccessful because the static universe with cosmological constant was unstable so, Λ was discarded.

In the early 1990s, the phenomena of expansion of the universe was not very well

known and explained but later in 1998 the Hubble space telescope (HST) observed that the expansion of universe is slower than supernova crisp [8,9]. Due to the gravity of mass of the universe, there is enough energy density to stop expansion of the universe so it was difficult to believe that universe can expand, however, observations showed its expansion but at that time no one knew the reason of the expansion.

The cosmological constant was the first interpretation of the expansion of the universe. Regardless this misguided motivation of Einstein of introduction of the cosmological term, adding this constant in the equations, nothing is inconsistent. In fact recent techniques have found that a positive value of Λ explains the expansion of the universe. The beauty of the cosmological term, Λ, is that it gives results which extensively improves the agreement between observations and theory. The most remarkable example of this are the recent efforts to measure the expansion of the universe since the last few billion years. Due to the gravity of matter present in the universe the expansion should be slow down, imparted by the Big Bang [10] but when astronomers observed supernova in order to calculate the rate of the expansion of the universe over the last few billion years. The results showed that the expansion of the universe is not slowed down but infact it is accelerating and there is bizarre matter or energy which is the reason of accelerating universe; which means that this mass or energy has gravitationally repulsive nature. This means that the cosmological constant is this type of energy.

The existence of quantum mechanical vacuum energy is another reason to expect a cosmological constant because quantum mechanical theory predicts that the vacuum has some amount of energy associated with it. In General Relativity, all forms of

matter and energy gravitates so the cosmological constant, Λ, can be associated with the vacuum energy. Much work needed to explain this mystery. Einstein took the cosmological constant as an independent parameter such that we have

$$(\Lambda g^{\gamma\beta})_{;\beta} = 0. \tag{1.38}$$

The vacuum energy is constant and given by

$$\rho_{vac} = \frac{\Lambda}{8\pi}. \tag{1.39}$$

The cosmological constant has negative pressure, given by

$$P_{vac} = -\rho_{vac}. \tag{1.40}$$

The positive cosmological constant induces a repulsive gravitational force. This results in the expansion of the universe. This means that the cosmological constant, Λ, is thus associated with non-zero vacuum energy. In general relativity these terms are now used interchangeably. In our universe around 68 percent is dark energy and about 27 percent is black substance and rest 5 percent is the matter. The mater we know is just a small part of the universe. Though we do not know much about dark energy but its effects can be seen by the expansion of the universe.

The Fig. 1.6 shows how the rate of expansion of the universe is changing from it's birth (fifteen billion years ago) till now. The shallow of the curve indicates that the expansion of the universe is faster. After 7.5 billion years the expansion is rapidly increasing and objects in the universe started moving away at much faster rate. The

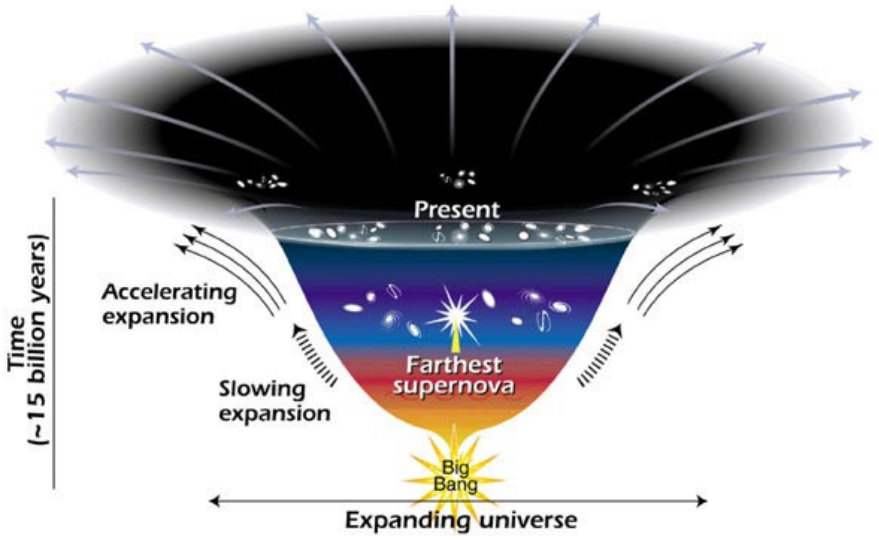

Figure 1.6: The expansion of the universe from its birth till now [11].

rate of this expansion is because of a mysterious dark energy [11].

1.5 Gravitational Collapse

In hydrostatic equilibrium, the gravity of a massive body is counter balanced by its pressure. With the passage of time this pressure starts decreasing and gravity starts dominating and the gravitational collapse occurs. When a distribution of matter collapses then different hierarchy of structures are born like cluster of galaxies, stellar groups, stars, planets etc. For example, if the gravitational collapse of the cloud of interstellar matter occurs gradually then a new star is born. When the temperature at the centre of the star is increased by the compression caused by the collapse then nuclear fuel ignites and the collapse starts to halt and the star gains dynamic equilibrium between gravity and pressure.

A normal star is a ball of gas held by its gravity and at the end of its life time the

gravitational collapse occurs, this is called the death of the star. So stars are born at gravitational collapse and with the time these again undergo a gravitational collapse which form new stars. The end states of a gravitational collapse are called compact stars [12]. There are different types of these compact stars:

I. "White dwarfs"

II. "Neutron Stars"

III. "Black Holes".

The collapse from stars to white dwarfs takes place in more than ten thousand of years while the stars blow off their outer shell to form planetary nebula. The size of a white dwarf is about 1.4 solar mass. If there are some companion stars near white dwarf then it can accrete their mass to reach a limit called Chandrasekhar limit i.e. when its mass crosses the limit of 1.4 solar mass and it blows off completely in type 1a supernova. The neutron stars are born by collapse of such massive stars.

If the star is very massive then collapse continues and nothing can stop it and when it reaches within the Schwarzschild radius then even light can not escape. At this point the star transforms to a black hole.

Classically, a black hole is the region in space from which not even light can escape. There is a surface around the black hole which is called event horizon which is also called the point of no return. The events beyond the event horizon can not affect an outside observer. If an observer approaches the event horizon then it slows down as seen by an outside observer and never crosses the event horizon. Although the interior of a black hole is invisible but we can detect the black hole from its interaction with other matter. By tracking the moments of group of stars, orbiting in a

region, we can infer black hole. If there is a companion star near a black hole then its gas starts to fall into black hole, it spirals inwards and is heated to very high temperature. This emits a large amount of radiations which can be detected from the telescope orbiting around the earth.

At the center, $r = 0$, of a black hole lies the singularity where the curvature is not finite. For non-rotating black holes, it is a single point and for rotating black holes it is a ring, which lies in the plane of rotation. The whole mass of a black hole lies in the singular region and its density is infinite. There is a famous theorem in Relativity called "*no hair theorem*", which states,

"*All black hole solutions of the EMFEs of gravitation and electromagnetism in general relativity can be completely characterized by only three externally observable classical parameters: mass, electric charge, and angular momentum*" [13].

All information of the matter which forms the black hole or falls into it, is disappeared behind the event horizon and are not accessible for observers outside the event horizon. It is interesting that the no hair theorem is independent of frame of reference and hence it tells nothing about the position and velocity of a black hole.

1.5.1 The Schwarzschild Black Hole Solution

Let us consider an isolated point of mass m. We consider the spacetime to be static and spherically symmetric. The line element is given as

$$ds^2 = -e^{\mu(r)}dr^2 - r^2 d\theta^2 - r^2 \sin^2\theta d\phi^2 + e^{\zeta(r)}dt^2. \tag{1.41}$$

There is vacuum all around the source so the stress-energy tensor is zero i.e. $T_{\gamma\beta} = 0$, for all γ and β. Then the EFEs become $R_{\gamma\beta} = 0$ i.e. the Ricci scalar is zero. For a diagonal metric given in Eq. (1.41), there are 4 independent component of the Ricci scalar. Solving the EFEs, the metric in Eq. (1.41) becomes

$$ds^2 = -(1 - \frac{2m}{r})^{-1}dr^2 - r^2 d\theta^2 - r^2 \sin^2\theta d\phi^2 + (1 - \frac{2m}{r})dt^2, \tag{1.42}$$

which is called the Schwarzschild solution [14]. Here, we have two singularities, the essential singularity, $r = 0$, that can not be removed and the coordinate singularity, $r = 2m$, that can be removed by using appropriate coordinate transformations. For example one can use Eddington-Finkelstein coordinate transformations

$$t = \tilde{t} \pm 2m \ln(1 - \frac{\tilde{r}}{2m}) \quad \text{for} \quad \tilde{r} < 2m, \tag{1.43}$$

$$t = \tilde{t} \pm 2m \ln(\frac{\tilde{r}}{2m} - 1) \quad \text{for} \quad \tilde{r} > 2m, \tag{1.44}$$

$$r = \tilde{r}. \tag{1.45}$$

Under these transformations the metric (1.42) becomes

$$ds^2 = -(1 + \frac{2m}{\tilde{r}})d\tilde{r}^2 \pm \frac{4m}{\tilde{r}}d\tilde{t}d\tilde{r} - \tilde{r}^2 d\theta^2 - \tilde{r}^2 \sin^2\theta d\phi^2 + (1 - \frac{2m}{\tilde{r}})d\tilde{t}^2. \tag{1.46}$$

Clearly the coordinate singularity, $\tilde{r} = 2m$, is removed while the essential singularity, $\tilde{r} = 0$, is not removed. The observer in the outer region $\tilde{r} > 2m$ can not get any information about the events happening in the inner region $r < 2m$ because no object can escape the hypersurface $\tilde{r} = 2m$.

1.5.2 The Reissner-Nordstrom Black Hole Solution

The Schwarzschild black hole has mass only. If the source also has charge then the solution of the EFEs along with the Maxwell field equations is known as the Rissner-Nordstrom black hole. To find the solution we assume

1. The spacetime to be static and spherically symmetric.

2. The source to be a charged source, having charge q.

3. There is vacuum around the charged source.

The electromagnetic potential for spherical symmetric spacetime is

$$\boldsymbol{A} = (A_0, 0, 0, 0), \tag{1.47}$$

where $A_0 = \phi(t, r)$ is the electric potential. For static case we have $A_0 = \phi(r)$. The electric field is

$$\mathbf{E} = (E(r), 0, 0). \tag{1.48}$$

The magnetic field is zero, $\mathbf{B} = 0$. Using Eq. (1.48) and $\mathbf{B} = 0$ in Eq. (1.36) we have

$$T^{\gamma}_{\beta} = diag(-\rho - E^2/2, -E^2/2, E^2/2, E^2/2). \tag{1.49}$$

The Einstein-Maxwell field equations (EMFEs) lead to the metric [15]

$$ds^2 = -(1 - \frac{2m}{r} + \frac{q^2}{r^2})^{-1}dr^2 - r^2 d\theta^2 - r^2 \sin^2\theta d\phi^2 + (1 - \frac{2m}{r} + \frac{q^2}{r^2})dt^2, \tag{1.50}$$

where the event horizon(s) can be calculated from

$$1 - \frac{2m}{r} + \frac{q^2}{r^2} = 0, \tag{1.51}$$

which gives two event horizons, the outer event horizon, r_+, and the inner event horizon, r_-, are given as

$$r_\pm = m \pm \sqrt{m^2 - q^2},\ m \geq q. \tag{1.52}$$

1.5.3 The Kerr-Neuman Black Hole Solution

The Schwarzschild black has mass only and if we add spin to it we get Kerr black hole. Similarly if we add spin to the Reissner-Nordstrom black hole then we get the Kerr-Neuman black hole. The mass of the Kerr-Neuman black hole is m, the charge is q, and the rotation is given as $\bar{a} = \frac{j}{m}$, where j is the angular momentum. So the most general stationary solution of the EMFEsis the Kerr-Newman black hole. Using the Boyer-Linquist coordinates the metric of Kerr-Newman black hole can be written as [16]

$$\begin{aligned} ds^2 &= -\frac{\Delta^2}{\rho^2}(dt - \bar{a}\sin^2\vartheta d\varphi)^2 + \frac{\Delta^2}{\rho^2}dr^2 + \rho^2 d\vartheta^2 \\ &+ \frac{\sin^2\vartheta}{\rho^2}(\bar{a}dt - (r^2 + \bar{a}^2)d\varphi)^2, \end{aligned} \tag{1.53}$$

where

$$\Delta^2 = r^2 - 2mr + \bar{a}^2 + q^2, \quad \rho^2 = r^2 + \bar{a}^2\cos^2\vartheta. \tag{1.54}$$

This solution shows that the charged and rotating bodies can undergo gravitational collapse and can form charged rotating black hole. The inner and outer event hori-

zons are given as

$$r_{\pm} = m \pm \sqrt{m^2 - q^2 - \bar{a}^2}. \tag{1.55}$$

1.6 Dark Energy and Dark Matter

In 1937 Zwicky [17] estimated the mass of the large cluster of galaxies. Then he estimated the average mass per galaxy. The average mass of the galaxy was many times more than their luminous mass. It means there is mass in galaxies which is non-luminous. Later, others also observed the same and found that about 95% of mass of galaxies is dark matter [17]. Other evidence of dark mater is provided by the X-ray emission from galaxies. From these emissions, luminosity of the galaxies can be measured. As luminosity depends on the temperature, volume, and density of the galaxies so much more mass is needed to hold very hot gasses. The luminous mass of galaxies is not sufficient to hold it, so the dark matter is responsible for holding the galaxies. Also the gravitational lensing gives presence of the dark matter by giving the measurement of total mass of galaxies.

The nature of dark matter particles is unknown. We do not know yet whether these particles are stable or have a finite life time. As the interaction of dark mater and ordinary mater is very weak (or we do not know yet) so direct detection of the dark mater is not possible. Although many experiments are running but no positive results are found, for example, at the Large Hadron Collider (LHC), the researches are trying to create the conditions of the very early universe so that they can detect the dark matter particles, by assuming that dark matter particles will be produced

in pairs according to standard model of Particles in Physics.

Einstein assumed that our universe is static but later observations form the Hubble telescope revealed that our universe is expanding. It means that there is some energy which is responsible for the expansion i.e. dark energy. As gravity has positive pressure which makes it attractive force so dark energy has negative pressure i.e. it is repulsive in nature. Basically the cosmological constant gives energy density of vacuum and has negative pressure. Generally the dark energy density can be expressed as

$$\rho_d \propto \rho_0 a^{-3(w+1)}, \tag{1.56}$$

where ρ_d is the energy density of the dark energy, ρ_0 is the initial value of the dark energy and can be associated with cosmological constant, a is the scale factor of the FLRW model, and $w = \frac{P_d}{\rho_d}$ is the parameter of equation of state. If $w = 0$ then it gives matter dominated universe, $w = \frac{1}{3}$ gives universe with pure radiation and $w = -1$ corresponds to the cosmological constant.

Many researchers consider cosmological constant and dark energy same however, there are other models for dark energy as well for example Quintessence, Phantom energy and Quintom energy.

1.7 Some Models for a Compact Object

The exact solutions of the EMFEs for the static symmetrically symmetric geometry are of great interest. In Relativistic Astrophysics solutions of the EMFEs which satisfy some physical criterion are of real interest because these can be used to model

the compact objects like stars, neutron stars, quark stars etc. This helps us in understanding the highly dense distribution of matter of the interior of relativistic compact objects. The EMFEs are nonlinear so it is very difficult to find the exact solutions, although many solutions have been obtained [6]. Only few exact solutions of the EMFEs fulfil the physical criterion to be considered as the relativistic compact objects. In literature the physical criterion is discussed in detail [18, 19]. There are regularity conditions which solution should satisfies.

To find the solution of the EMFEs, one can take any equations of state of the form $p_r = f(\rho)$. The equation of state plays important role for the relativistic compact matter. It gives relation between the radial pressure, p_r, and the density, ρ. Mostly the solutions of the EMFEs do not satisfy any equation of state. However, one may choose an equation of state and then solve the EMFEs for physically valid solutions. In Literature many solutions of the EMFEs have been obtained by assuming different types of the equations of state. Thirukkanesh et al. [20], Feroze [21], Sunzu et al. [22], and Malaver [23] assumed linear equation of state, $p_r = A\rho + B$. Feroze et al. [24, 25], Maharaj et al. [26], Mafa et al. [27], and Shrama et al. [28] considered quadratic equation of state, $p_r = A\rho^2 + B\rho + C$. Takisa et al. [29], and Malaver [30] assumed the polytropic equation of state, $p_r = k\rho^{\Gamma}$, where $\Gamma = 1 + \frac{1}{\eta}$ and η is the ploytropic index. Malaver [31], Thirukkanesh et al. [32] assumed Van der Waals modified equation of state, $p_r = \alpha\rho^2 + \frac{\gamma\rho}{1+\beta\rho}$, while in [33] Malaver assumed Van der Waals modified equation of state of type $p_r = \alpha\rho^{\Gamma+1} + \frac{\beta\rho^{\Gamma}}{1+\gamma\rho^{Y}\Gamma}$.

To model a relativistic stellar object, one generally assumes that the pressure distribution is isotropic and homogeneous but in the presence of the electromagnetic field

pressure is anisotropic. Anisotropy is defined as $p_t - p_r$, where p_t is the transverse pressure. This represents an anisotropic force which is repulsive in nature if $p_t > p_r$ and attractive if $p_t < p_r$. Many compact astrophysical objects like "X-ray pulsar", "Her-x-1", "X-ray buster $4U1820-30$", "millisecond pulsar SAXJ1804.4 $-$ 3658", and etc have anisotropic pressures.

Many solutions of the EMFEs have been obtained for anisotropic pressures. Feroze [21], Malaver [23, 30, 31, 33], Sunzu et al. [22], Feroze et al. [24, 25], Maharaj et al. [26, 29], Takisa et al. [27] and Sharma et al. [28] obtained solutions of the EMFEs for charged spherically symmetric static spacetimes by assuming anisotropic pressure. In general, in all these solutions radial pressure is positive.

1.7.1 Classification of the Solutions

In order to find some new classes of the solutions of the EMFEs, we divided the problem as fellows. First we categorized the electromagnetic field to be without source ($T = 0$) or with source ($T \neq 0$). Then we divided the problem further by assuming the electromagnetic field to be null or non-null and then in each case we investigated the solution by considering the pressure to be isotropic or anisotropic. The summary of the scheme is shown in Fig. 1.7.

The electromagnetic field is called null field if it satisfies the following conditions

$$\mathbf{E}.\mathbf{B} = 0, \tag{1.57}$$

$$\mathbf{E}^2 = \mathbf{B}^2, \tag{1.58}$$

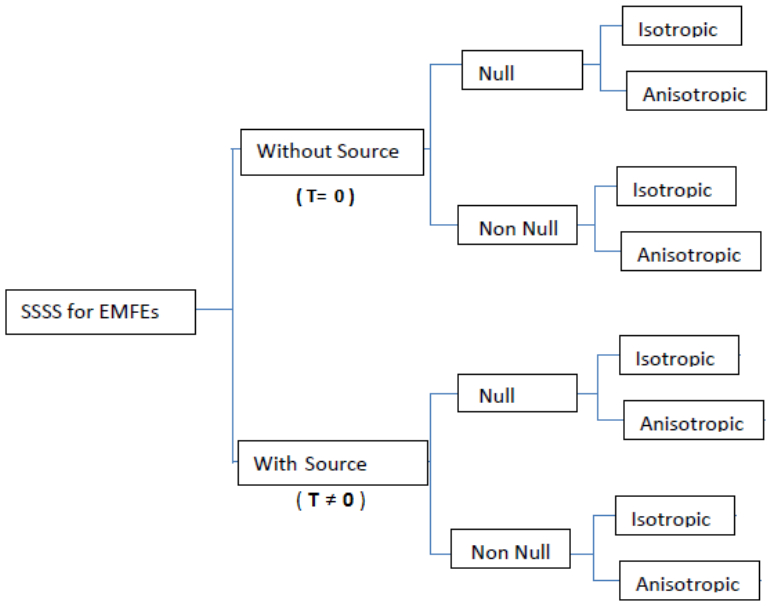

Figure 1.7: Some Classes of the spherically symmetric static solutions (SSSS) of the EMFEs.

where **E** is the electric field and **B** is the magnetic field. If any of the above conditions fail then electromagnetic field is called non-null field. If the electric field or magnetic field is zero then field is called magnetostatic or electrostatic field respectively.

We can classify solutions of the EMFEs in different ways. One of the interesting classification is the Segre classification which depends on the eigenvectors and eigenvalues of the trace free Ricci tensor, $R_{\gamma\beta}$, [6]. The Segre tensor, $S_{\gamma\beta}$, is given as

$$S_{\gamma\beta} = R_{\gamma\beta} - \frac{1}{4} R g_{\gamma\beta}. \tag{1.59}$$

Another way to write the Segre tensor is to write its components in null tetrad form $(k^\beta, l^\beta, m^\beta, \overline{m}^\beta)$. The null tetrad is a complex basis for the metric, $g_{\gamma\beta}$. Mathemati-

cally the metric, $g_{\gamma\beta}$, can be written in terms of null tetrad as

$$g_{\gamma\beta} = 2(m_\gamma \overline{m}_\beta) - 2(k_\gamma l_\beta). \tag{1.60}$$

The components of null tetrad satisfy the following conditions

$$k^\gamma l_\gamma = -1, \tag{1.61}$$

$$m^\gamma \overline{m}_\gamma = 1. \tag{1.62}$$

In terms of the null tetrad the Segre tenor can be written as 3×3 Hermitian matrix $\phi_{ij}(i, j = 0, 1, 2)$

$$\phi_{00} = \frac{1}{2} S_{ab} k^\alpha k^\beta, \tag{1.63}$$

$$\phi_{01} = \frac{1}{2} S_{ab} k^\alpha m^\beta, \tag{1.64}$$

$$\phi_{02} = \frac{1}{2} S_{ab} m^\alpha m^\beta, \tag{1.65}$$

$$\phi_{11} = \frac{1}{4} S_{ab} (k^\alpha l^\beta + m^\alpha \overline{m}^\beta), \tag{1.66}$$

$$\phi_{12} = \frac{1}{2} S_{ab} l^\alpha m^\beta, \tag{1.67}$$

$$\phi_{22} = \frac{1}{2} S_{ab} l^\alpha l^\beta. \tag{1.68}$$

The static spherically symmetric metric is given as

$$ds^2 = -e^{2\zeta(r)} dt^2 + e^{2\eta(r)} dr^2 + r^2 (d\theta^2 + sin^2\theta d\phi^2), \tag{1.69}$$

and the components of the null tetrad can be expressed as functions of the coefficients of the metric, mathematically

$$k^{\beta} = 1/\sqrt{2}(-e^{-\zeta}\partial/\partial t - e^{-\eta}\partial/\partial r), \tag{1.70}$$

$$l^{\beta} = 1/\sqrt{2}(-e^{-\zeta}\partial/\partial t + e^{-\eta}\partial/\partial r), \tag{1.71}$$

$$m^{\beta} = 1/r\sqrt{2}(\partial/\partial\theta + \frac{\imath}{\sin\theta}\partial/\partial\phi), \tag{1.72}$$

$$\overline{m}^{\beta} = 1/r\sqrt{2}(\partial/\partial\theta - \frac{\imath}{\sin\theta}\partial/\partial\phi). \tag{1.73}$$

Now question is how to know a given metric contains null or non-null electromagnetic field? The first way is to check whether the electric and magnetic fields satisfy the conditions (1.57) and (1.58) or not. The second method is to check the Segre type of the metric and then tell either it contains null or non-null electromagnetic field. For this we have

1. If ϕ_{00} is the only non-zero component of the Segre tensor then the electromagnetic field null.

2. If ϕ_{11} is the only non-zero component then the electromagnetic field non-null [5, 34].

The non-zero components of the ϕ_{ij} for the metric (1.69) are

$$\phi_{00} = \frac{1}{2r}e^{-2\eta}(\eta' + \zeta'), \tag{1.74}$$

$$\phi_{22} = \frac{1}{2r}e^{-2\eta}(\eta' + \zeta'), \tag{1.75}$$

$$\phi_{11} = \frac{1}{4}e^{-2\eta}(\zeta'' + \zeta'^2 - \zeta'\eta' - \frac{1}{4r^2}) + \frac{1}{4r^2}. \tag{1.76}$$

For the null electromagnetic field we set $\phi_{00} \neq 0$, $\phi_{11} = 0$ and $\phi_{22} = 0$. We can choose ζ and η such that $\phi_{11} = 0$ in Eq. (1.76) but if we set $\phi_{22} = 0$ in Eq. (1.75) then ϕ_{00} in Eq. (1.74) also becomes zero which is not possible. This means for the static charged spherical symmetric spacetime the null electromagnetic field is not possible.

For the non-null electromagnetic field we need $\phi_{11} \neq 0$, $\phi_{00} = 0$ and $\phi_{22} = 0$. If we have

$$\eta' + \zeta' = 0, \tag{1.77}$$

then $\phi_{00} = 0$, $\phi_{22} = 0$ and $\phi_{11} \neq 0$. We choose the stress-energy tensor, $T_{\gamma}{}^{\beta}$, as

$$T_{\gamma}{}^{\beta} = diag(-\rho - \frac{E^2}{2}, p_r - \frac{E^2}{2}, p_t + \frac{E^2}{2}, p_t + \frac{E^2}{2}), \tag{1.78}$$

where ρ is the density, $\mathbf{E}$ is the electric field, p_r and p_t are the radial and transverse pressures respectively. Here, we only consider the electric field and magnetic field is taken to be zero. The EMFEs for the metric (1.69) are

$$\begin{aligned}
\frac{1}{r^2}((1 - e^{-2\eta})) + \frac{2\eta'}{r}e^{-2\eta} &= \rho + \frac{E^2}{2}, & (1.79)\\
-\frac{1}{r^2}(r(1 - e^{-2\eta}) + \frac{2\zeta'}{r}e^{-2\eta}) &= p_r - \frac{E^2}{2}, & (1.80)\\
e^{-2\eta}(\zeta'' + \zeta'^2 + \frac{\zeta'}{r} + \zeta'\eta' - \frac{\eta'}{r}) &= p_t + \frac{E^2}{2}, & (1.81)\\
\sigma &= \frac{1}{r^2}e^{-\eta}(r^2E)'. & (1.82)
\end{aligned}$$

For non-null case, using $\phi_{00} = 0$ in the EMFEs, we get the following equation of state

$$p_r = -\rho. \tag{1.83}$$

Using $\zeta' = -\eta'$ in source less electromagnetic field i.e. $T = 0$ we have

$$r^2(e^{-2\eta})'' + 4r(e^{-2\eta})' + 2e^{-2\eta} - 2 = 0, \tag{1.84}$$

which is a Cauchy-Euler Equation. Solving it we get

$$e^{-2\eta} = \frac{c_1}{r^2} + \frac{c_2}{r} + 1. \tag{1.85}$$

For anisotropic case we get $p_r = -p_t$ which is not physically possible so there is no solution in this case. However, if we take isotopic case, $p_r = p_t$, then other parameters are

$$p = 0,\ \rho = 0,\ E^2 = \frac{2c_1}{r^2}, \tag{1.86}$$

$$\sigma = 0,\ e^{2\zeta} = \frac{c_1}{r^2} + \frac{c_2}{r} + 1. \tag{1.87}$$

So the metric in this case becomes

$$ds^2 = -(\frac{c_1}{r^2} + \frac{c_2}{r} + 1)dt^2 + (\frac{c_1}{r^2} + \frac{c_2}{r} + 1)^{-1}dr^2 + r^2(d\theta^2 + sin\theta^2 d\phi^2), \tag{1.88}$$

Choosing $c_1 = q^2$ and $c_2 = -m$, where q is the charge and m is the mass then it is Reissner-Nordstrom metric. This metric is the most general metric containing mass and charge for the spherically symmetric static metric. Hence, the Reissner-Nordstrom metric is the unique solution of the EMFEs for the non-null and electric field without source with isotropic matter.

If the trace, T, of the stress energy tensor is non-zero i.e. $T \neq 0$ then one needs to be careful in order to find out the relation between null/non-null field with its Segre

type. Here, we are adding matter with non-null electromagnetic field. To find out the Segre type we need to write the stress energy tensor for this case. In [6] the Segre type for the non-null electromagnetic field along with the perfect fluid is discussed. If the fluid velocity vector u and the null principle directions of the electromagnetic field are coplanar then the Segre type is $[1, 1(11)]$ and non-zero components of ϕ_{ij} are $\phi_{00} = \phi_{22}$ and ϕ_{11} and if they are non-coplanar then Segre type is $[1, 111]$. Generally for non-null electromagnetic field with perfect fluid the Segre type is [1,1(11)]. In literature many solutions have been obtained for this Segre type.

It is clear that we can classify the electromagnetic field into two categories, traceless and with trace. When we add matter with electric field then spacetime can be further classified into isotropic and anisotropic. By taking the static spherically symmetric spacetime we have checked all possible solutions of the EMFEs for each case. We find out independently that for isotropic spacetime with non-null traceless electric field, the Reissner-Nordstrom metric is the unique solution of the EMFEs and there is no solution for anisotropic spacetime with non-null traceless electric field. There exists many solutions for the isotropic/anisotropic spacetime with non-null electric field with $T \neq 0$. One can discuss the Segre type of each case.

Chapter 2

A New Solution of the Einstein-Maxwell Field Equations with Linear Equation of State

In literate many solutions of the EMFEs have been obtained which are physically valid solutions [18 – 33]. The spacetime is taken to be static and spherically symmetric. Generally pressure is taken to be isotropic pressure i.e. the pressure is same in all directions but for the charged fluid spheres pressure does not need to be same in all directions. This is called anisotropy.

The Christoffel's symbols for the metric (1.69) are

$$\Gamma^0_{00} = \zeta', \tag{2.1}$$

$$\Gamma^1_{00} = e^{2\zeta-2\eta}\zeta', \tag{2.2}$$

$$\Gamma^1_{11} = \eta', \tag{2.3}$$

$$\Gamma^1_{22} = -re^{-2\eta}, \tag{2.4}$$

$$\Gamma^1_{33} = -r\sin^2\theta e^{-2\eta}, \tag{2.5}$$

$$\Gamma^2_{21} = \frac{1}{r}, \tag{2.6}$$

$$\Gamma^2_{33} = -\cos\theta\sin\theta, \tag{2.7}$$

$$\Gamma^3_{31} = \frac{1}{r}, \tag{2.8}$$

$$\Gamma^3_{32} = \frac{\cos\theta}{\sin\theta}. \tag{2.9}$$

The components of the Ricci tensor, $R_{\gamma\beta}$, are

$$R_{11} = \frac{e^{-2\eta+2\zeta}(2 - r\eta^{'}\zeta^{'} + r(\zeta^{'})^2 + r\zeta^{''})}{r}, \tag{2.10}$$

$$R_{22} = \frac{\eta^{'}(2 + r\zeta^{'}) - r((\zeta^{'})^2 + \zeta^{''})}{r}, \tag{2.11}$$

$$R_{33} = e^{-2\eta}(-1 + e^{2\eta} + r\eta^{'} - r\zeta^{'}), \tag{2.12}$$

$$R_{44} = e^{-2\eta}\sin^2\theta(-1 + e^{2\eta} + r\eta^{'} - r\zeta^{'}). \tag{2.13}$$

The EMFEs for the metric (1.69) with the stress-energy momentum tensor in Eq. (1.78) are

$$\frac{1}{r^2}(1 - e^{-2\eta}) + \frac{2\eta'}{r}e^{-2\eta} = \rho + \frac{E^2}{2}, \tag{2.14}$$

$$-\frac{1}{r^2}(1 - e^{-2\eta}) + \frac{2\zeta'}{r}e^{-2\eta} = p_r - \frac{E^2}{2}, \tag{2.15}$$

$$e^{-2\eta}(\zeta'' + \zeta'^2 + \frac{\zeta'}{r} + \zeta'\eta' - \frac{\eta'}{r}) = p_t + \frac{E^2}{2}, \tag{2.16}$$

$$\sigma = \frac{1}{r^2}e^{-\eta}(r^2E)', \tag{2.17}$$

where σ is the current density.

2.1 Basic Physical Criterion for a Compact Object

The solution of the EMFEs is considered as a model for a compact object if it satisfies the physical criterion. The basic conditions for a physically valid solution are [35–37]:

(I) The solution should be free from the geometric singularities. This means the metric coefficients should be well defined and finite. Also the density, ρ, radial pressure, p_r, transverse pressure, p_t, and electric field, $\mathbf{E}$, should also be well defined and finite for the region, $0 \leq r \leq R$, where R is the radius of the stellar compact object.

(II) The density, ρ, must be positive and monotonically decreasing function of the radius, r. Mathematically, we have

$$\rho(r) \geq 0, \qquad \frac{d\rho}{dr} \leq 0. \tag{2.18}$$

(III) The radial pressure, p_r, should be positive and monotonically deceasing function of the radius, r. i.e.

$$p_r(r) \geq 0, \qquad \frac{dp_r}{dr} \leq 0. \tag{2.19}$$

(IV) The radial pressure, p_r, must be zero at the boundary of the relativistic compact object. We can write it mathematically as

$$p_r(R) = 0. \tag{2.20}$$

There are some stability conditions which solution must satisfy. These are:

(V) For the equilibrium the matter must be stable against the local collapse of region. For this solution must satisfy the local stability condition known as "*Le Chatelier's principle*", which stats that the radial pressure, p_r, must be monotonically increasing function of the density, ρ. Mathematically

$$\frac{dp_r}{d\rho} \geq 0. \tag{2.21}$$

(VI) The radial and transverse pressures must be same at the $r = 0$ i.e. $p_r(r = 0) = p_t(r = 0)$.

(VII) For a stable star the radial sound velocity, $\frac{dp_r}{d\rho}$, should be greater than the transverse sound velocity, $\frac{dp_t}{d\rho}$. We define Θ as

$$\Theta = \frac{dp_r}{d\rho} - \frac{dp_t}{d\rho}, \tag{2.22}$$

then Θ must be positive i.e. $\Theta > 0$ for the stable region.

(VIII) The solution must satisfy the casuality condition that the speed of sound should not be greater than the speed of light, mathematically, we have

$$0 < \frac{dp_r}{d\rho} \leq 1. \tag{2.23}$$

The solution should satisfies the following energy conditions:

(IX) The weak energy condition states that density is non-negative, $\rho \geq 0$, throughout the interior of the compact object.

(X) The strong energy condition states that the density, ρ, should be greater than

the radial pressure, p_r, i.e. $\rho \geq p_r$.

(XI) The trace of the stress-energy tensor $T^{\alpha}_{\alpha} = \rho - p_r - 2p_t > 0$.

The solution must satisfy the following matching conditions:

(XII) For the charged case the solution at the boundary, $r = R$, must match with the Reissner-Nordstrom exterior solution, i.e.

$$g_{00} = -(1 - \frac{2m}{r} + \frac{q^2}{r^2}), \tag{2.24}$$

where m is the mass and q is the charge of the compact object at the boundary. In case of uncharged compact object the solution must match the exterior Schwarzschild solution.

(XIII) The red shift, g_{00}, should be well defined and monotonically decreasing function of the radius. In particular, the red shift at the centre and boundary of the compact object must be finite and positive.

If the solution satisfies all the above conditions then it is called a physically valid solution and it can be considered as a model for the compact object.

As discussed in Chapter 1, one may obtain solutions of the EMFEs by choosing some equation of state. In this chapter we obtain a class of new solutions of the EMFEs by taking linear equation of state, $p_r = f(\rho)$. Also we discuss validity of the solution in detail by examining whether the solution satisfies the physical criteria or not. Later, we discuss the stability of the solution. This solution can be used as the model of a compact object.

2.2 A New Solution for Charged Spherically Symmetric Spacetime

We choose the spacetime metric to be spherically symmetric given by Eq. (1.69) and a linear equation of state given as

$$p_r = \alpha\rho + \beta, \tag{2.25}$$

where $\alpha > 0$ and β is any arbitrary constant. Using Eq. (2.25) in Eqs. (2.14)-(2.17) we have

$$\begin{aligned}
\frac{1}{r^2}(1-e^{-2\eta}) + \frac{2\eta'}{r}e^{-2\eta} &= \rho + \frac{E^2}{2}, &(2.26)\\
\frac{e^{2\eta}r}{2}(\frac{1}{r^2}(1-e^{-2\eta}) + \alpha\rho + \beta - \frac{E^2}{2}) &= \zeta', &(2.27)\\
e^{-2\eta}(\zeta'' + \zeta'^2 + \frac{\zeta'}{r} - \zeta'\eta' - \frac{\eta'}{r}) &= p_t + \frac{E^2}{2}, &(2.28)\\
\sigma &= \frac{1}{r^2}e^{-\eta}(r^2E)'. &(2.29)
\end{aligned}$$

The above system of equations (2.26)-(2.29) has six unknowns while the total equations are 4. To find the solution we need to choose any two unknowns. For simplicity we choose η and the electrical field, $\mathbf{E}$, as

$$\eta = -\frac{1}{2}\ln(\frac{1}{1+ar^2}), \tag{2.30}$$

$$E^2 = \frac{kar^2(5+ar^2)}{(1+ar^2)^3}, \tag{2.31}$$

where $a > 0$ and $k > 0$. For uncharged case we have $k = 0$. Using Eqs. (2.30) and (2.31) in Eqs. (2.26)-(2.29) we have

$$\rho = \frac{a(6+8ar^2-5kr^2+2a^2r^4-akr^4)}{2(1+ar^2)^3}, \tag{2.32}$$

$$\zeta = \frac{1}{8a(1+ar^2)}[(1+\alpha)\{-4k+(2a-k)(1+ar^2)^2-3k(1+ar^2)\ln(1+ar^2)\}$$
$$+(1+ar^2)^3\beta+4a\alpha\ln(1+ar^2)], \tag{2.33}$$

$$\sigma = \frac{ak(15+4ar^2+a^2r^4)}{(1+ar^2)^3\sqrt{ak(5+ar^2)}}, \tag{2.34}$$

$$p_t = \frac{1}{16(1+ar^2)^5}[4\beta(4+r^2\beta)+44a^6r^{10}(1+\alpha+r^2\beta)^2$$
$$-4a^5r^8A+8a^3kr^6B+32a^3r^4C+D], \tag{2.35}$$

where

$$A = kr^2(1+\alpha)(1+\alpha+r^2\beta)-2(3+7\alpha+4\alpha^2+8r^2\beta+7r^2\alpha\beta+3r^4\beta^2), \tag{2.36}$$

$$B = 5kr^2(1+\alpha)^2-2(27+36\alpha+23\alpha^2+18r^2\beta+18r^2\alpha\beta), \tag{2.37}$$

$$C = 5+19\alpha+12\alpha^2+36r^2\beta+22r^2\alpha\beta+10r^4\beta^2, \tag{2.38}$$

$$D = a^2kr^4E+4a^2r^2F+a^4kr^8G+4a^4r^6H+4aI, \tag{2.39}$$

$$E = 25kr^2(1+\alpha)^2-4(48+41\alpha+15\alpha^2+16r^2\beta+16r^2\alpha\beta), \tag{2.40}$$

$$F = 3+32\alpha+9\alpha^2+58r^2\beta+26r^2\alpha\beta+150r^4\beta^2, \tag{2.41}$$

$$G = k^2r^4(1+\alpha)^2-4kr^2(10+17\alpha+9\alpha^2+8r^2\beta+8r^2\alpha\beta), \tag{2.42}$$

$$H = 12+30\alpha+22\alpha^2+48r^2\beta+36r^2\alpha\beta+15r^4\beta^2, \tag{2.43}$$

$$I = 5kr^2(6+r^2\beta+\alpha(4+r^2\beta))-6(\alpha(2+r^2\beta)+r^2\beta(4+r^2\beta)), \tag{2.44}$$

which is the solution of the EMFEs.

2.3 Physical Validity

The conditions for a physically valid solution are discussed in detail in Section 2.1. In this section we discuss either the solution we obtained satisfies these conditions or not.

(I) The obtained solution is well-defined because there is no singularity in the solution as it is clear from Eqs. (2.30)-(2.35) that the metric coefficients, density, electrical field, charged density, radial and transverse pressures are all well defined functions of the radial parameter, r.

(II) As the density must be positive and non-increasing function of the radial parameter, r we set $a > \frac{5k}{8}$ in Eq. (2.32). It is clear that the density, ρ, is positive for the chosen values of the parameters. Taking derivative of Eq. (2.32) with respect to radial parameter, r, we get

$$\frac{d\rho}{dr} = \frac{-ar}{(1+ar^2)^4}(5k + 10a + r^2(12a^2 - 8ak) + r^4(2a^3 - ka^2)). \tag{2.45}$$

Clearly $\frac{d\rho}{dr} < 0$ if we choose the parameters as $a > \frac{2}{3}k$. Hence, the density, ρ, is positive and decreases monotonically if we set values of the parameters k and a as $a > \frac{2}{3}k$. For example if $k = 2$ and $a = 2$ then density and its derivative are

$$\rho = \frac{6 + 6r^2 + 4r^4}{(1+2r^2)^3}, \tag{2.46}$$

$$\frac{d\rho}{dr} = \frac{-4r(15 + 8r^2 + 4r^4)}{(1+2r^2)^4}. \tag{2.47}$$

In Fig.2.1, we plot the density for $a = k = 2$ against the radial parameter, r. From the Fig. 2.1 it is clear that density, ρ, satisfies the physical conditions i.e. it is

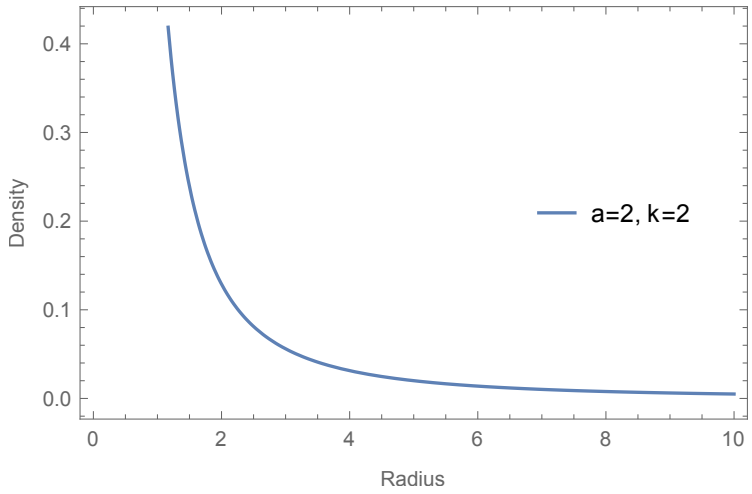

Figure 2.1: The density, ρ, is plotted by setting $a = k = 2$. It is well defined, positive and non-increasing function of radial parameter, r.

positive and is a non-increasing function of radial parameter, r.

If we set a=constant, then we can check the behaviour of the density for k. The plot of the density, ρ, for different values of k against the radial parameter, r, is given in Fig. 2.2. From Fig. 2.2 it is clear that density is positive and well defined for different values of the parameter k. Similarly if we fix k then we can check the behaviour of the density, ρ, for the parameter a. In Fig. 2.3 we set $k = 2$ and plot the density, ρ, for different values of the parameter, a. It is clear from the Fig. 2.3 that the density is well defined, positive and a decreasing function of the radial parameter, r, for different values of the parameter, a.

(III) The radial pressure, $p_r = \alpha\rho + \beta$, is positive as the density, $\rho > 0$, for $a > \frac{2}{3}k$ and also $\alpha > 0$ and $\beta > 0$. To check it is a decreasing function of r or not, we have

$$\frac{dp_r}{dr} = \alpha\frac{d\rho}{dr}, \tag{2.48}$$

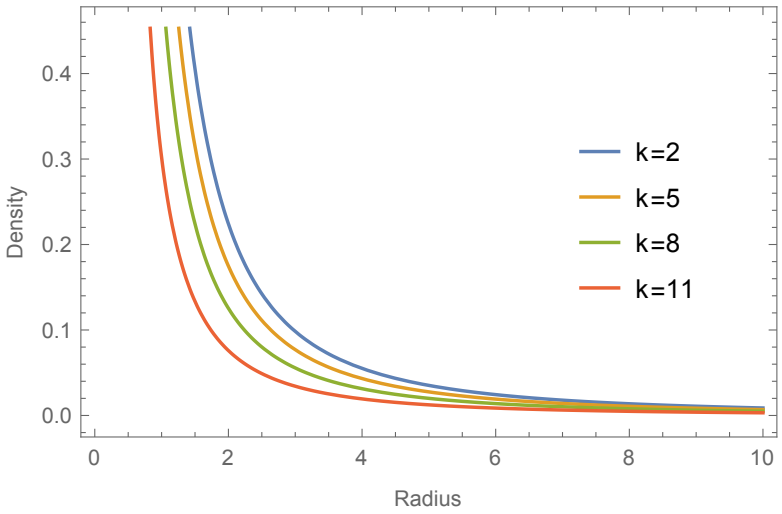

Figure 2.2: The density, ρ, is plotted for $k = 2, 5, 8$, and 11 by taking $a = 8$. It is well defined, positive and non-increasing function of radial parameter, r.

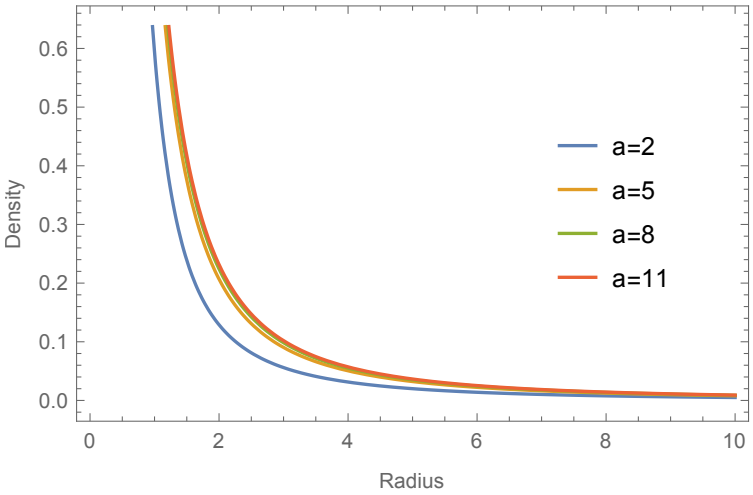

Figure 2.3: The density, ρ, is plotted for $a = 2, 5, 8$, and 11 by taking $k = 2$. It is well defined, positive and non-increasing function of radial parameter, r.

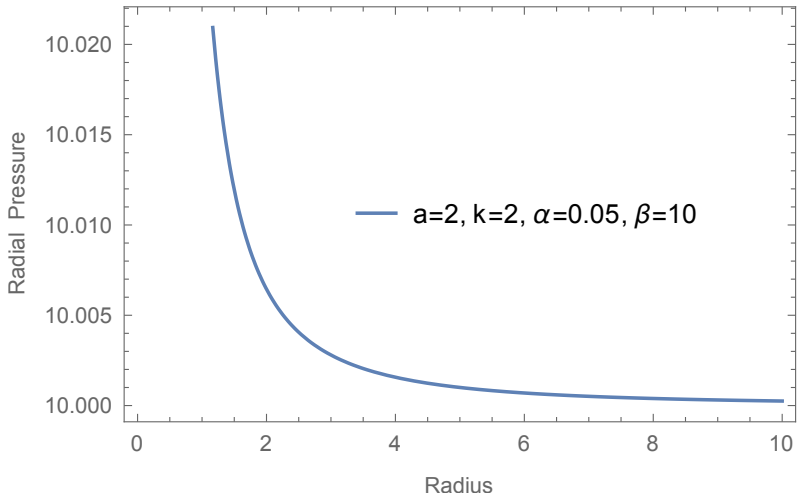

Figure 2.4: The radial pressure, p_r, is plotted against the radial parameter, r, by setting $a = k = 2$, $\alpha = 0.05$ and $\beta = 10$. It is well defined, positive and non-increasing function of r.

and $\frac{d\rho}{dr} < 0$ for $a > \frac{2k}{3}$, this mean we have

$$\frac{dp_r}{dr} = \alpha \frac{d\rho}{dr} < 0. \tag{2.49}$$

Hence the radial pressure, p_r, is a decreasing function of radial parameter, r. Graph of the radial pressure, p_r, for $a = k = 2$, $\alpha = 0.05$ and $\beta = 10$ is given in Fig. 2.4. From Fig. 2.4 it is clear that the radial pressure, p_r, is positive and non-increasing function of r. In Fig. 2.5 the radial pressure is plotted for $k = 2, 5, 8$, and $k = 11$ by fixing $a = 8$. Fig. 2.5 shows that the radial pressure, p_r, is well defined and positive for different values of k, it also shows that the radial pressure is maximum at the center and gradually decreases with the increases of the radial parameter, r. Similarly, in Fig. 2.6 the radial pressure, p_r, is plotted for $a = 2, 5, 8$, and 11 against the radial parameter, r, by setting $k = 2$, $\alpha = 0.05$ and $\beta = 10$. Fig. 2.6 shows that the radial pressure is well defined, positive and non-increasing function of the radial

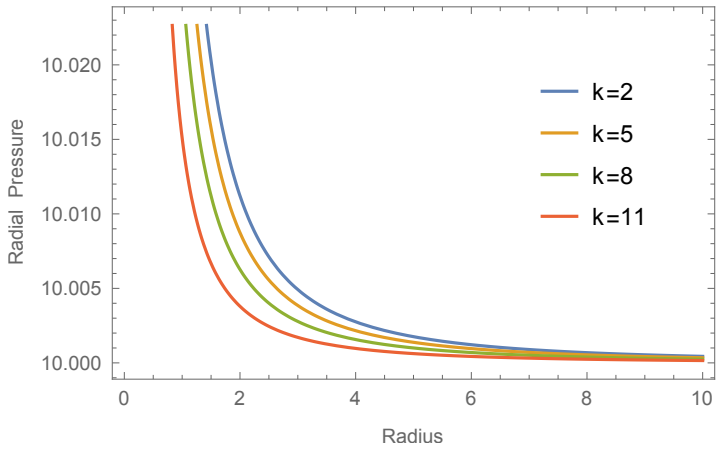

Figure 2.5: The radial pressure, p_r, is plotted for different values of k: $k = 2, 5, 8$, and 11 against the radial parameter, r, by setting $a = 8$, $\alpha = 0.05$ and $\beta = 10$. It is well defined, positive and non-increasing function of r.

parameter for different values of a.

In Fig. 2.7 the radial pressure is plotted for different values of α: $\alpha = 0.05, 0.1, 0.15$, and 2 by fixing $a = 2$, $k = 2$, and $\beta = 10$. The radial pressure is well defined, positive and non-increasing. In Fig. 2.8 the radial pressure is plotted for different values of β: $\beta = 5, 10, 15$, and 20 by fixing $a = 2$, $k = 2$, and $\alpha = 10$. The radial pressure is well defined, positive and non-increasing function of the radial parameter.

To check how transverse pressure, p_t, varies with respect to the parameter a we plotted the transverse pressure, p_t, in Fig. 2.9 for different values of a: $a = 2, 4, 6$, and 8 against the radial parameter, r, by fixing $k = 2$, $\alpha = 1$, and $\beta = 1$. Fig. 2.9 shows that the transverse pressure is positive and well defined.

In Fig. 2.10 the transverse pressure, p_t, is plotted for $k = 2, 4, 6$, and 8 against the radial parameter, r, by fixing $a = 6$, $\alpha = 1$, and $\beta = 1$. Fig. 2.10 shows that the transverse pressure is positive and well defined.

In Fig. 2.11 the transverse pressure, p_t, is plotted for different values of α: $\alpha = 1, 2, 3$,

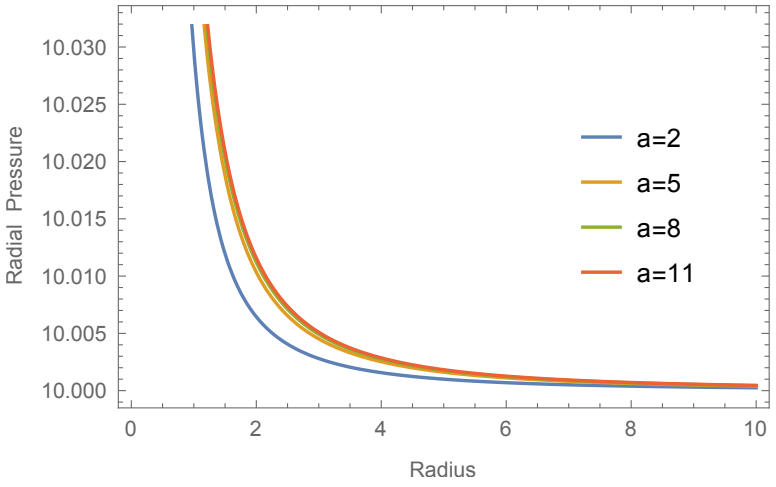

Figure 2.6: The radial pressure, p_r, is plotted for different values of a: $a = 2, 5, 8,$ and 11 against the radial parameter, r, by setting $k = 2$, $\alpha = 0.05$ and $\beta = 10$. It is well defined, positive and non-increasing function of r.

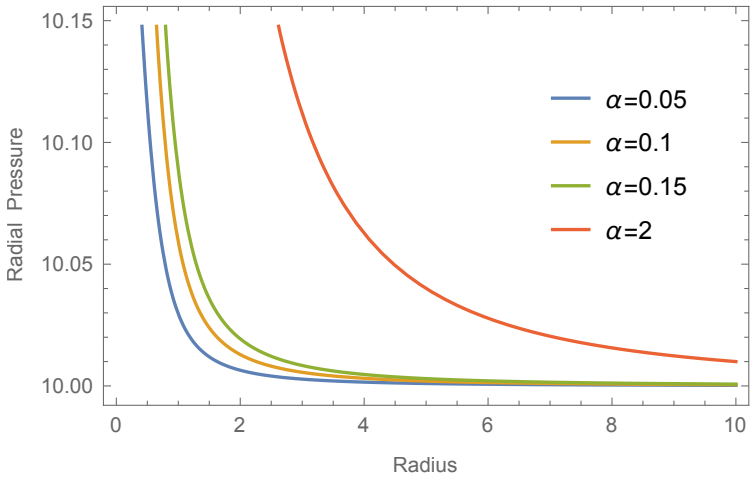

Figure 2.7: The radial pressure, p_r, is plotted for different values of α: $\alpha = 0.05, 0.1, 0.15,$ and 2 against the radial parameter, r, by setting $a = 2$, $k = 2$ and $\beta = 10$. It is well defined, positive and non-increasing function of r.

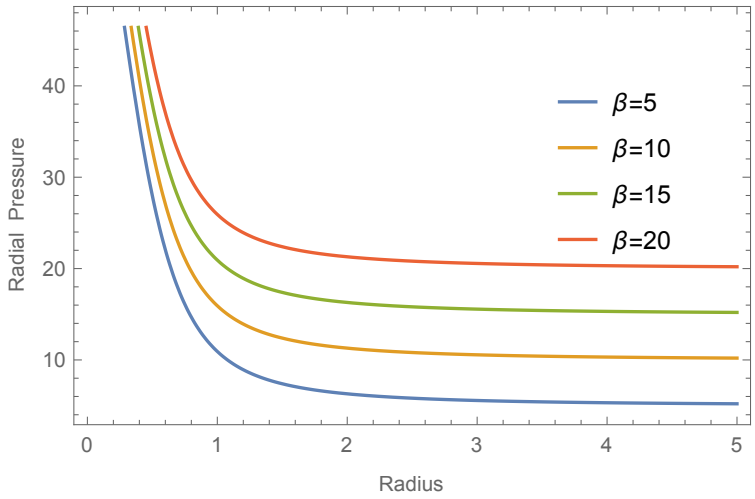

Figure 2.8: The radial pressure, p_r, is plotted for different values of β: $\beta = 5, 10, 15$ and 20 against the radial parameter, r, by setting $a = 2$, $k = 2$ and $\alpha = 10$. It is well defined, positive and non-increasing function of r.

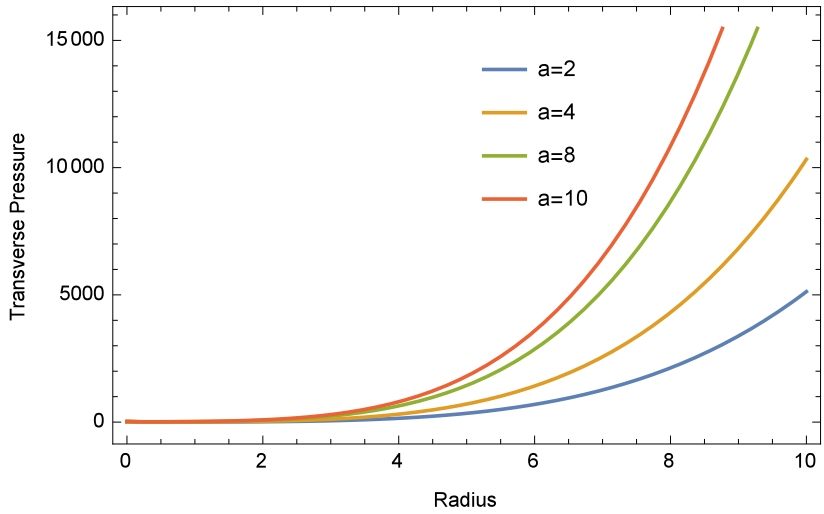

Figure 2.9: The transverse pressure, p_t, is plotted for $a = 2, 4, 6$, and 8 against the radial parameter, r, by fixing $k = 2$, $\alpha = 1$, and $\beta = 1$. It is well defined and positive.

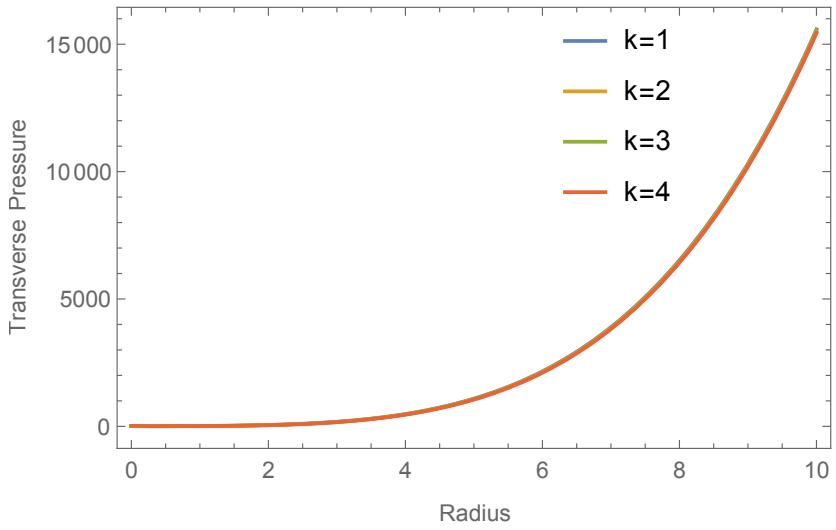

Figure 2.10: The transverse pressure, p_t, is plotted for $k = 2, 4, 6$, and 8 against the radial parameter, r, by setting $a = 6$, $\alpha = 1$, and $\beta = 1$. It is well defined and positive.

and 4 against the radial parameter, r, by fixing $a = 2$, $k = 2$, and $\beta = 1$. Fig. 2.11 shows that the transverse pressure is positive and well defined.

In Fig. 2.12 the transverse pressure, p_t, is plotted for different values of β: $\beta = 1, 2, 3$, and 4 against the radial parameter, r, by fixing $a = 2$, $k = 2$, and $\alpha = 1$. Fig. 2.12 shows that the transverse pressure is positive and well defined.

(IV) To find the value of the radial pressure, p_r, at the boundary, $r = R$, we have

$$p_r(R) = \frac{a\alpha(6 + 8aR^2 - 5kR^2 + 2a^2R^4 - akR^4) + \beta 2(1 + aR^2)^3}{2(1 + aR^2)^3}. \tag{2.50}$$

For physical validity of the solution, one can set values of the parameters α, β, k, and a so that the radial pressure becomes zero at the boundary i.e. $p_r(R) = 0$.

(V) As the density, ρ, is positive i.e. $\rho > 0$ so the weak energy condition is satisfied.

(VI) From Eq. (2.25) we have

$$\frac{dp_r}{d\rho} = \alpha. \tag{2.51}$$

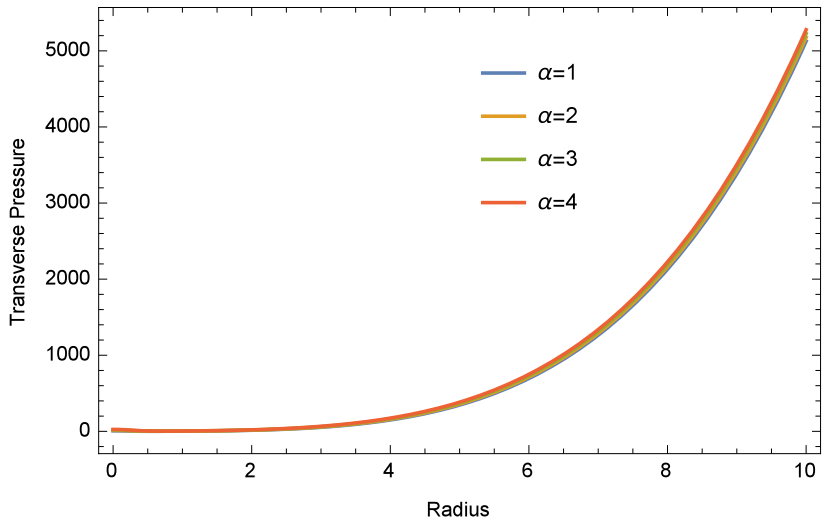

Figure 2.11: The transverse pressure, p_t, is plotted for $\alpha = 1, 2, 3$, and 4 against the radial parameter, r, by fixing $a = 2$, $k = 2$, and $\beta = 1$. It is well defined and positive.

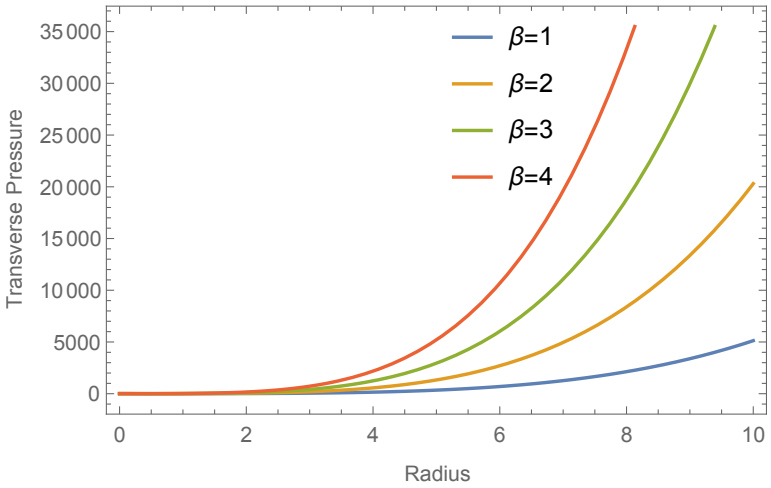

Figure 2.12: The transverse pressure, p_t, is plotted for $\beta = 1, 2, 3$, and 4 against the radial parameter, r, by fixing $a = 2$, $k = 2$, and $\alpha = 1$. It is well defined and positive.

If we set $0 < \alpha < 1$ then the causality condition $0 < \frac{dp_r}{d\rho} < 1$ is satisfied.

(VII) From Eq. (2.30), the red shift at the origin $r = 0$ is

$$e^{-2\eta}(0) = 1, \tag{2.52}$$

and the red shift on the boundary, $r = R$, is

$$e^{-2\eta}(R) = \frac{1}{1 + aR^2}. \tag{2.53}$$

as $a > 0$, so the red shift at the centre and at the boundary is positive and finite.

(VIII) As from Eqs. (2.25) and (2.35) we have

$$p_r(0) = p_t(0) = 3\alpha a + \beta, \tag{2.54}$$

so at the origin the radial and transverse pressures are same.

(IX) As we take the spacetime to be charged spherically symmetric so solution should match with the Reissner-Nordstrom exterior solution at the boundary, $r = R$. For Reissner-Nordstrom solution we have

$$g_{00} = -(1 - \frac{2m}{R} + \frac{q^2}{R^2}), \tag{2.55}$$

$$E(R) = \frac{q}{R^2}, \tag{2.56}$$

where m is the mass and q is the charge of the spactime.

By matching the solution obtained and the Reissner-Nordstrom exterior solution at

the boundary, $r = R$, we get

$$\frac{1}{1+aR^2} = 1 - \frac{2m}{R} + \frac{q^2}{R^2}, \tag{2.57}$$

$$\frac{q^2}{R^6} = \frac{ak(5+aR^2)}{(1+aR^2)^3}. \tag{2.58}$$

Using Eq. (2.57) and $a > \frac{2k}{3}$, we have

$$\frac{m}{R} < \frac{aR^2(2+5a^2R^4+19aR^2)}{4(1+aR^2)}, \tag{2.59}$$

which gives an upper bound on the mass-radius, $\frac{m}{r}$, ratio.

Also using Eq. (2.58) and $a > \frac{2k}{3}$ we get the bound on the charge-radius ratio as

$$\frac{q^2}{R^2} < \frac{3a^2R^4(5+aR^2)}{2(1+aR^2)^3}. \tag{2.60}$$

2.4 Stability Analysis

The behaviour of the radial sound velocity, $V_r^2 = \frac{dp_r}{d\rho}$, and transverse sound velocity, $V_t^2 = \frac{dp_t}{d\rho}$, determine the stability of a star. The stability region is the region where $V_r^2 > V_t^2$ i.e. the transverse sound velocity is less than the radial sound velocity. From Eq.(2.25) we have

$$V_r^2 = \alpha, \tag{2.61}$$

and from Eqs. (2.32) and (2.35) we have

$$V_t^2 = \frac{J}{4\beta^2 + 8a^7r^{12}\beta(1+\alpha+r^2\beta)+K}, \tag{2.62}$$

where

$$
\begin{aligned}
J &= -8a(1+ar^2)^2(5k+2a^3r^4+a(10-8kr^2)+a^2(12r^2-kr^4)), && (2.63)\\
K &= -4a^6r^8L-8aN-4a^5r^6P+a^4r^4(Q1+Q2)\\
&\quad -2a^3r^2(S1+S2)+a^2(T1+T2), && (2.64)\\
L &= 1+3\alpha^2-12r^2\beta+r^4(k-13\beta)\beta+\alpha(4-12r^2\beta+kr^4\beta), && (2.65)\\
N &= -\beta(2+3\alpha+4r^2\beta)+5k(3+r^2\beta+\alpha(2+r^2\beta)), && (2.66)\\
P &= 12\alpha^2+\alpha(4-34r^2\beta)-4r^2\beta(8+9r^2\beta)\\
&\quad +kr^2(-5-4\alpha^2+6r^2\beta+\alpha(-7+6r^2\beta)), && (2.67)\\
Q1 &= -5k^2r^4(1+\alpha)^2+4(6-6\alpha^2+48r^2\beta+55r^4\beta^2+8\alpha(-3+7r^2\beta)), && (2.68)\\
Q2 &= -8kr^2(-7-5\alpha^2+11r^2\beta+\alpha(-2+11r^2\beta)), && (2.69)\\
S1 &= 5k^2r^4(1+\alpha)^2+2kr^2(-63+24\alpha^2+40r^2\beta+5\alpha(-3+8r^2\beta)), && (2.70)\\
S2 &= -4(4+6\alpha^2+21r^2\beta+25r^4\beta^2+\alpha(-26+27r^2\beta)), && (2.71)\\
T1 &= 75k^2r^4(1+\alpha)^2+4(3+9\alpha^2+20r^2\beta+27r^4\beta^2+28\alpha(-1+r^2\beta)), && (2.72)\\
T2 &= -4kr^2(-24+30\alpha^2+33r^2\beta+\alpha(2+33r^2\beta)). && (2.73)
\end{aligned}
$$

If we define $\Theta = V_r^2 - V_t^2$ then

$$\Theta = \alpha - \frac{J}{4\beta^2+8a^7r^{12}\beta(1+\alpha+r^2\beta)+K}. \tag{2.74}$$

Here, we can choose the parameters such that $\Theta > 0$, for example taking $\alpha = 0.05, a = k = 2$ and $\beta = 10$ we have

$$\Theta = \frac{494+2630r^2+5678r^4+9890r^6+18826r^8+23846r^{10}+16909r^{12}+5120r^{14}}{274+9080r^2+52121r^4+167071r^6+366278r^8+476928r^{10}+338176r^{12}+102400r^{14}}. \tag{2.75}$$

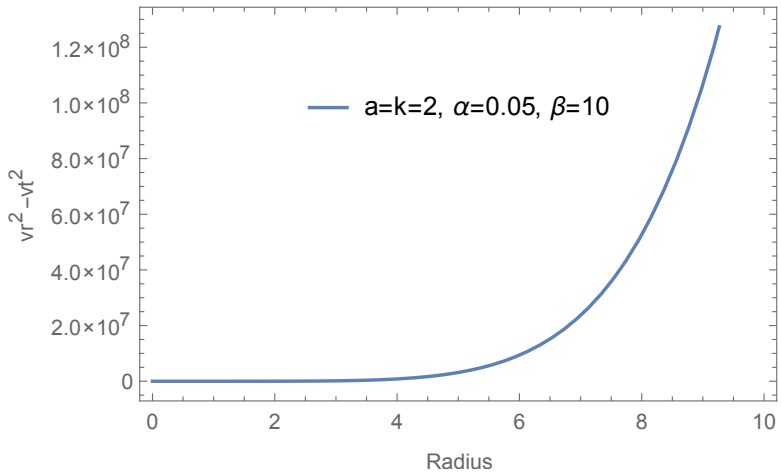

Figure 2.13: The stability parameter, $\Theta = V_r^2 - V_t^2$, is plotted for $a = k = 2, \alpha = 0.05$ and $\beta = 10$ against the radial parameter, r. It is well defined and positive function of r.

Clearly the expression of Θ shows that it is positive so the solution is stable. The graph of Θ is shown in Fig. 2.13. To check how stability is varied by the different values of parameters we plotted the stability parameter, Θ, for different values of the parameters. In Fig. 2.14 the stability parameter is plotted for a: a: $a = 2, 4, 6,$ and 8 against the radial parameter, r, by fixing $k = 2$, $\alpha = 1$, and $\beta = 1$. Fig. 2.14 shows that the stability parameter, Θ, is positive so the solution is stable.

In Fig. 2.15 the stability parameter, Θ, is plotted for $k = 2, 4, 6,$ and 8 against the radial parameter, r, by fixing $a = 6$, $\alpha = 1$, and $\beta = 1$. Fig. 2.15 shows that the stability parameter is positive and well defined.

In Fig. 2.16 the stability parameter, Θ, is plotted for different values of α: $\alpha = 1, 2, 3,$ and 4 against the radial parameter, r, by fixing $a = 2$, $k = 2$, and $\beta = 1$. Fig. 2.16 shows that the stability parameter is positive and well defined.

In Fig. 2.17 the stability parameter, Θ, is plotted for different values of β: $\beta = 1, 2, 3,$

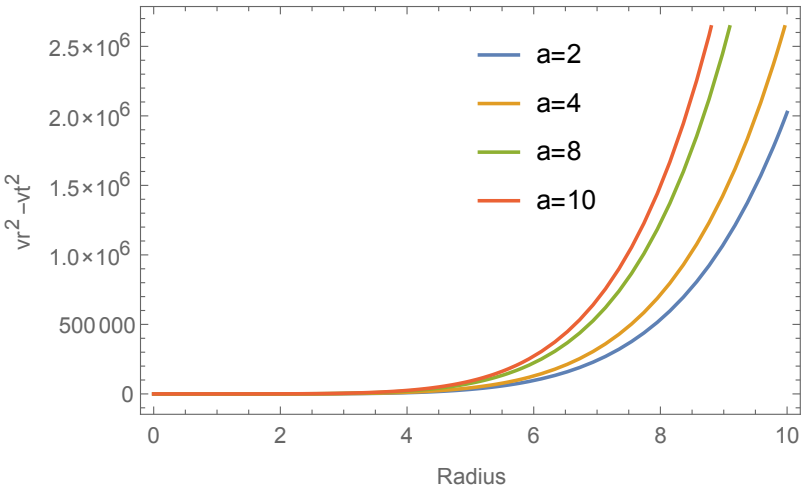

Figure 2.14: The stability parameter, $\Theta = V_r^2 - V_t^2$, is plotted for a: a: $a = 2, 4, 6,$ and 8 against the radial parameter, r, by fixing $k = 2$, $\alpha = 1$, and $\beta = 1$. It is well defined and positive.

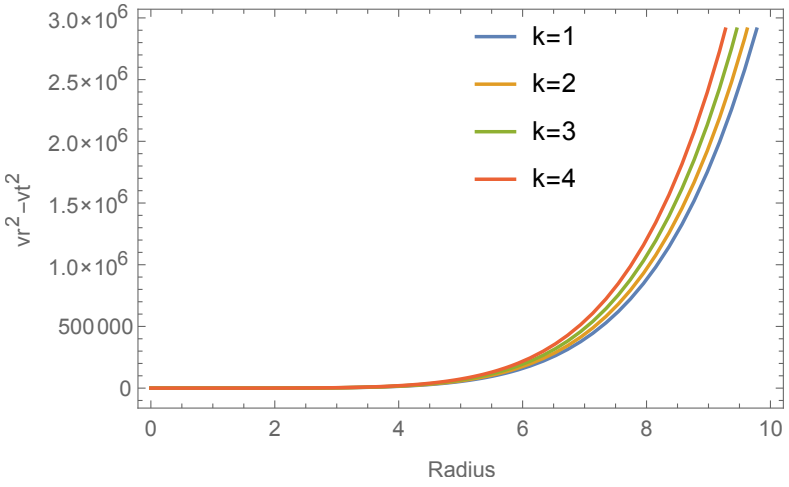

Figure 2.15: The stability parameter, $\Theta = V_r^2 - V_t^2$, is plotted for $k = 2, 4, 6,$ and 8 against the radial parameter, r, by fixing $a = 6$, $\alpha = 1$, and $\beta = 1$. It is well defined and positive.

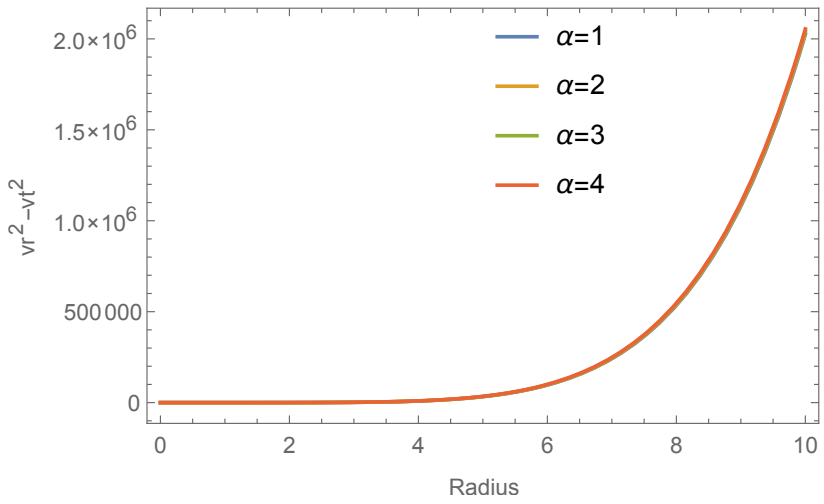

Figure 2.16: The stability parameter, $\Theta = V_r^2 - V_t^2$, is plotted for $\alpha = 1, 2, 3$, and 4 against the radial parameter, r, by fixing $a = 2$, $k = 2$, and $\beta = 1$. It is well defined and positive.

and 4 against the radial parameter, r, by fixing $a = 2$, $k = 2$, and $\alpha = 1$. Fig. 2.17 shows that the stability parameter is positive and well defined.

Hence, we can find stable region by choosing appropriate values of the parameters a, k, α, and β. There is a wide range of parameters for which the solution is stable. Hence, the solution satisfies the all physical criteria and stability conditions. So this solution may be considered as a model for a compact object having linear equation of state.

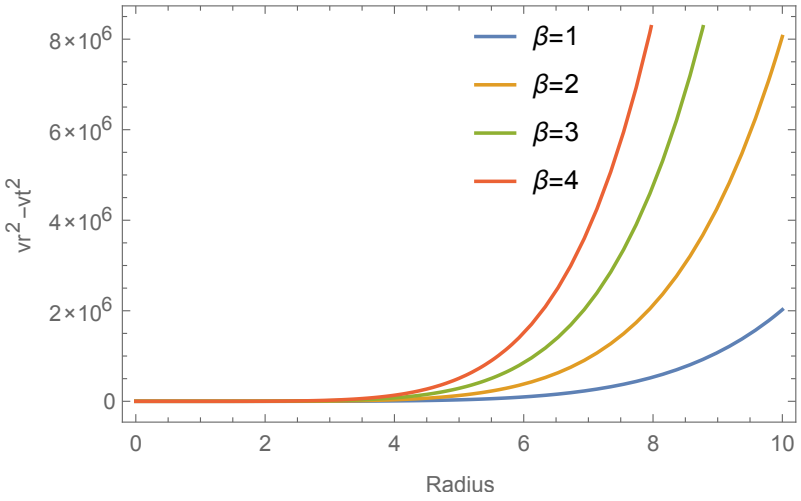

Figure 2.17: The stability parameter, $\Theta = V_r^2 - V_t^2$, is plotted for $\beta = 1, 2, 3$, and 4 against the radial parameter, r, by fixing $a = 2$, $k = 2$, and $\alpha = 1$. It is well defined and positive.

Chapter 3

A Model for the Dark Energy Star

The study of dark energy stars is of interest these days due to the fact that universe is expanding with acceleration which was suggested by High-z supernova Search Team in 1998 by observing type 1a supernova [13]. The acceleration of the universe can be explained by dark energy present in the universe which is about 26 percent of the total mass energy of the universe. Dark energy possess strong negative pressure which helps in explaining the acceleration of the expanding universe. In literature, a number of well behaved exact solutions of the EMFEs are obtained to model strange quark stars, neutron stars and pulsars for example in [22, 23]. The expansion of the universe raises interest to study of the dark energy objects. The dark energy has some unusual properties like it violates energy conditions. The dark energy parameter is define as

$$w = \frac{p_r}{\rho} < \frac{-1}{3}, \tag{3.1}$$

where p_r is the radial pressure and ρ is the density. If $w < \frac{-1}{3}$ then dark energy violates the strong energy condition and if $w < -1$ then the dark energy violates null or weak energy condition. For accelerating expansion the dark energy parameter

satisfies the following condition

$$w < \frac{-1}{3}. \tag{3.2}$$

For the Einstein cosmological constant we have $w = -1$. Current observations show that for accelerating unverse the value of the dark energy parameter is $-1.38 < w < -0.82$. As the dark energy plays fundamental role in Cosmology so it is desirable to find astrological models for it.

In Relativity, Astrophysics, Particle Physics, and many other fields, the concept of a black hole is well established and it is accepted in all these fields. Sometimes we encounter scepticism regarding the physical reality of the solutions of the EMFEs and the theory of black holes fail to interpret some observational data, especially, at its event horizon [39]. For example, the Schwarzschild black hole has one dynamical singularity at the origin, $r = 0$, and one corrdinate singularity at the event horizon, $r = 2m$, . This motivated many people to find out the alternative of a black hole which avoids the possibility of the singularities and the event horizons.

Recently Mazur and Mottola [40] gave an interesting alternative to black hole called "*Gravastar*", which means "*gravitational vacuum star*". They took static spherically symmetric spacetime with isotropic pressure. They obtained a static solution of the EFEs. They took quantum considerations by replacing the critical surface by a thin shell of relativistic fluid of soft quanta which obeys $\rho = p$. Such a solution does not have any singularity and does not posses horizon which makes it very significant because it can be considered as alternative to black holes when gravitational collapse is occurred. The existence of the solution requires that near $r = R_s$, the gravity must undergoes a vacuum rearrangement phase transition, where R_s is the Schwarzschild

radius. At Planck's level where $\hbar \neq 0$, the energy, $E = \hbar\omega\frac{1}{(1-\frac{2m}{r})}$, of the infrared photon is divergent at the event horizon. Also the Hawking temperature, $T_H = \frac{\hbar}{8\pi k_B m}$, shows that the black hole is unstable to thermodynamic fluctuations.

Mazur and Mottola took the interior of the compact object as the de-Sitter space and there is a thin shell of stiff matter around, which is surrounded by the Schwarzschild vacuum. They assumed the isotropic matter i.e. the radial and the transverse pressures are equal. The line element is given as [40]

$$ds^2 = -g(r)dt^2 + \frac{dr^2}{f(r)} + r^2(d\theta^2 + \sin^2\theta d\phi^2). \tag{3.3}$$

The equation of state for three regions of the gravastar are:

I. $\rho = -p$ for interior region $0 \leq r \leq r_1$,

II. $\rho = p$ for thin shell region $r_1 \leq r \leq r_2$,

III. $\rho = p = 0$ for exterior region $r_2 < r$.

The Einstein field equations are

$$\frac{1}{r^2}\frac{d}{dr}(r(1-f)) = 8\pi G\rho, \tag{3.4}$$

$$\frac{f}{rf}\frac{df}{dr} + \frac{1}{r^2}(f-1) = 8\pi G p. \tag{3.5}$$

Solving these equations for the interior region we have

$$g(r) = Cf(r) = C(1 - H_0^2 r^2), \quad 0 \leq r \leq r_1, \tag{3.6}$$

where H_0 and C are arbitrary constants of integration. This de-Sitter spacetime is free from the singularity at the origin. On the scale of the Schwarzschild radius the

quantum fluctuations dominate the time and radial components of the stress-energy tensor, they both grow so large that the equation of state becomes $\rho = p$. For the thin shell Mazur et al. considered a dimensionless variable, $w = 8\pi G r^2 p$, so the EFEs become

$$\frac{dr}{r} = \frac{dh}{1-w-f}, \tag{3.7}$$

$$\frac{dh}{f} = -\frac{1-w-f}{1+3-3f}\frac{dw}{w}. \tag{3.8}$$

The Eq. (3.7) gives

$$f = 1 - \frac{\mu}{r}, \tag{3.9}$$

where $d\mu = w dr$. Mazur et al. numerically obtained the solution of Eq. (3.8) for the limit $0 < f \ll 1$ because the shell is very thin. They obtained that $r_1 \simeq H_0^{-1} \simeq r_2 2Gm$ and the functions g and f of order $0 < \varepsilon \ll 1$ and constant approximately. This means there is no event horizon as g and f are not zero for $r_1 < r < r_2$. The thickness of the shell is $\ell \sim \varepsilon^{\frac{3}{2}} R_s$, which is very small then the Schwarzschild radius, R_s.

The third region is the exterior Schwarzschild spacetime i.e.

$$g(r) = f(r) = 1 - \frac{2m}{r}. \tag{3.10}$$

The energy of the shell is $E \sim \varepsilon^2 m$, which is very small this means that all the mass of the object comes from the energy density of the interior, while the thin shell is responsible for all its entropy. The solution obtained by Mazur et al. is stable and compact with no singularities. So we can say that at the end of a gravitational col-

lapse we get gravastar if the quantum gravitational vacuum phase transition occurs before the event horizon can form.

Lobo [42] in 2006 found a model for the dark energy star with equation of state $p_r = w\rho$, taking the metric and the stress-energy tensor as

$$ds^2 = -e^{\int_r^\infty h(r)dr}dt^2 + \frac{dr^2}{1-\frac{2m(r)}{r}} + r^2(d\theta^2 + \sin\theta d\phi^2), \tag{3.11}$$

$$T_{\mu\nu} = (\rho + p_t)\mathbf{V}_\mu\mathbf{V}_\nu + p_t g_{\mu\nu} + (p_r - p_t)X_\mu X_\nu, \tag{3.12}$$

where $\mathbf{V}$ is the four vector velocity and $\mathbf{X}$ is a spacelike vector in radial direction. Using the EFEs he found the solution and discussed the stability. He showed that for $w < \frac{-1}{3}$, the solution at the boundary matches with the Schwarzschild solution. To avoid the event horizon he imposed a condition on the boundary, $r = R > 2m$ i.e. the boundary should be greater than that Schwarzschild radius. In Phantom region, $w \leq -1$, the null energy condition is violated which means that the energy density becomes less than the negative radial pressure, p_r. This censorious negative radial pressure changes the topology of the spacetime. This may result in opening a tunnel which makes the dark energy star into a wormhole [43, 44].

Yazadjiev [45] found a model for the compact object having ordinary matter and dark energy. He expressed the dark energy with scalar field which has negative kinetic energy and is known as the Phantom scalars. The negative kinetic energies may lead to some quantum instabilities but there are claims that these instabilities can be avoided [46]. If we consider the Phantom scalar as an effecting field theory resulting from some fundamental theory with positive energy then we can avoid the instabilities [46, 47]. In the presence of the dark energy the EFEs taken by

Yazadjiev [45] are

$$R_{\alpha\beta} = 8\pi(T_{\alpha\beta} - \frac{1}{2}Tg_{\alpha\beta}) - 2\partial_\alpha\varphi\partial_\beta\varphi, \tag{3.13}$$

$$\nabla_\alpha\nabla^\alpha\varphi = 4\pi\rho_D, \tag{3.14}$$

where ρ_D is the density of the dark energy. The dark energy charges are the sources for the dark energy. The interaction between the dark energy and the matter is not known so the interaction is taken to be zero in the field equations. The metric is given as

$$ds^2 = -e^{2V}dt^2 + e^{-2V+2U}(e^{-2\chi})dr^2 + r^2(d\theta^2 + \sin\theta^2 d\phi^2), \tag{3.15}$$

where $V = V(r)$ and $U = U(r)$. The solution of the EFEs is obtained as

$$e^{2V} = e^{2U\cosh\beta}, \tag{3.16}$$

$$\rho = e^{2V-2U}(\rho_E\cosh\beta + 3(\cosh\beta - 1)p_E), \tag{3.17}$$

$$p = e^{2V-2U}p_E, \tag{3.18}$$

$$\rho_D = e^{2V-2U}(\rho_E + 3p_E)\sinh\beta, \tag{3.19}$$

$$\varphi = \sinh(\beta U). \tag{3.20}$$

Some exact interior and exterior solutions are also discussed by Yazadjiev which in some cases lead to wormhole solutions.

In this chapter we extend the work of Yazadjiev by adding charge to find an exact solution of the EFEs along with the Maxwell field equations i.e. we find a model for a dark energy object with charge. We check the physical validity and stability of our solution. We assume the equation of state to be $p_r = -\rho$. This approach is different

from other previous attempts to find the models for dark energy object. Our model of the dark energy star consists solely of dark energy (i.e. with no ordinary hadronic matter admixed in). Also we have not assumed the de-Sitter spacetime in the interior of the dark energy star as chosen in [40] nor we assume some thin boundary around the star. We will discuss the EMFEs for the negative radial pressure by taking the equation of state as $p_r = -\rho$ and we obtain a class of solutions and discuss its validity.

3.1 Field Equations for Charged Dark Energy Star

The metric for charged static spherically symmetric spacetimes is given in (1.69). We assume the parameter of the dark energy, $w = -1$, then equation of state becomes

$$p_r = -\rho. \tag{3.21}$$

Here, radial pressure is negative which corresponds to the dark energy. Using Eq. (3.21) in the EMFEs (2.14) and (2.15), we have

$$\zeta = -\eta. \tag{3.22}$$

Using Eq. (3.22) in the EMFEs (2.14)-(2.17), we get

$$\frac{1}{r^2}(r(1-e^{-2\eta})' = \rho + \frac{E^2}{2}, \tag{3.23}$$

$$e^{-2\eta}(-\eta'' - \frac{2\eta'}{r}) = p_t + \frac{E^2}{2}, \tag{3.24}$$

$$\sigma = \frac{1}{r^2}e^{-\eta}(r^2E)'. \tag{3.25}$$

Using the transformation $Z = e^{-2\eta}$ in Eqs. (3.23)-(3.25), we finally have following set of three equations with five unknowns Z, ρ, E, p_t, and σ.

$$1 - Z - rZ' = r^2(\rho + \frac{E^2}{2}), \tag{3.26}$$

$$r^2Z'' + 2rZ' = 2r^2(p_t + \frac{E^2}{2}), \tag{3.27}$$

$$\sigma = \frac{1}{r^2}e^{-\eta}(r^2E)'. \tag{3.28}$$

3.2 A New Class of Solutions

In order to obtain solution of the system of Eqs. (3.26)-(3.28), we assume the electric field, **E**, and the gravitational potential, Z, as

$$E = \sqrt{kar^2\frac{5 + ar^2}{(1 + ar^2)^3}}, \tag{3.29}$$

$$Z = (1 + ar^2)^{-1}. \tag{3.30}$$

Using Eqs. (3.29) and (3.30) in Eqs. (3.26)-(3.28), the remaining unknowns are obtained as

$$\rho = \frac{a(6 + 8ar^2 - 5kr^2 + 2a^2r^4 - akr^4)}{2(1 + ar^2)^3}\ , \tag{3.31}$$

$$p_t = \frac{-a(6 + 5kr^2 + ar^2(-2 + kr^2))}{2(1 + ar^2)^3}, \tag{3.32}$$

$$\sigma = \frac{\sqrt{ak}(15 + 4ar^2 + a^2r^4)}{(1 + ar^2)^3\sqrt{5 + ar^2}}, \tag{3.33}$$

and the metric (1.69) takes the form

$$ds^2 = -(1 + ar^2)^{-1}dt^2 + (1 + ar^2)dr^2 + r^2(d\theta^2 + \sin^2\theta d\phi^2). \tag{3.34}$$

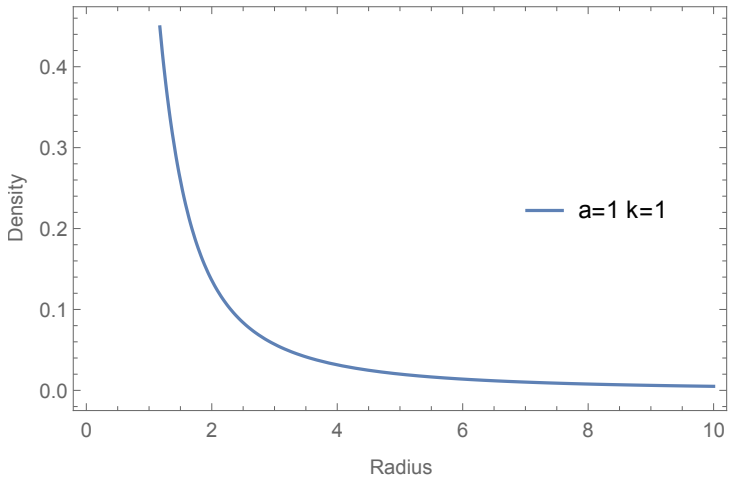

Figure 3.1: The density, ρ, is plotted for $a = k = 1$ against the radial parameter, r. It is well defined, positive and a non-increasing function of radial parameter, r.

3.3 Physical Validity

The solution obtained is physically acceptable as it satisfies the following conditions:

(I) There is no physical or geometrical singularities as Z, E, ρ, p_r, p_t, and σ for $a > \frac{2}{3}k$ are well defined.

(II) Density, ρ, is well defined for all r and its value at the origin is $\rho(0) = 3a$, where $a > 0$. From Eq. (3.31) it is clear that density is positive for all r if $8a - 5k > 0$ and $2a^2 - ak > 0$ which give $a > \frac{5k}{8}$.

Taking derivative of Eq. (3.31) we have

$$\frac{d\rho}{dr} = \frac{-ar(5k + 10a + r^2(12a^2 - 8ak) + r^4(2a^3 - ka^2)}{(1 + ar^2)^4}. \tag{3.35}$$

We can set suitable values of parameters a and k so that $d\rho/dr < 0$, i.e. ρ becomes monotonically decreasing with respect to r. If we set $12a^2 - 8ak > 0$ and $2a^3 - ka^2 > 0$ then we have $a > \frac{2}{3}k$. For this the density becomes monotonically decreasing. But

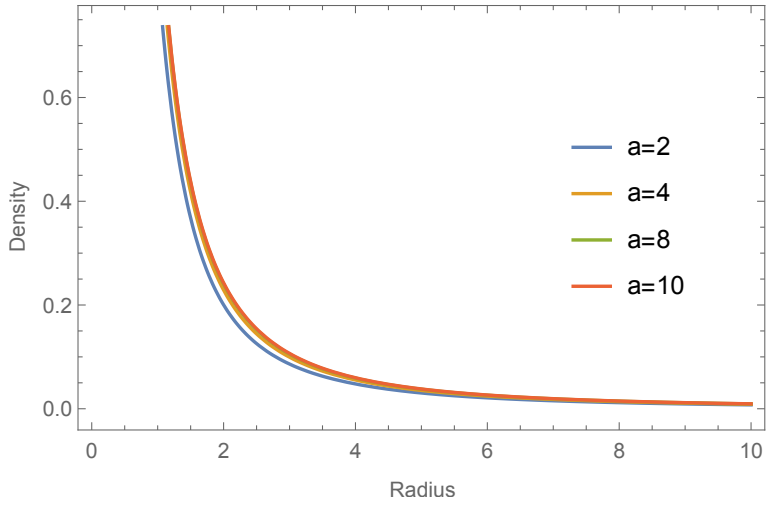

Figure 3.2: The density, ρ, is plotted for $k = 1$ and $a = 2, 4, 8$, and 10 against the radial parameter, r. It is well defined, positive and a non-increasing function of radial parameter, r.

it is positive definite if $a > \frac{5k}{8}$, so we can say that the density is positive definite and monotonically decreasing if $a > \frac{2k}{3}$. For example if we choose $a = 1$ and $k = 1$ we get $\rho > 0$ and $d\rho/dr < 0$ which is also shown in Fig. 3.1.

We can check the behaviour of the density with respect to the parameter a by taking the parameter k constant. For this we fix $k = 1$ and then plot the density for different values of the parameter a. In Fig. 3.2 the density, ρ, is plotted for $a = 2, 4, 8$, and 10 by fixing the parameter $k = 1$. It is clear from the Fig. 3.2 that density is well defined and a non-increasing function of the radial parameter for different values of the parameter a.

Similarly we can check the behaviour of the density with respect to the parameter k. In Fig. 3.3 we fix the parameter $a = 6$ and plot the density for $k = 2, 4, 6$, and 8. From the Fig. 3.3 it is clear that the density is well defined and it is maximum at the centre and gradually decreases with the increase in the radial parameter.

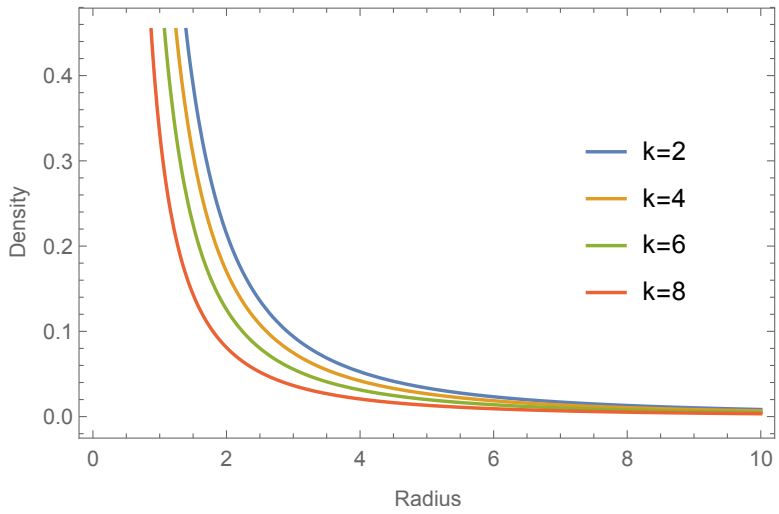

Figure 3.3: The density, ρ, is plotted for $a = 6$ and $k = 2, 4, 6$, and 8 against the radial parameter, r. It is well defined, positive and a non-increasing function of radial parameter, r.

(III) From Eq. (3.21) it is clear that radial pressure is not positive i.e. it is negative and also not a decreasing function of the radial parameter. To require that the radial pressure is zero at the boundary, $r = R$, we have

$$6 + 8aR^2 - 5kR^2 + 2a^2R^4 - akR^4 = 0. \tag{3.36}$$

The radial pressure, p_r, depends on the radial parameter, r, the parameters a and k. To check how radial pressure changes with respect to the parameter a we need to plot it for different values of a by taking the parameter k constant. In Fig. 3.4 the radial pressure, p_r, is plotted for $a = 2, 4, 6$, and 8 with $k = 1$. From the Fig. 3.4 it is clear that the radial pressure is well defined and negative as we required for the dark energy object.

To check behaviour of the radial pressure, p_r, with respect to the parameter k we plot the radial pressure, p_r, in Fig. 3.5 for different values of k i.e. for $k = 2, 4, 6$,

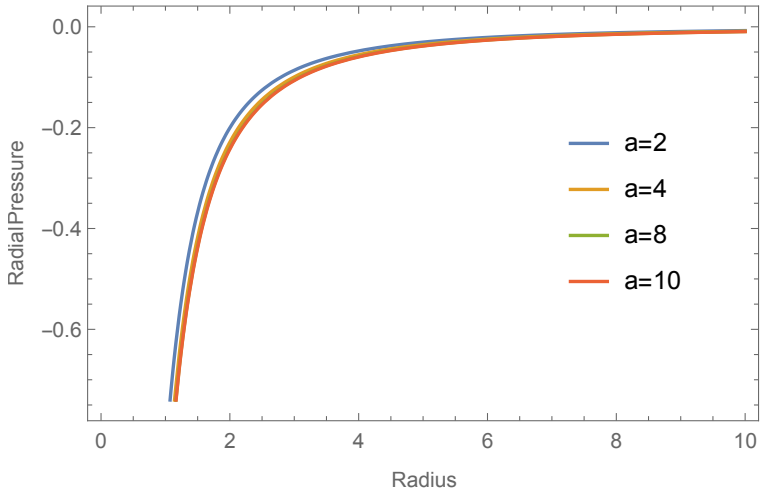

Figure 3.4: The radial pressure, p_r, is plotted for $k = 1$ and $a = 2, 4, 6$, and 8 against the radial parameter, r. It is well defined and negative.

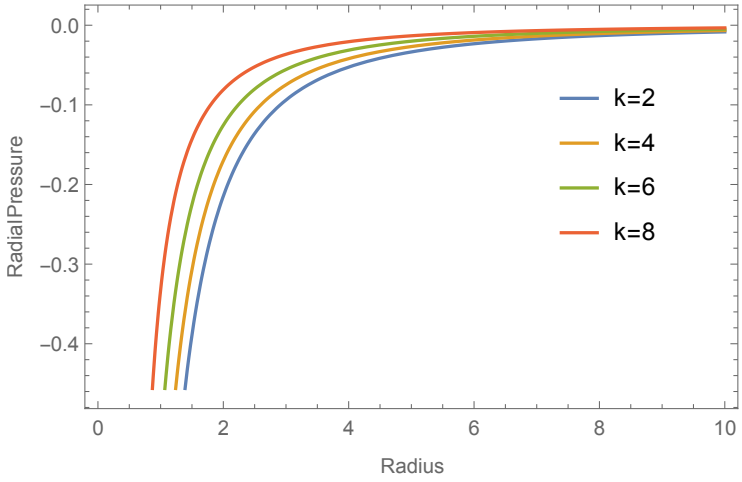

Figure 3.5: The radial pressure, p_r, is plotted for $a = 6$ and $k = 2, 4, 6$, and 8 against the radial parameter, r. It is well defined and negative.

and 8.

(IV) As $\rho > 0$ for all r so solution satisfies the weak energy condition.

(V) From Eq. (3.21) $dp_r/d\rho = -1$, so the causality condition is not satisfied. It is also discussed in [48] in detail.

(VI) The red shift at the origin, $Z(0)$, and on the boundary, $Z(R)$, are finite and positive. From Eq.(3.30), we get $Z(0) = 1 > 0$ and $Z(R) = \frac{1}{1+aR^2} > 0$, $(a > 0)$, where $r = R$ is the boundary.

(VII) From Eq.(3.29) it is clear that the electrical field is well defined within the star.

(VIII) Radial and transverse pressures are same at the origin. Eq. (3.21) with Eq. (3.32) gives $p_r(0) = p_t(0) = -3a$.

In Fig. 3.6 the transverse pressure, p_t, is plotted for $a = 2, 4, 8$, and 10 by fixing $k = 1$. Fig. 3.6 shows that the transverse pressure is well defined for the parameter a. In Fig. 3.7 the transverse pressure, p_t, is plotted for $k = 2, 4, 6$, and 8 by fixing $a = 6$. Fig. 3.7 shows that the transverse pressure is well defined for the parameter k.

(IX) The mass of the dark energy star is

$$M = 4\pi \int_0^R t^2 \rho(t) dt. \tag{3.37}$$

Using Eq. (3.31) in Eq. (3.37) we get

$$M = \frac{2\pi a R^3 \left(2aR^2 - kR^2 + 2\right)}{\left(aR^2 + 1\right)^2}. \tag{3.38}$$

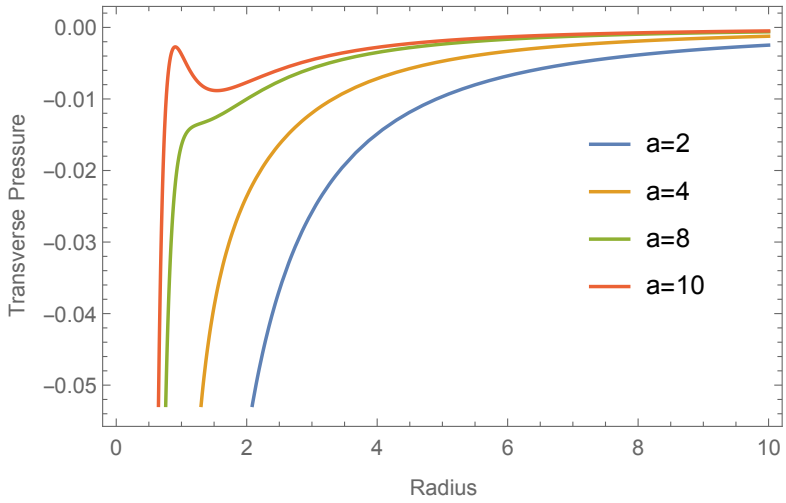

Figure 3.6: The transverse pressure, p_t, is plotted for $k = 1$ and $a = 2, 4, 8$, and 10 against the radial parameter, r. It is well defined for all values of r.

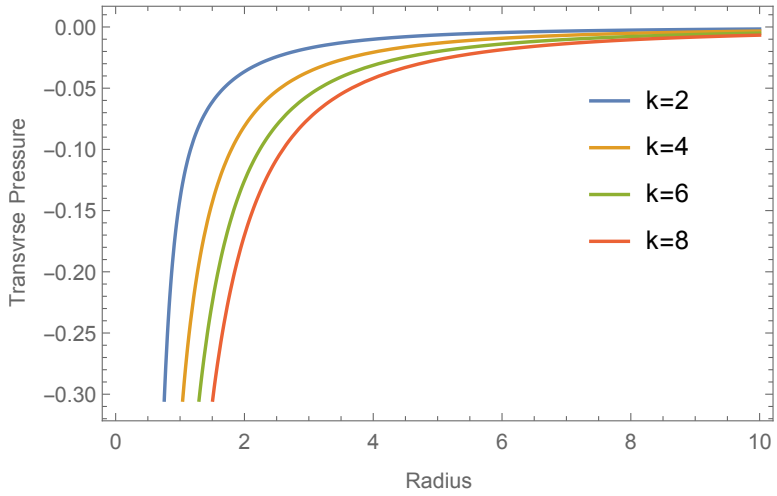

Figure 3.7: The graph of the transverse pressure, p_t, is plotted against the radial parameter, r, for $k = 2, 4, 6$, and 8 and by fixing $a = 6$. It is well defined for all values of r.

The requirement that the solution matches with the Riessner-Nordstrom exterior solution at the boundary, with $g_{00} = -(1 - \frac{2m}{R} + \frac{q^2}{R^2})$ and $E(R) = \frac{q}{R^2}$, gives

$$\frac{1}{1+aR^2} = 1 - \frac{2m}{R} + \frac{q^2}{R^2}, \tag{3.39}$$

$$\frac{q^2}{R^6} = \frac{ak(5+aR^2)}{(1+aR^2)^3}. \tag{3.40}$$

Using Eq. (3.40) and $a > \frac{2k}{3}$, we have

$$\frac{m}{R} < \frac{aR^2(2+5a^2R^4+19aR^2)}{4(1+aR^2)}, \tag{3.41}$$

which gives bound on the mass-radius ratio.

Also using Eq. (3.40) and $a > \frac{2k}{3}$ we get the bound on the charge-radius ratio as

$$\frac{q^2}{R^2} < \frac{3a^2R^4(5+aR^2)}{2(1+aR^2)^3}. \tag{3.42}$$

As we choose the same metric as in Chapter 2 so we get same mass-radius and charge-radius ratios.

3.4 Stability Analysis

As from Section 3 of this chapter the dark energy objects with linear equation of state, $p_r = -\rho$ do not satisfy the causality condition; however, we can check the stability region for the dark energy object. As discussed in Chapter 2, we can check the stability with the help of the stability parameter, $\Theta = V_r^2 - V_t^2$. From Eq.(3.21)

the radial velocity of sound, V_r^2, is given as

$$V_r^2 = -1. \tag{3.43}$$

From Eq. (3.32) the transverse velocity of sound , V_t^2, is given as

$$V_t^2 = \frac{a^2r^2\left(kr^2-4\right)+4a\left(2kr^2+5\right)-5k}{-2a^3r^4+a^2r^2\left(kr^2-12\right)+2a\left(4kr^2-5\right)-5k}. \tag{3.44}$$

Using Eqs. (3.43) and (3.44) we get the value of the stability parameter, Θ, as

$$\Theta = -\frac{2(a-k)\left(a^2r^4+8ar^2-5\right)}{2a^3r^4+a^2\left(12r^2-kr^4\right)+a\left(10-8kr^2\right)+5k}. \tag{3.45}$$

For the stability Θ should be positive i.e. $\Theta > 0$. As the stability parameter, Θ, depends on the parameters a, k and the radial parameter, r. We can choose appropriate values of parameters a, and k so that the stability parameter is positive, for example, if we choose the parameter $a = 2$, and $k = 1$ then the stability parameter, Θ, becomes

$$\Theta = -\frac{1.6\left(0.81r^4+7.2r^2-5\right)}{1.458r^4+0.9\left(10-0.8r^2\right)+0.81\left(12r^2-0.1r^4\right)+0.5}. \tag{3.46}$$

To check that Θ in Eq. (3.46) is positive or not, we plot the stability parameter against the radial parameter in Fig. (3.8). From Fig. (3.8) it is clear that the stability parameter is positive for some region, which means that the dark energy star is stable for this region.

Further work is needed to investigate stability of the dark energy objects. To check how the parameters a and k effect stability of the dark energy object the stability

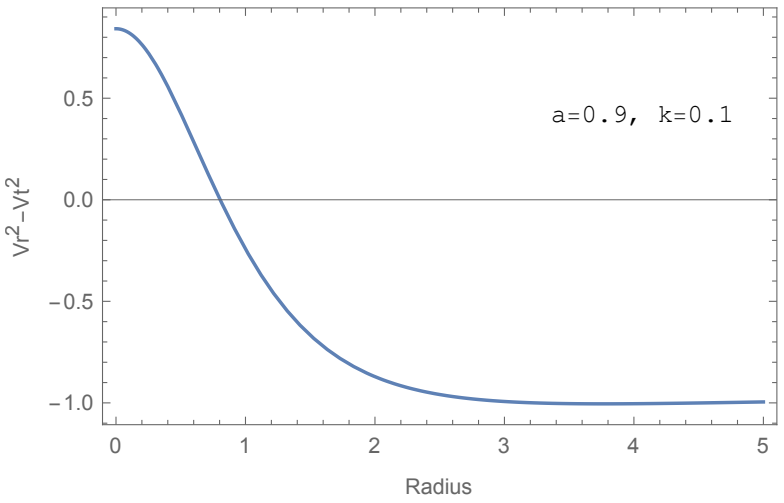

Figure 3.8: The stability parameter, Θ, is plotted for $a = 2$, $k = 1$ against the radial parameter, r. It is well defined and positive for some region.

parameter for different values of a but taking k constant and vice versa is plotted.

In Fig. 3.9 Θ is plotted against the radial parameter, r, for different values of a: $a = 0.2, 0.25, 0.3$, and 0.35 by taking $k = 0.1$. From Fig. 3.9 it is clear that the stability parameter is stable for some region. We can choose such values of the parameter a for which this stable region is large.

In Fig. 3.10 the stability parameter is plotted for different values of k: $k = 0.1, 0.25, 0.5$, and 0.6 by taking $a = 0.9$. From Fig. 3.10 it is clear that the stability parameter is stable for some region. We can choose such values of the parameter k for which this stable region is large.

Hence, the solution obtained can be considered as a model for the dark energy object as it satisfies the physical criterion and is stable.

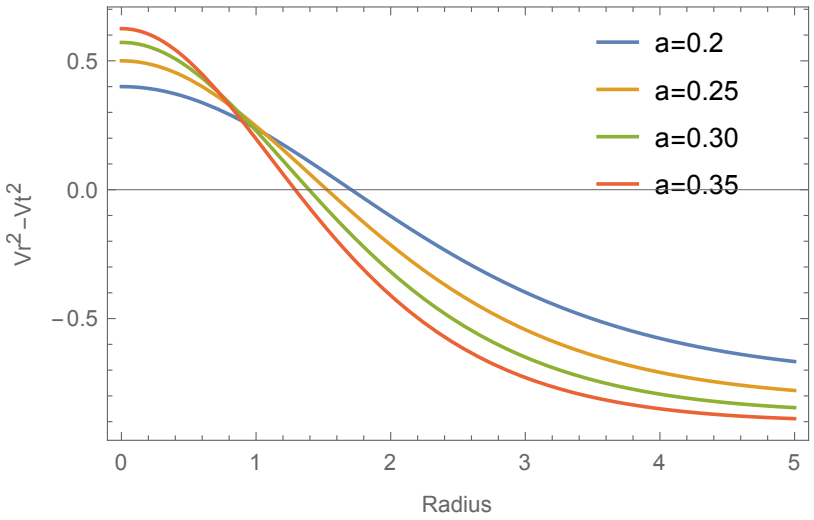

Figure 3.9: The stability parameter, Θ, is plotted for a: $a = 0.2, 0.25, 0.3$, and 0.35 against the radial parameter, r, by taking $k = 0.1$. It is well defined and positive for some region.

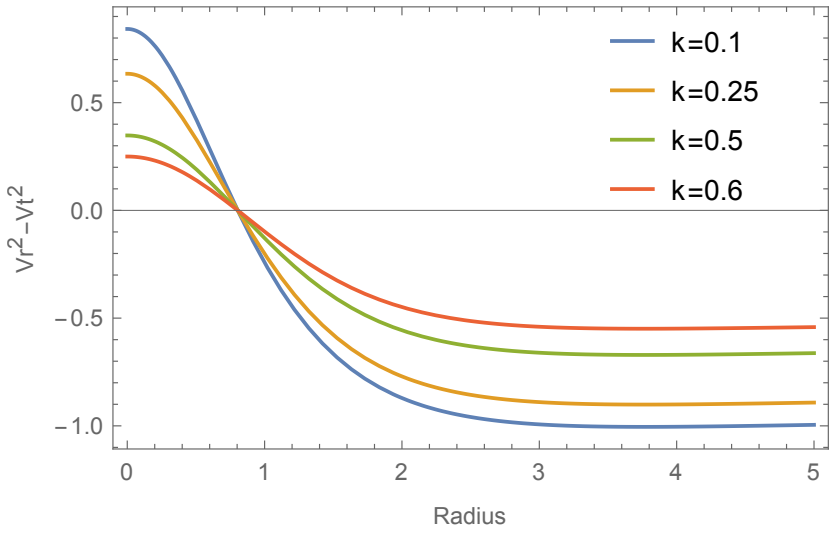

Figure 3.10: The stability parameter, Θ, is plotted for k: $k = 0.1, 0.25, 0.5$, and 0.6 against the radial parameter, r, by taking $a = 0.9$. It is well defined and positive for some region.

Chapter 4

Initial Data for Cauchy Evolutions for the Einstein-Maxwell Field Equations

4.1 Initial Data

Due to nonlinearly of the EMFEs it is difficult to find the analytical solutions. In many areas like perturbed black holes, cosmological models, and neutron stars we need to find numerical solutions of the EMFEs. There are many methods to find solutions in Numerical Relativity but among them the Cauchy method is widely used. However, in all these methods the gravitational field is applied on some hypersurfaces with some initial data and the evolution of this data on the neighbouring hypersurfaces [49]. In this chapter we discuss the initial data needed for the cauchy evolution of the EMFEs. However, in this section we discuss the cauchy evolution equations for the EFEs. The initial data can not be specified freely because of the nonlinearity of the EFEs.

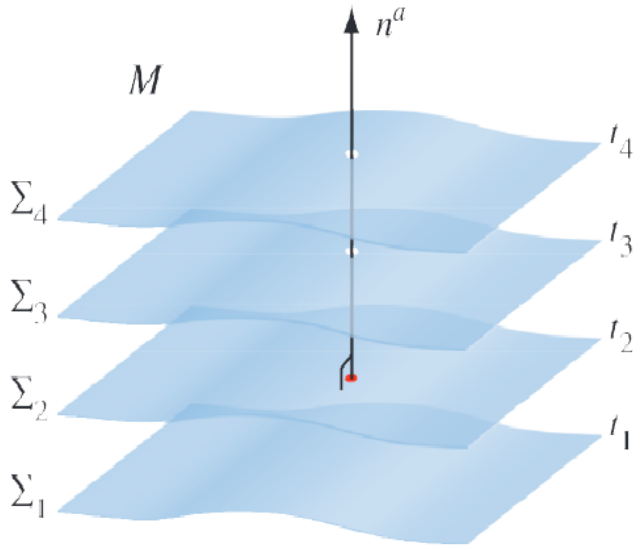

Figure 4.1: The foliation of the spacetime into hypersurfaces at constant times, t. The unit normal of the hypersurfaces is n^α [51].

By considering the EFEs as Cauchy problem we get ten equations in which four are the constraints, also called initial value equations and the rest six are the dynamic or evolution equations. In Cauchy problem the spacetime of the EFEs is foliated by a 3-dimensional hypersurface called slices and this is a spacelike set. If the initial value equations are satisfied on some hypersurface (at t = 0) then the Bianchi identities ensure that the evolution equations preserve these constraints on the spacelike neighbouring hypersurfaces. This is called (3+1) decomposition of the spacetime. The the 4-dimensional curvature quantities can be expressed into3-dimensional curvature quantities in any spacetime such that these give the evolution and constraints equations for the Cauchy-Einstein field equations. The hypersurfaces are also called the level surfaces of time, t, as t is constant for each hypersurface as shown in Fig.

4.1. The metric of the spacetime is $g_{\alpha\beta}$. The unit normal, n^{α}, is defined as

$$n^{\alpha} = -\epsilon\omega^{\alpha}, \tag{4.1}$$

where ω_{α} is the co-vector defined as

$$\omega_{\alpha} = \nabla_{\alpha} t. \tag{4.2}$$

The lapse function, ϵ, measures how the time has elapsed between the neighbouring hypersurfaces along the normal vector, ω^{α}. The lapse function, ϵ, is positive which makes the normal vector, ω^{α}, to be timelike and hence, the hypersurfaces become spacelike. The normalized normal vector, n^{α}, can be considered as the 4-vector velocity of the observer whose worldlines are normal to the hypersurfaces. The metric, $g_{\gamma\beta}$, induces a 3-dimensional hypersurface, η_{ij}, where

$$\eta_{\gamma\beta} = g_{\gamma\beta} + n_{\gamma} n_{\beta}, \tag{4.3}$$

The metric, $\eta_{\gamma\beta}$, is spatial because it is within the hypersurfaces so there is no component along the normal vector, n^{α}, i.e.

$$n^{\gamma}\eta_{\gamma\beta} = 0. \tag{4.4}$$

The Riemannian curvature tensor, $\overline{R}^{\alpha}_{\beta\nu\mu}$, for the metric, $\eta_{\gamma\beta}$, is defined as

$$\nabla_{\alpha}\nabla_{\beta} v^{\rho} - \nabla_{\beta}\nabla_{\alpha} v^{\rho} = \overline{R}^{\rho}_{a\alpha\beta} v^{a}, \tag{4.5}$$

where ∇_β is the covariant derivative.

The Riemannian curvature tensor, $\overline{R}^{\alpha}_{\beta\nu\mu}$, measures the intrinsic curvature of the metric, $\eta_{\gamma\beta}$, but it does not give any idea about how the hypersurfaces are embedded in the 4-dimensional geometry. For this we define the extrinsic curvature, $K_{\alpha\beta}$, which is infact the 2nd fundamental form of the spacetime. In fact the extrinsic curvature, $K_{\alpha\beta}$, measures how the hypersurfaces deform along n^α i.e. it gives the rate of deformation. The extrinsic curvature, $K_{\alpha\beta}$, for the metric, $\eta_{\gamma\beta}$, is given as

$$K_{\alpha\beta} = -\frac{1}{2}\text{Ł}_n \eta_{\alpha\beta}, \tag{4.6}$$

where Ł_n is the Lie derivative in the direction of n^μ.

4.2 Constraint Equations

The Gauss-Codazzi-Mainardi equations are

$$\begin{aligned} \overline{R}_{\gamma\beta\mu\nu} + K_{\gamma\mu}K_{\beta\nu} - K_{\gamma\nu}K_{\mu\beta} &= \eta^a_\gamma \eta^b_\beta \eta^c_\mu \eta^d_\nu R_{abcd}, & (4.7)\\ \nabla_\gamma K_{\beta\mu} - \nabla_\beta K_{\gamma\mu} &= \eta^a_\gamma \eta^b_\beta \eta^c_\mu n^d R_{abcd}, & (4.8) \end{aligned}$$

where $a, b, c, d = 0, 1, 2, 3$ and R_{abcd} is the Ricci tensor for $g_{\gamma\beta}$. Using Eqs. (4.7) and (4.8) in the EFEs we get the constraint equations as

$$\begin{aligned} \overline{R} + K^2 - K_{\gamma\beta}K^{\gamma\beta} &= 16\pi\rho, & (4.9)\\ \nabla_\beta (K^{\gamma\beta} - \eta^{\gamma\beta}K) &= 8\pi J^\beta, & (4.10) \end{aligned}$$

where $\overline{R}$ is the Ricci scalar for $\eta_{\gamma\beta}$, K is the mean curvature defined as

$$K = \eta^{\gamma\beta} K_{\gamma\beta}, \tag{4.11}$$

$\rho = n_\gamma n_\beta T^{\gamma\beta}$ is the total energy density and $J^\gamma = -\eta^{\gamma\beta} n^\mu T_{\beta\mu}$ is the matter momentum density. The Eq. (4.9) is known as the scalar constraint or Hamiltonian constraint while Eq. (4.10) is called the vector constraint or the momentum constraint. These four constraint equations are the required conditions which the extrinsic curvature, $K_{\gamma\beta}$, and the metric, $\eta_{\gamma\beta}$ must satisfy.

Now we choose the line element of the spacetime as [49]

$$ds^2 = \epsilon^2 dt^2 + \eta_{ij}(dx^i + \varepsilon^i dt)(dx^j + \varepsilon^j dt), \tag{4.12}$$

where ϵ is lapse function, η_{ij} is the induced metric for 3-dimensional hypersurface and ε^i is the shift vector. This is the $(3+1)$ decomposition of the 4-dimensional spacetime. The shift vector, ε^i, measures shifting of the spatial coordinates within a time slice. The constraint equarions (4.9) and (4.10) for the 3-dimensional metric, η_{ij}, can be wriiten as

$$\overline{R} + K^2 - K_{ij}K^{ij} = 16\pi\rho, \tag{4.13}$$

$$\nabla_j (K^{ij} - \eta^{ij} K) = 8\pi J^j, \tag{4.14}$$

where $\overline{R}$ is the Ricci scalar, K_{ij} is the extrinsic curvature, and K is the mean curvature for the metric, η_{ij}. These four constraint equations are the required conditions which the extrinsic curvature, K_{ij}, and 3-dimensional hypersurface, η_{ij}, must sat-

isfy but these equations do not specify which components are free and which are constrained. To find this we need a method which decomposes the constrains equations [49, 50, 52, 53]. To specify the Cauchy evolution of the EFEs the minimal set of initial data is η_{ij} and K_{ij}.

4.3 York Lichnerowicz Conformal Decompositions

The York Lichnerowicz conformal decompositions are widely used to decompose the constraints. These decompositions decompose the metric, η_{ij}, and the extrinsic curvature, K_{ij}. The metric, η_{ij}, is decomposed into an auxiliary 3-metric, $\tilde{\eta}_{ij}$, along with a conformal factor ψ [49]

$$\eta_{ij} = \psi^4 \tilde{\eta}_{ij}. \tag{4.15}$$

The auxiliary 3-metric, $\tilde{\eta}_{ij}$ is also referred as the background 3-metric or the conformal metric. The relationship between $\overline{R}$ and $\tilde{R}$ is given as

$$\overline{R} = \tilde{R}\psi^{-4} - 8\psi^{-5}\tilde{\nabla}^2\psi, \tag{4.16}$$

where $\tilde{R}$ is the Ricci scalar for the metric, $\tilde{\eta}_{ij}$. We can rewrite the extrinsic curvature, $K_{\alpha\beta}$ in trace and trace free parts, given in [49], as

$$K_{ij} = A_{ij} + \frac{1}{3}\eta_{ij}K, \tag{4.17}$$

where A_{ij} is the trace free part of the extrinsic curvature. In the conformal quantities we have

$$K_{ij} = \frac{K}{3}\tilde{\eta}_{ij} + \psi^{-2}\tilde{A}_{ij}, \tag{4.18}$$

where $\tilde{A}_{ij}$ is the trace free part of the extrinsic curvature in the conformal metric, $\tilde{\eta}_{ij}$.

Using Eq. (4.16) in Eq. (4.9) we get the scalar constraint equation (Hamiltonian equation) for the conformal metric (auxiliary 3-metric), $\tilde{\eta}_{ij}$, as

$$\tilde{\nabla}^2\psi - \frac{1}{8}\psi\tilde{R} - \frac{1}{8}\psi^5 K^2 + \frac{1}{8}\psi^5 K_{ij}K^{ij} = -2\pi\psi^5\rho, \tag{4.19}$$

where $\tilde{\nabla}^2 = \tilde{\nabla}.\tilde{\nabla}$ is the scalar Laplace operator, and $\tilde{\nabla}_i$ is the covariant derivative in the metric $\tilde{\eta}_{ij}$.

Using Eq. (4.18) in Eq. (4.10) we get the vector constraint (momentum constraint) as

$$\tilde{\nabla}_i\tilde{A}^{ij} - \frac{2\psi^6\tilde{\eta}^{ij}}{3}\tilde{\nabla}_i K = 8\pi\psi^{10}J^i. \tag{4.20}$$

These constraint equations are nonlinear in ψ and are difficult to solve, however, if we choose vacuum initial data such that ρ and J^i are zero then we can solve these numerically.

In 1957 Lindquist and Wheeler [54] obtained an inhomogeneous black hole model. They considered a 3-sphere. The hyper-spherical coordinates of a 3-sphere of radius a are given as

$$\begin{aligned} x^0 &= a\cos\varphi, \\ x^1 &= a\sin\varphi\cos\theta, \\ x^2 &= a\sin\varphi\sin\theta\cos\phi, \\ x^3 &= a\sin\varphi\sin\theta\sin\phi. \end{aligned} \tag{4.21}$$

The metric for the 3-sphere is given as

$$d\tilde{s}^2 = d\varphi^2 + a^2 \sin^2 \varphi d\theta^2 + a^2 \sin^2 \varphi \sin^2 \theta d\phi^2. \tag{4.22}$$

The Ricci scalar, $\tilde{R}$, for the metric (4.22) is constant and we have

$$\tilde{R} = 6. \tag{4.23}$$

T. Clifton in [55] took the auxiliary 3-metric as the spherically symmetric metric so the line element is given as

$$ds^2 = \psi^4(d\rho^2 + \rho^2 d\theta^2 + \rho^2 \sin^2 \theta d\phi^2), \tag{4.24}$$

which gives $\tilde{R} = 0$ and $K_{ij} = 0$ so the constraint equation (4.19) becomes

$$\tilde{\nabla}\psi = 0. \tag{4.25}$$

Solving the above equation gives

$$\psi = 1 + \frac{m}{2\rho}. \tag{4.26}$$

Hence, the line element (4.24) becomes

$$ds^2 = (1 + \frac{m}{2\rho})^4(d\rho^2 + \rho^2 d\theta^2 + \rho^2 \sin^2 \theta d\phi^2). \tag{4.27}$$

There is a singularity at $\rho = 0$. If we use the following transformation

$$\rho = \frac{m \tan \frac{\varphi}{2}}{2}, \tag{4.28}$$

in the metric (4.27), we have

$$ds^2 = (\frac{\sqrt{m}}{2\sin\frac{\varphi}{2}} + \frac{\sqrt{m}}{2\cos\frac{\varphi}{2}})^4(d\varphi^2 + \sin^2\varphi(d\theta^2 + \sin^2\theta d\phi^2)), \tag{4.29}$$

The first term in the conformal factor is divergent at $\varphi = 0$ and the second term is divergent at $\varphi = \pi$. However, both terms satisfy the Helmholtz equation (4.25) so the general solution is

$$\psi = \Sigma_{j=1}^{N} \frac{\sqrt{\bar{m}_j}}{2f_j(\varphi, \theta, \phi)}, \tag{4.30}$$

where $\bar{m}_j$ is the mass parameter of the jth mass, N is the total number of the masses, and $f_j(\varphi, \theta, \phi)$ are the source functions given as

$$f_j = \sin(arccos(h_j)), \tag{4.31}$$

where h_j are defined as

$$h_j = x_j^0 \cos\varphi + x_j^1 \sin\varphi + x_j^2 \sin\varphi\cos\phi + x_j^3 \sin\varphi\sin\theta\sin\phi, \tag{4.32}$$

which is divergent at $(x_j^0, x_j^1, x_j^2, x_j^3)$. These divergent points correspond to the locations of point like masses in the initial data. There are cosmological models corresponding to different masses i.e. $N = 5, 8, 16, 24, 120$, or $N = 600$ for an identically regular polyhedra 3-sphere with a Schwarzschild mass at the center.

4.4 5-Mass Cosmological Models

The 5-mass cosmological model consists of 5 tetrahedra. The position of masses are at the center of the tetrahedra. In the cartesian coordinates the positions of masses

in a 5-mass model are given as [55]:

1. $(1, 0, 0, 0)$,

2. $(-\frac{1}{4}, \frac{\sqrt{15}}{4}, 0, 0)$,

3. $(-\frac{1}{4}, -\frac{\sqrt{5}}{\sqrt{48}}, \frac{\sqrt{5}}{\sqrt{6}}, 0)$,

4. $(-\frac{1}{4}, -\frac{\sqrt{5}}{\sqrt{48}}, -\frac{\sqrt{5}}{\sqrt{24}}, \frac{\sqrt{5}}{\sqrt{8}})$,

5. $(-\frac{1}{4}, -\frac{\sqrt{5}}{\sqrt{48}}, -\frac{\sqrt{5}}{\sqrt{24}}, -\frac{\sqrt{5}}{\sqrt{8}})$.

Using these one can obtain the functions, f_j [55]. In Fig. 4.2 the hypersurfaces are shown for different masses [55]. We can visualized the geometry by taking a slice trough it. In Fig. 4.2 a slice of 5-model mass is shown at $\varphi_0 = \cos^{-1}(\frac{-1}{4})$. This slice passes through the 4 masses only. The metric for this geometry is given as

$$dl^2 = \frac{15}{16}\psi^4(\varphi_0, \theta, \phi)d\Omega^2. \tag{4.33}$$

4.5 8-Mass Cosmological Models

In the 8-mass cosmological model the cells are cubes. For the 8-mass cosmological model the positions of masses are found with the help of dual lattice [55] and are given as

1. $(1, 0, 0, 0)$,

2. $(-1, 0, 0, 0)$,

3. $(0, 1, 0, 0)$,

4. $(0, -1, 0, 0)$,

5. $(0, 0, 1, 0)$,

6. $(0, 0, -1, 0)$,

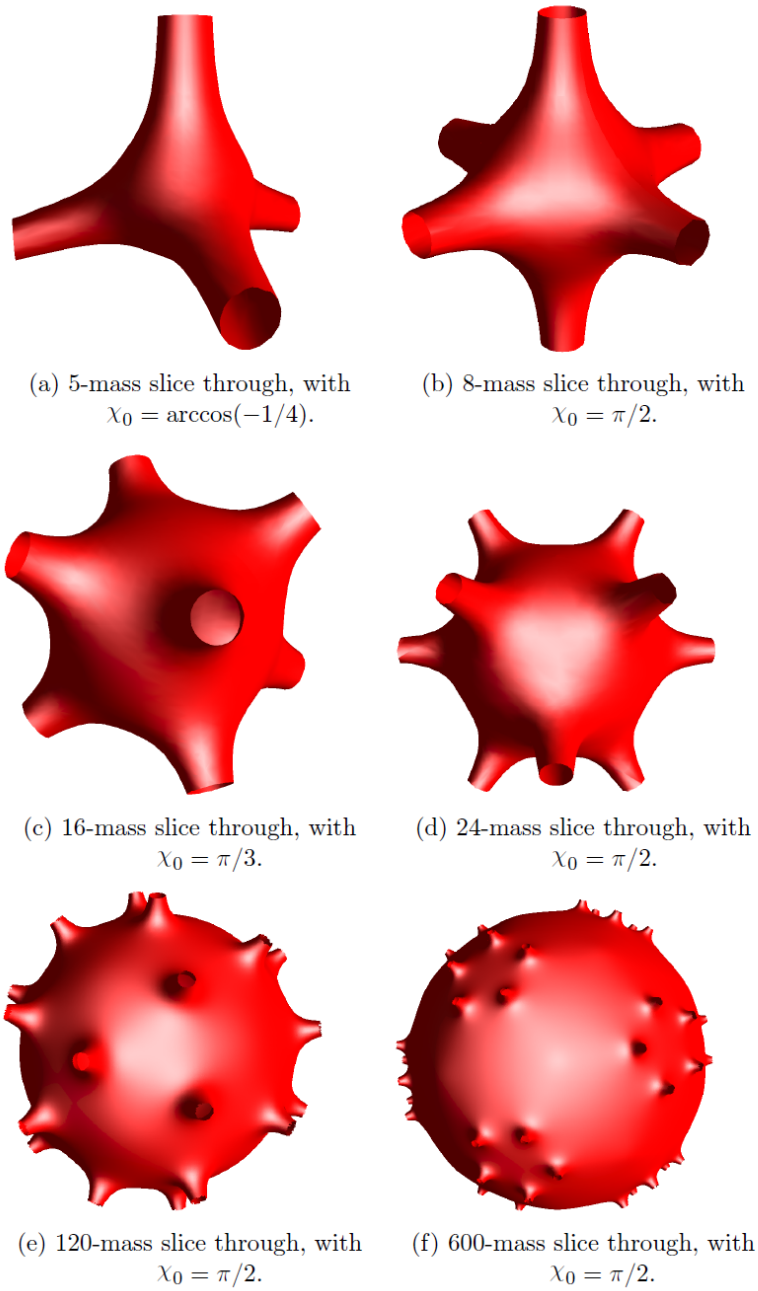

(a) 5-mass slice through, with $\chi_0 = \arccos(-1/4)$.

(b) 8-mass slice through, with $\chi_0 = \pi/2$.

(c) 16-mass slice through, with $\chi_0 = \pi/3$.

(d) 24-mass slice through, with $\chi_0 = \pi/2$.

(e) 120-mass slice through, with $\chi_0 = \pi/2$.

(f) 600-mass slice through, with $\chi_0 = \pi/2$.

Figure 4.2: Slices through the hypersurfaces in which positions of masses are represented by the tubes [55].

7. $(0, 0, 0, 1)$,

8. $(0, 0, 0, -1)$.

Using these positions we can find the values of the functions f_j. Using Eq. 4.31 values of the functions f_j are

$$\begin{aligned}
f_1 &= \sin\frac{\varphi}{2}, \\
f_2 &= \cos\frac{\varphi}{2}, \\
f_3 &= \sin(\frac{1}{2}\cos^{-1}(\cos\theta\sin\varphi)), \\
f_4 &= \cos(\frac{1}{2}\cos^{-1}(\cos\theta\sin\varphi)), \\
f_4 &= \cos(\frac{1}{2}\cos^{-1}(\cos\theta\sin\varphi)), \\
f_5 &= \sin(\frac{1}{2}\cos^{-1}(\cos\phi\sin\theta\sin\varphi)), \\
f_6 &= \cos(\frac{1}{2}\cos^{-1}(\cos\phi\sin\theta\sin\varphi)), \\
f_7 &= \sin(\frac{1}{2}\cos^{-1}(\sin\phi\sin\theta\sin\varphi)), \\
f_8 &= \cos(\frac{1}{2}\cos^{-1}(\sin\phi\sin\theta\sin\varphi)).
\end{aligned} \tag{4.34}$$

In Fig. 4.2 the 8-mass cosmological model is shown which passes through only 6 masses.

4.6 Horizons

For a cosmological model these discrete models should not have over lapping regions i.e. the horizons should not be overlapped. In [55] it is shown that these models do

not have overlapping regions if

$$(\psi^4 \sin\psi)_{,\varphi} = 0, \tag{4.35}$$

which is a good approximation.

4.7 Comparison with FLRW

The metric for Friedmann Lemaitre Robertson Walker (FLRW) is given as

$$dl^2_{FLRW} = -U(t)dt^2 + a^2(t)(d\varphi^2 + h(\varphi)d\Omega^2), \tag{4.36}$$

where $U(t)$ is a free function and $h(\varphi) = \sin\varphi$ with spatial curvature $K = 1$, or $h(\varphi) = \varphi$ with spatial curvature $K = 0$, or $h(\varphi) = \sinh\varphi$ with spatial curvature $K = -1$, the scale factor, $a(t)$, is defined as

$$\frac{1}{U}\frac{\dot{a}^2}{a^2} = \frac{8\pi\rho}{3} - \frac{K}{a^2}, \tag{4.37}$$

where $\rho(t)$ is the density of the fluid.

The lattices can be compared with FLRW universe. By comparing the line elements of FLRW and the lattice solution we have [55]

$$\frac{dl_{Discrete}}{dl_{FLRW}} = \frac{3\pi\overline{m}_j}{16Nm}(\Sigma_{j=1}^{N} f_j^{-1})^2, \tag{4.38}$$

where $\overline{m}_j$ is the effective mass and m is the proper mass. The proper mass is a mass observed by an observer in the asymptotically flat region far from the Einstein-Rosen bridge shown in Fig. 4.3. Which is the mass of the geometry in the limit $\varphi \to 0$. It

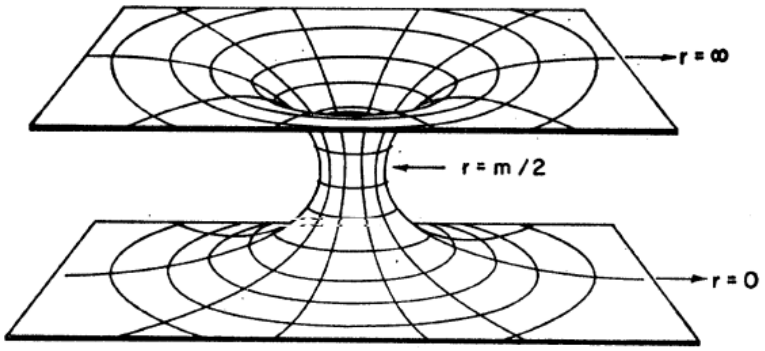

Figure 4.3: The Einstein-Rosen Bridge which shows the embedding of the unchaged black hole where the singularities, $r \to 0$, and $r \to \infty$ are mapped into asymptotical infinities [60].

Shape of Cell	**No. Masses**	$\frac{\mathbf{m}_{eff}}{\mathbf{m}}$
Tetrahedron	600	0.0010
Dodecahedron	120	0.0052
Octahedron	24	0.029
Tetrahedron	16	0.045
Cube	8	0.11
Tetrahedron	5	0.2

Table 4.1: The ratio of the effective and proper masses $\frac{m_{eff}}{m}$ for different n-mass cosmological models [55].

is given as [55]

$$m_j = \sum_{i \neq j}^{N} \frac{\sqrt{\overline{m}_i \overline{m}_j}}{2 \sin(\frac{\varphi_{ij}}{2})}, \tag{4.39}$$

where φ_{ij} is the coordinate distance between the jth and ith points. The ratio of the effective and proper masses is given in Table. 4.1.

Chapter 5

Cosmological Models with Charged Black Holes

The standard model of cosmology assumes an FLRW solution to the EFEs with a stress energy tensor corresponding to that of a homogeneous and isotropic perfect fluid. However, the non-commutativity between averaging and evolution gives rise to correction terms. This phenomena is called backreaction and is the effect of inhomogeneities which are on small scale on the dynamics of the universe [56–59]. Constructing toy models of the universe with inhomogeneities allows for investigation of this phenomena, and an idea of to what extent the universe can be modelled by an FLRW solution. Inhomogeneous models are then part of a broader class of models that contain FLRW as a limiting case.

Particularly interesting subsets of inhomogeneous cosmologies are those that consist of a lattice of black holes, or Schwarzschild spacetimes. These build on the works of the Misner initial data with n black holes [60, 61]. Existing work is either numerical, [62–66], which is a numerical evolution of a lattice containing eight black holes,

or perturbative, [67], which also uses a cubic lattice. An exact solution of six lattice model was constructed in [55], and has since been generalised to include a non-zero cosmological constant [68]. The lattices in [55] are exact solutions of the EFEs with vacuum and requiring no matching conditions. These solutions consist of a linear superposition of Schwarzschild black holes. The black holes are arranged in one of six ways to tessellate a hypersphere (either using 5, 8, 16, 24, 120, or 600 masses) and therefore result in closed, inhomogeneous surfaces. The work in this chapter generalises the eight mass model to include charge, and therefore requires a comparison to the Reissner-Nordstrom solution, which is a solution to the EMFEs of electromagnetism and gravitation. This is the first treatment of backreaction using an exact solution consisting of charged black holes in the literature.

The motivation for now including electric charge to these models is that it gives relatively simple generalisation of the previous work which gives new insight into the nature of these inhomogeneous cosmologies. In addition, an FLRW universe has limitations that it does not allow charged regions of spactime because of the cosmological principle of homogeneity and isotropy. By constructing an inhomogeneous cosmology with charge we overcome this limitation imposed by an FLRW cosmology. The work in this chapter also differs from the existing work in [55] in that the lattice is longer rotationally symmetric, as the black holes now contain charge and are therefore not identical.

5.1 Geometrostatics with an Electric Field

The EMFEs for the electromagnetic field with gravitation are given by

$$R^{\mu}{}_{\nu} - \frac{1}{2}\delta^{\mu}{}_{\nu}R = F_{\nu\alpha}F^{\alpha\mu} - \frac{1}{4}\delta^{\mu}{}_{\nu}F_{\alpha\beta}F^{\alpha\beta} \equiv T^{\mu}{}_{\nu}. \tag{5.1}$$

The electromagnetic Maxwell tensor, $F_{\nu\mu}$, satisfies the following differential conditions:

$$F^{\nu\mu}_{;\mu} = 0, \tag{5.2}$$

$$F_{[\nu\mu;\beta]} = 0. \tag{5.3}$$

The solution to the above EMFs gives the model of a universe having N black holes which are electrically charged.

We choose a spacelike 3-dimensional hypersurface, η_{ij}, with normal vector n^j then the four constraints from Eq. (5.1) can then be found to be

$$\overline{R} + K^2 - K_{ij}K^{ij} = 2\rho, \tag{5.4}$$

$$(K^{j}{}_{i} - \delta^{j}{}_{i}K)_{:j} = s_i, \tag{5.5}$$

where $\overline{R}$ is called the Ricci scalar, K_{ij} is called the extrinsic curvature, and $\rho \equiv T_{\mu\nu}u^{\mu}u^{\nu}$ is the energy density and $s_i \equiv -\delta^{j}{}_{i}u^{\mu}T_{\mu j}$ is the momentum density of the 3-dimensional hypersurface. Here, all indices in above equations can be lowered or raised with the help of η_{ij}. If our initial hypersurface and matter fields are time-symmetric then we immediately have $K_{ij} = 0$, while $F_{i\mu} = -E_i u_{\mu}$ and $F_{ij} = 0$. This

gives $\rho = E_i E^i$ and $s_i = 0$, so that the constraints Eqs. (5.4) and (5.5) become

$$\overline{R} = E_i E^i, \tag{5.6}$$

$$s_i = 0. \tag{5.7}$$

The differential conditions in Eqs. (5.2) and (5.3) give

$$E^i{}_{;j} = 0. \tag{5.8}$$

If Eqs. (5.6) and (5.8) are both satisfied, then we obtain a solution to the constraint equations. This gives the initial data for evolution under the EMFS (5.1) such that this evolution is unique.

Let us now make the following ansătze: firstly, let us write the metric as

$$ds^2 = g^2 f^2 h_{ij} dx^i dx^j \,, \tag{5.9}$$

where $f = f(x^1, x^2, x^3)$ and $g = g(x^1, x^2, x^3)$, and h_{ij} is a 3-dimensional conformal metric to η_{ij} which has constant Ricci curvature i.e. $\mathcal{R} =$ constant. Secondly, we choose as in [60]

$$E_i = [\ln (g/f)]_{,i} \,. \tag{5.10}$$

Using Eq. (5.10) into Eqs. (5.6) and (5.8) we have

$$\overline{\nabla}^2 g = \frac{\mathcal{R}}{8} g, \tag{5.11}$$

$$\overline{\nabla}^2 f = \frac{\mathcal{R}}{8} f, \tag{5.12}$$

where $\overline{\nabla}^2$ is a covariant Laplacian of conformal 3-space with metric h_{ij}. This means both f and g satisfy the Helmholtz equations. The solutions of the Helmholtz equation are easy to obtain, and it can be seen that $E_i \neq 0$ if g and f are not proportional directly.

5.2 A Universe Full of Charged Black Holes

To find cosmologically interesting configurations of black holes, it is convenient to choose h_{ij} to be the metric of a 3-sphere as

$$d\bar{s}^2 = h_{ij}dx^i dx^j = dr^2 + \sin^2 r \left(d\theta^2 + \sin^2\theta\, d\phi^2\right) , \tag{5.13}$$

so that $\mathcal{R} = 6$. As Eqs. (5.11) and (5.12) are both linear and $h \propto 1/\sin(r/2)$ is a solution, it can be seen that the general solution is as follows:

$$g = \sum_{j=1}^{N} \frac{a_j}{2\sin(r_j/2)}, \tag{5.14}$$

$$f = \sum_{j=1}^{N} \frac{b_j}{2\sin(r_j/2)}, \tag{5.15}$$

where $j = 1, 2, 3, ...N$, and where a_j and b_j are arbitrary constants which we need to be obtained for the solution. The solutions of the Eqs. (5.14) and (5.15) have N poles on h_{ij} which are located at arbitrarily chosen positions, and the symbol r_j is intended to denote the value of the r coordinate after rotating the metric, h_{ij}, in such a way that the jth pole is shifted at $r_j = 0$. Here, each pole represents the electrically charged mass point which is located at the heart of a black hole in the model of cosmological universe.

5.2.1 Cosmological Universe Containing 2 Reissner-Nordstrom Black Holes

In principle, Eqs. (5.14) and (5.15) represent exact initial data for N electrically charged black holes in a hyper-spherical cosmology. In order for the solution to be fully obtained, the constants a_i and b_i must be related with the charge, q_i, and mass, m_i, of each black hole, To make this connection, it is useful to recall that the Reissner-Nordstrom (1.50). By making the transformation

$$r = \rho\left(1 + \frac{m}{2\rho}\right)^2 - \frac{q^2}{4\rho}\,, \tag{5.16}$$

we can write a time-symmetric slice of metric from Eq.(1.50) as

$$ds^2 = \left((1 + \frac{m+q}{2\rho})(1 + \frac{m-q}{2\rho})\right)^2 \left(d\rho^2 + \rho^2 d\theta^2 + \rho^2 \sin^2\theta d\phi^2\right)\,. \tag{5.17}$$

A further transformation, to cast this metric in the form of Eqs. (5.9), (5.14) and (5.15), is given by $\rho = k\tan(\sigma/2)$. This transforms the conformal three-space from a plane to a sphere, and results in

$$ds^2 = \frac{l^2}{4}\left((\frac{1}{\cos(\sigma/2)} + \frac{m+q}{2k\sin(\sigma/2)})(\frac{1}{\cos(\sigma/2)} + \frac{m-q}{2k\sin(\sigma/2)})\right)^2 d\bar{s}^2\,, \tag{5.18}$$

where $d\bar{s}^2$ is the metric of 3-sphere (5.13). Finally, if we choose

$$2l = \sqrt{m+q}\sqrt{m-q}, \tag{5.19}$$

then we have

$$ds^2 = \left((\frac{\sqrt{m+q}}{2\cos(\sigma/2)} + \frac{\sqrt{m-q}}{2\sin(\sigma/2)})(\frac{\sqrt{m-q}}{2\cos(\sigma/2)} + \frac{\sqrt{m+q}}{2\sin(\sigma/2)}) \right)^2 d\bar{s}^2 \,. \qquad (5.20)$$

If we set $a_1 = b_2 = \sqrt{m+q}$ and $a_2 = b_1 = \sqrt{m-q}$ then metric (5.20) becomes exactly the same as form as Eqs. (5.9), (5.14) and (5.15). This shows that the initial data for the time-symmetric Reissner-Nordstrom black hole solution is a solution of our more general initial data. Here, one mass, $m_1 = m$, with positive charge $q_1 = +q$ is located at $\sigma = 0$ and second mass, $m_2 = m$, with negative charge, $q_2 = -q$ is located at $\sigma = \pi$.

5.2.2 N Electrically Charged Black Holes

Now we consider the case, in which we choose the arbitrarily positioned N masses. In the vicinity of a mass point, and by using Eq. (5.18), we can relate a_i and b_i to the mass, m_i, and charge ,q_i, of each black hole. If we have N masses $m_1, m_2, m_3 ..... m_N$ with charges $q_1, q_2, q_3 ..... q_N$ then the solution for N charged black holes universe is given as

$$ds^2 = (1 + \sum_{j=1}^{N} \frac{m_j - q_j}{2r})^2 (1 + \sum_{j=1}^{N} \frac{m_j + q_j}{2r})^2 (dr^2 + r^2 d(\theta)^2 + r^2 \sin^2(\theta) d\phi^2). \quad (5.21)$$

The first step in this is rotating coordinates so that the jth mass appears at $r = 0$. In the limit when $r \to 0$ then using Eq. (5.9) we get

$$ds^2 = (\frac{a_l}{r} + \sum_{j \neq l} \frac{a_l}{2\sin(r_{lj}/2)})^2 (\frac{b_l}{r} + \sum_{j \neq l} \frac{b_l}{2\sin(r_{lj}/2)})^2 d\bar{s}^2 \,, \qquad (5.22)$$

where r_{lj} is the coordinate distance between the masses located at lth and jth positions. Comparing Eq. (5.22) with Eq. (5.20) around $r = 0$, we get

$$l = \frac{1}{2a_i b_i}\left(a_i \sum_{j\neq i} \frac{b_j}{2\sin(r_{ij}/2)} + b_i \sum_{j\neq i} \frac{a_j}{2\sin(r_{ij}/2)}\right) - \frac{q^2}{2a_i b_i}, \tag{5.23}$$

and

$$m_i = a_i \sum_{j\neq i} \frac{b_j}{2\sin(r_{ij}/2)} + b_i \sum_{i\neq j} \frac{a_j}{2\sin(r_{ij}/2)}\,. \tag{5.24}$$

The Eq. (5.23) relates our N electrically charged black hole solution and the coordinate systems of the Reissner-Nordstrom solution in the vicinity of one of mass points. While Eq. (5.24) gives the mass of each black holes. This means if N black holes solution is obtanied with all a_is and b_i are known, then the geometry near each black hole will be similar to a Reissner-Nordstrom having mass m given in Eq. (5.24).

It now remains to find the electric charge, q_i, on each black hole. The electric charge within a region Υ is given as [60]

$$q_i \equiv \int_{\partial\Upsilon} \frac{E_i n^i}{4\pi} dS, \tag{5.25}$$

where E_i is the electric field of the ith black hole and n^i is the unit normal pointing inward. We choose the boundary $\partial\Upsilon$ to be asymptotic infinity and the unit normal as

$$n^i = \left(\frac{-1}{fg}, 0, 0\right)\,, \tag{5.26}$$

and

$$dS = f^2 g^2 r^2 \sin\theta d\theta d\phi, \tag{5.27}$$

where both g and f are evaluated in limiting case, $r \to 0$. Evaluating Eq. (5.25) in this limiting case, $r \to 0$ and using Eqs. (5.14), (5.15) and (5.26) in it we get

$$q_l = a_l \sum_{j \neq l} \frac{b_j}{2\sin(r_{lj}/2)} - b_l \sum_{j \neq l} \frac{a_j}{2\sin(r_{lj}/2)} \,. \tag{5.28}$$

This gives the charge on the lth mass located at $r_l = 0$. With the help of Eq. (5.28) we can calculate the charge on other black holes in N black holes solution. It is interesting that Eq. (5.28) immediately gives

$$\sum_i q_i = 0. \tag{5.29}$$

This means that in the cosmological universe, the total charge must be zero, irrespective of how the black holes are located at arbitrary positions and how masses are distributed. This is physically acceptable because the lines of flux terminate on masses in a closed cosmology.

From Eqs. (5.24) and (5.28) we have

$$m_i + q_i = a_i \sum_{l \neq i} \frac{b_l}{\sin(r_{il}/2)} \,, \tag{5.30}$$

$$m_i - q_i = b_i \sum_{l \neq i} \frac{a_l}{\sin(r_{il}/2)} \,. \tag{5.31}$$

This gives a system of nonlinear equations, and solution of these give the values of the constants $\{a_i\}$ and $\{b_i\}$. Due to nonlinearity these are difficult to solve.

5.3 A Regular Universe with 8 Electrically Charged Black Holes

If we consider the simplest case: extremal case with $m_i = q_i$ and find the solution to Eqs. (5.30) and (5.31) by labelling one black hole as $i = 1$. As total charge is zero so $q_1 = -\sum_{j\neq 1} q_j = -\sum_{i\neq 1} m_j$ then the only solution is

$$m_1 = -q_1, \tag{5.32}$$

which is the initial data for a Majumdar-Papapetrou [69, 70]. In the next section we present an example with non-extremal black holes, in which exact solution for $\{a_i\}$ and $\{b_i\}$ can be obtained after the mass, m_i, and charge, q_i, of each black hole have been specified.

5.3.1 Non-Extremal Black Holes Solution

To find a regular arrangement of black holes in a closed cosmological model, we can choose to tile the conformal hypersphere from our 3-dimensional initial data with eight cubic lattice cells. It corresponds to the structure one would obtain by placing a hypercube within the hypersphere in a 4-dimensional Euclidean embedded space,such that the all vertices of the hypercube were touching the hypersphere i.e. cube is circumscribed within the sphere. If we connect the points where these two structures touch we get the lines which form the edges of eights equal sized cubes, which can be used as the primitive lattice cells of our tiling. If we place one mass point at the centre of each of these cells, then we have a completely regular lattice in

which each mass is completely at equal distant from each of its nearest neighbours.

One of the nice features of the regular eight-mass universe is that each black hole will be antipodal to another black hole, same as in the time-symmetric slice through the Reissner-Nordstrom solution discussed earlier. The Table 5.1 gives the coordinates of the location of each mass in Cartesian coordinates in the 4-dimensional Euclidean space, and in hyperspherical coordinates. We choose the values of $\{a_i\}$ and $\{b_i\}$ in such a way that the a_i from each mass is equal to the b_i of the antipodal mass then we have

$$e - d = a_1 = a_3 = a_5 = a_7 = b_2 = b_4 = b_6 = b_8 \,, \tag{5.33}$$

$$e + d = a_2 = a_4 = a_6 = a_8 = b_1 = b_3 = b_5 = b_7 \,, \tag{5.34}$$

where e and d are constants need to be determined. This choice then very conveniently allows us to determine from Eqs. (5.30) and (5.31) that

$$(1 + 6\sqrt{2})e^2 + d^2 \;=\; m_1 = m_2 = m_3 = m_4 = m_5 = m_6 = m_7 = m_8 \,, \tag{5.35}$$

$$-2(1 + 3\sqrt{2})ed \;=\; q_1 = -q_2 = q_3 = -q_4 = q_5 = -q_6 = q_7 = -q_8 \,, \tag{5.36}$$

so that every black hole in the universe has same mass but having an equal and opposite charge to its antipodal black hole. The requirement that the total electric charge of all black holes, $\sum q_i$, must zero is satisfied.

mass number, i	(x^0, x^1, x^2, x^3)	$(r,\ \theta,\ \phi)$
1	(1, 0, 0, 0)	$(0,\ \frac{\pi}{2},\ \frac{\pi}{2})$
2	(-1, 0, 0, 0)	$(\pi,\ \frac{\pi}{2},\ \frac{\pi}{2})$
3	(0, 1, 0, 0)	$(\frac{\pi}{2},\ 0,\ \frac{\pi}{2})$
4	(0, -1, 0, 0)	$(\frac{\pi}{2},\ \pi,\ \frac{\pi}{2})$
5	(0, 0, 1, 0)	$(\frac{\pi}{2},\ \frac{\pi}{2},\ 0)$
6	(0, 0, -1, 0)	$(\frac{\pi}{2},\ \frac{\pi}{2},\ \pi)$
7	(0, 0, 0, 1)	$(\frac{\pi}{2},\ \frac{\pi}{2},\ \frac{\pi}{2})$
8	(0, 0, 0, -1)	$(\frac{\pi}{2},\ \frac{\pi}{2},\ \frac{3\pi}{2})$

Table 5.1: The coordinate positions the eight black holes in the conformal 3-sphere.

In this case Eqs. (5.30) and (5.31) take the form

$$m_1 + q_1 = \frac{2a_1(\frac{b_2}{2} + (b_3 + b_4 + b_5 + b_6 + b_7 + b_8))}{\sqrt{2}}, \tag{5.37}$$

$$m_2 + q_2 = \frac{2a_2(\frac{b_1}{2} + (b_3 + b_4 + b_5 + b_6 + b_7 + b_8)}{\sqrt{2}}, \tag{5.38}$$

$$m_3 + q_3 = \frac{2a_3(\frac{b_4}{2} + (b_1 + b_2 + b_5 + b_6 + b_7 + b_8))}{\sqrt{2}}, \tag{5.39}$$

$$m_4 + q_4 = \frac{2a_4(\frac{b_3}{2} + (b_1 + b_2 + b_5 + b_6 + b_7 + b_8))}{\sqrt{2}}, \tag{5.40}$$

$$m_5 + q_5 = \frac{2a_5(\frac{b_6}{2} + (b_3 + b_4 + b_1 + b_2 + b_7 + b_8))}{\sqrt{2}}, \tag{5.41}$$

$$m_6 + q_6 = \frac{2a_6(\frac{b_5}{2} + (b_3 + b_4 + b_1 + b_2 + b_7 + b_8))}{\sqrt{2}}, \tag{5.42}$$

$$m_7 + q_7 = \frac{2a_7(\frac{b_8}{2} + (b_3 + b_4 + b_5 + b_6 + b_1 + b_2))}{\sqrt{2}}, \tag{5.43}$$

$$m_8 + q_8 = \frac{2a_8(\frac{b_7}{2} + (b_3 + b_4 + b_5 + b_6 + b_1 + b_2))}{\sqrt{2}}, \tag{5.44}$$

$$m_1 - q_1 = \frac{2b_1(\frac{a_2}{2} + (a_3 + a_4 + a_5 + a_6 + a_7 + a_8))}{\sqrt{2}}, \quad (5.45)$$

$$m_2 - q_2 = \frac{2b_2(\frac{a_1}{2} + (a_3 + a_4 + a_5 + a_6 + a_7 + a_8))}{\sqrt{2}}, \quad (5.46)$$

$$m_3 - q_3 = \frac{2b_3(\frac{a_4}{2} + (a_1 + a_2 + a_5 + a_6 + a_7 + a_8))}{\sqrt{2}}, \quad (5.47)$$

$$m_4 - q_4 = \frac{2b_4(\frac{a_3}{2} + (a_1 + a_2 + a_5 + a_6 + a_7 + a_8))}{\sqrt{2}}, \quad (5.48)$$

$$m_5 - q_5 = \frac{2b_5(\frac{a_6}{2} + (a_3 + a_4 + a_1 + a_2 + a_7 + a_8))}{\sqrt{2}}, \quad (5.49)$$

$$m_6 - q_6 = \frac{2b_6(\frac{a_5}{2} + (a_3 + a_4 + a_1 + a_2 + a_7 + a_8))}{\sqrt{2}}, \quad (5.50)$$

$$m_7 - q_7 = \frac{2b_7(\frac{a_8}{2} + (a_3 + a_4 + a_5 + a_6 + a_1 + a_2))}{\sqrt{2}}, \quad (5.51)$$

$$m_8 - q_8 = \frac{2b_8(\frac{a_7}{2} + (a_3 + a_4 + a_5 + a_6 + a_1 + a_2))}{\sqrt{2}}. \quad (5.52)$$

These are non-linear equations. Finally, Solving Eqs. (5.35) and (5.36) for e and d to get

$$e = \frac{\sqrt{(19 + 6\sqrt{2})m + \sqrt{(433 + 228\sqrt{2})m^2 - (91 + 120\sqrt{2})q^2}}}{\sqrt{(182 + 240\sqrt{2})}}, \quad (5.53)$$

$$d = -q/2(1 + 3\sqrt{2})e, \quad (5.54)$$

where $m = m_i$ is the mass of each black hole and $|q| = |q_i|$ is the magnitude of the charge on each black hole. Finally we have an exact solution with all black holes have same mass, m, and half of them have positive charge, q, while the other half have negative charge, $-q$.

If we arrange the charges of black holes differently then the solution will the solution would be same. To check this we arrange the black holes as given in the Table 5.2 and choose the coefficients as

Mass	(x^0, x^1, x^2, x^3)	(X, θ, ϕ)	Charge
m_1	(1, 0, 0, 0)	$(0, \frac{\pi}{2}, \frac{\pi}{2})$	$-$
m_2	(-1, 0, 0, 0)	$(\pi, \frac{\pi}{2}, \frac{\pi}{2})$	$+$
m_3	(0, 1, 0, 0)	$(\frac{\pi}{2}, 0, \frac{\pi}{2})$	-
m_4	(0, -1, 0, 0)	$(\frac{\pi}{2}, \pi, \frac{\pi}{2}$	$+$
m_5	(0, 0, 1, 0)	$(\frac{\pi}{2}, \frac{\pi}{2}, 0)$	$+$
m_6	(0, 0, -1, 0)	$(\frac{\pi}{2}, \frac{\pi}{2}, \pi)$	-
m_7	(0, 0, 0, 1)	$(\frac{\pi}{2}, \frac{\pi}{2}, \frac{\pi}{2})$	-
m_8	(0, 0, 0, -1)	$(\frac{\pi}{2}, \frac{\pi}{2}, \frac{3\pi}{2})$	$+$

Table 5.2: Another possible arrangement of the black holes.

$$a_1 = a_3 = a_6 = a_7 = \quad e - d \quad = b_2 = b_4 = b_5 = b_8, \tag{5.55}$$

$$a_2 = a_4 = a_5 = a_8 = \quad e + d \quad = b_1 = b_3 = b_6 = b_7. \tag{5.56}$$

Then solution is

$$m_1 = m_2 = ... = m_8 = (1 + 6\sqrt{2})e^2 + d^2, \tag{5.57}$$

$$q_1 = -q_2 = q_3 = -q_4 = -q_5 = q_6 = q_7 = -q_8 = -2(1 + 3\sqrt{2})ed. \tag{5.58}$$

Here also we get the same mass for all black holes and net charge is zero. In next section we will find out the distance between the black holes and the event horizons.

5.3.2 Comparison with FLRW Cosmology

With a cosmological solution in hand, it is interesting to check whether the large-scale properties of our space bear any resemblance to the predictions of the commonly used isotropic and homogeneous FLRW models. The first thing that one could compare, between these two cases, is the scale of the cosmological region with maximum

expansion. The initial data constructed above is time-symmetric so it is at maximum. The scale factor of dust dominated and closed FLRW model is given by

$$a(t_{\max}) = \frac{4M}{3\pi}\,, \tag{5.59}$$

where M is the total mass of the spacetime. We can compare it to the scale of our cosmological model and then we can find the result of condensing the mass into a finite number of points, with discretely distributed electric charges. It is an extension of previous results of uncharged black holes cosmological models, and will allow us to consider the cosmological effects of electrical charge.

The most natural way to determine the scale of our cosmological region is to compute the proper length the edge of one of our lattice cell. To find the scale we rotate our cosmological model in such a manner that one cell edge lies on a curve having θ =constant and ϕ = constant, then the proper distance, d of the edge is written as

$$d = \int_{r_1}^{r_2} \sqrt{g_{rr}} dr = \int_{r_1}^{r_2} f g dr\,, \tag{5.60}$$

where r_1 and r_2 are the coordinates of the end points of the edge i.e. the location of the vertices of the cell. The proper length, d_{FLRW}, of a curve in a closed FLRW model can be calculated as

$$d_{\mathrm{FLRW}} = \int_{r_1}^{r_2} a(t_{\max}) dr = (r_1 - r_2) a(t_{\max})\,, \tag{5.61}$$

where $a(t_{\max})$ is the scale factor from Eq. (5.59). In general, the value of the length, d, depends on both the mass, m, of the black holes and their charge, q, but on the

other hand the value of the length, $d_{\rm FLRW}$ depends only on the total mass, M, once the positions of the cell vertices have been chosen. If we take $M = 8m$, so that both cosmologies have the same total proper mass, then the comparison of scales for the both cosmologies is written as

$$\frac{a}{a_{\rm FLRW}} = \frac{d}{d_{\rm FLRW}}\,, \tag{5.62}$$

where d and $d_{\rm FLRW}$ are given by Eqs. (5.60) and (5.61). The ratio, $\frac{d}{d_{\rm FLRW}}$, is only a function of q/m, and in the limiting case, $q \to 0$, it gives the measurement of cosmological backreaction which is studied previously.

Fig. 5.1 shows the the value of the ratio of scale factors, $\frac{a}{a_{\rm FLRW}}$, as a function of the ratio of charge to mass, q/m. In the special case in which we have $q/m \to 0$ then it gives the results of the uncharged case, and in extremal case we have $q/m \to \pm 1$ i.e. black holes are extremal in this case. It can be seen that the difference between the predicted scale factor, $a_{\rm FLRW}$, and actual scale factor, a, is largest if we have uncharged black holes. If the charges of the black holes start increasing then the difference between the predicted scale factor, $a_{\rm FLRW}$, and actual scale factor, a, decreases, however the scale, a in our cosmology is always greater than $a_{\rm FLRW}$ in all cases either uncharged or extremal case. In Fig. 5.1 the orange line is for the case where along the cell edge all three associated cells have the same charge either negative or positive. While for the case where two cell have same charge (positive or negative) and the third has the opposite (negative or positive) the graph is shown with blue line. It is interesting to note that the results do not change if we choose the same charges in these two cases to be negative or positive i.e. the ratio of scale

factors, $\frac{a}{a_{\text{FLRW}}}$, remains same.

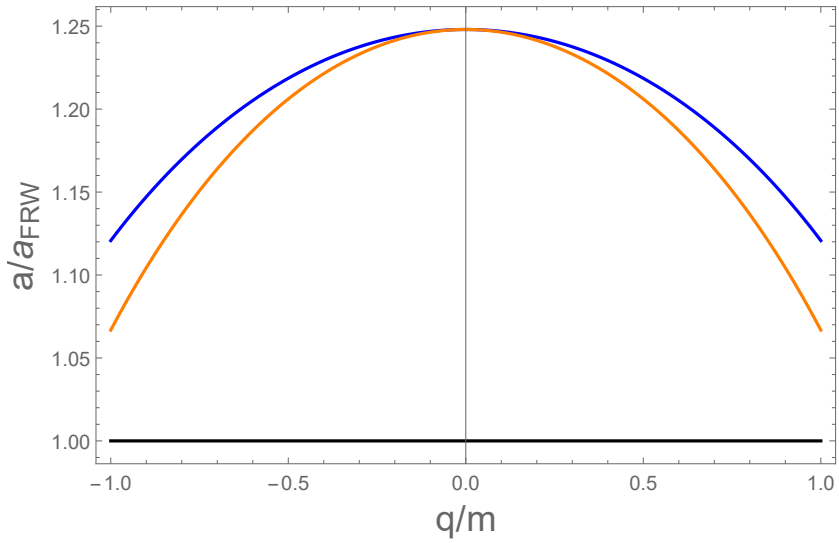

Figure 5.1: The ratio of scale of the cosmological region in our model, a, and scale of FLRW model, a_{FLRW} where the FLRW Model has same mass as our cosmological model.

It also of great interest to find the locations of the apparent horizons around the black holes. The solution is referred as a "*cosmological model*' if the horizons of the black holes do not overlap. For our purposes, the location of the event horizon is impossible to locate, as we do not have knowledge of the global spacetime. However, the locations of the apparent horizons can be obtained from the initial data.

As the apparent horizon is the outermost marginally outer trapped surface, by definition and for time-symmetric initial data this surface is extremal surface in this 3-space [71]. We can approximate its location by rotating 3-sphere such that one of the masses, m_i reaches the origin i.e. at $r_i = 0$. The area of 3-sphere centered on this mass, m_i, is written as

$$A = \int_0^{2\pi} \int_0^{\pi} f^2 g^2 \sin^2 r \sin\theta \, d\theta \, d\phi \,, \tag{5.63}$$

where r =constant. Integrating this quantity numerically, and determining the value of r that minimizes it i.e we calculate r_{min}. This gives the approximation of the position of the black hole horizon. The results are shown in Fig. 5.2, where we plot the ratio of the r coordinate of the apparent horizon and the distance between adjacent black holes against the ratio, $\frac{q}{m}$. When $q/m \to 0$ it can be seen that the horizon lengthen appositely 27% to the half of the distance between black holes. It is interesting to note that as the charge, q, of the black hole is increased (to either negative or positive values) then the horizon reaches back towards the centre of the black hole and in the limiting case $q/m \to \pm 1$ it reaches zero i.e $r_{\min} \to 0$ as $q/m \to 0$. The behaviour expected from a Reissner-Nordstrom black hole is also same, and verifies that the black holes horizons in our eight mass model never touch.

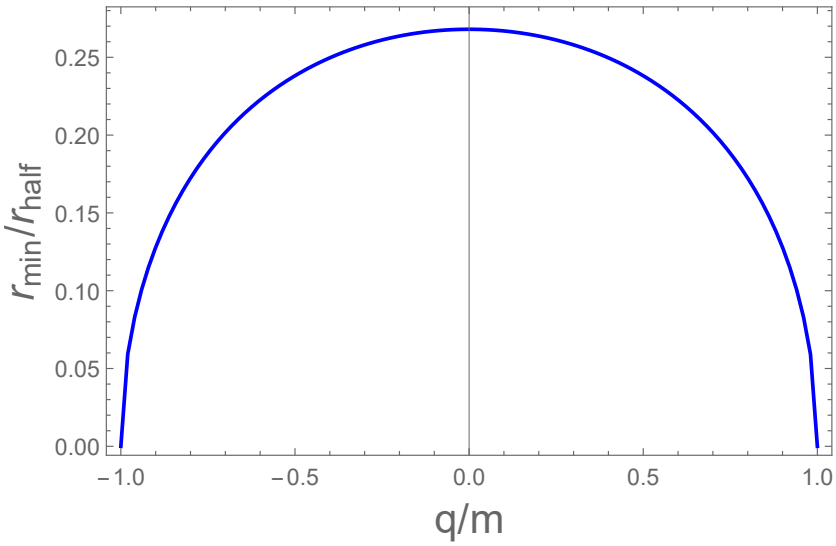

Figure 5.2: The location of the apparent horizon around one of the black holes with $r_{\min}$.

Chapter 6

Summery and Conclusion

In Chapter 1, we gave a brief introduction to the Einstein-Maxwell field equations (EMFEs) and some of its solutions. In order to find some new classes of the solutions of the EMFEs, we divided the problem as fellows. First we categorized the electromagnetic field to be without source ($T = 0$) or with source ($T \neq 0$). Then we divided the problem further by assuming the electromagnetic field to be null or non-null and then in each case we investigated the solution by considering the pressure to be isotropic or anisotropic.

For the case without source, it is shown that the solution with null electromagnetic field is not possible irrespective of the pressure being isotropic or anisotropic. However, in the case of non-null electromagnetic field the Reissner-Nordstrom is the only solution for the isotropic pressure and for anisotropic pressure no solution is possible. For the case with source, it is found that the solution for the null electromagnetic field is not possible, however, for the non-null electromagnetic field many solutions are possible for both isotropic and anisotropic cases. The summery of these results is shown in Fig. 6.1.

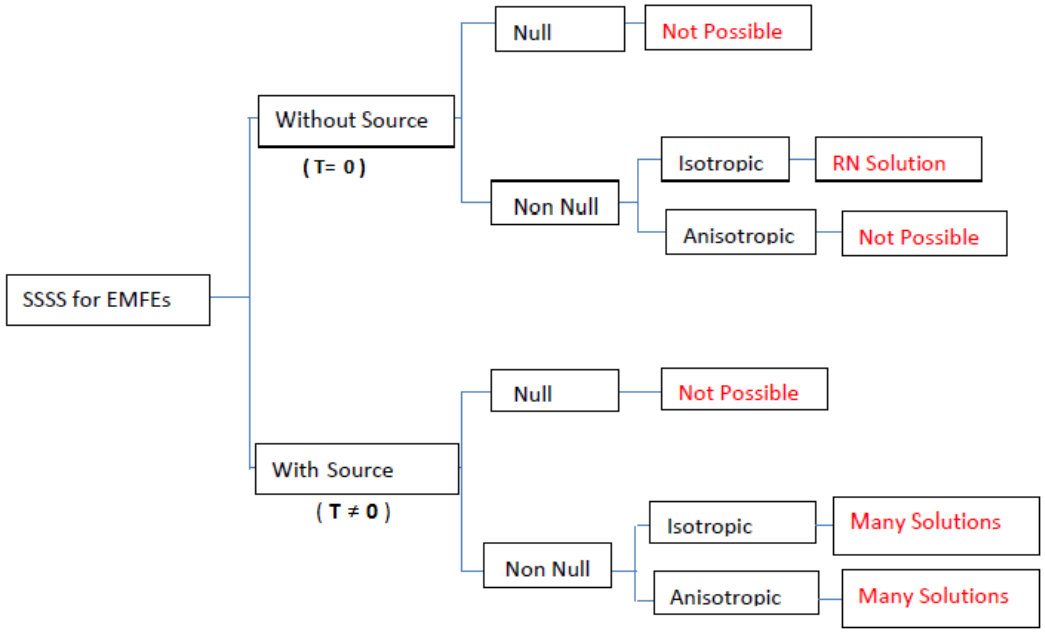

Figure 6.1: Results of the Classes of the spherically symmetric static solutions (SSSS) of the EMFEs.

Solutions of the EMFEs have significant importance in Relativity, Cosmology and Astrophysics. Among these solutions those which satisfy the physical criteria can be considered as models for the compact objects. The equation of the state also plays important role in finding the suitable models for the compact objects. Mostly the equation of the state is not known for the astrophysical objects but one can choose an equation of state and then find the physically valid solution of the EMFEs. Many solutions of the EMFEs have been obtained by choosing different equations of state. The motivation of this thesis was to find some exact solutions of the EMFEs which satisfy the physical criteria of the compact object. To find such models first question arises what should be the equation of state. As the equation of state is unknown so one may choose different types of the equation of states for example linear equation

of state, $p_r = \alpha\rho + \beta$, quadratic equation of state, $p_r = \alpha\rho^2 + \beta\rho + \gamma$, the polytropic equation of state, $p_r = k\rho^\alpha$, where $\alpha = 1 + \frac{1}{\eta}$ and η is the ploytropic index, the Van der Waals modified equation of state, $p_r = \alpha\rho^2 + \frac{\gamma\rho}{1+\beta\rho}$, or any other. After choosing the equation of state the solution of the EMFEs is obtained. The next step is to check whether the solution satisfies the physical criteria or not. In Literature many solutions of the EMFEs have been obtained by assuming different types of the equations of state and many of such solutions satisfy the physical criteria as well.

In Chapter 2, we discussed the physical criteria for the compact objects in detail. Also we choose the linear equation of state, $\alpha\rho + \beta$, and then we obtained a solution of the EMFEs. The solution satisfies all the physical conditions of a compact object. All metric coefficients, density, and radial and transverse pressures are well defined and there is no singularity present for the suitable values of the parameters. The density is positive and a non-increasing function of the radial parameter if $a > \frac{2k}{3}$. At the center the radial pressure, p_r, and the transverse pressure, p_t, are equal. The causality condition is also satisfied. The weak energy condition is also satisfied. The red shift at the center and at the boundary of the compact object is finite and positive. At the boundary the solution matches with the Reissner-Nordstrom exterior solution and it gives some bounds on the mass-radius and charge-radius ratios. The stability is discussed in detail and the stability parameter, Θ, is positive for $a > \frac{2k}{3}$. Hence solution can be treated as a model for a compact object.

The expansion of the universe raises interest in dark energy. It is interesting to find some models for the dark energy. In Chapter 3, we obtained a solution for the dark energy object by taking the equation of state as $p_r = -\rho$. The solution is physically

valid as it satisfies the physical criteria. All metric coefficients, density, and radial and transverse pressures are well defined and there is no singularity present for the suitable values of the parameters. For example the density is positive and a decreasing function of the radial parameter if $a > \frac{2k}{3}$. The red shift is also well defined and positive at the center and at the boundary. The weak energy condition is satisfied. The casuality condition is not satisfied. Ellis at al. (2007) have discussed violation of this condition for dark energy models. At the boundary the solution matches with the Reissner-Nordstrom metric and we get some bounds on mass-radius and charge-radius ratios. The solution also satisfies the stability condition for the appropriate vales of the parameters. Hence, the solution obtained fulfills all the requirements of a compact negative energy object.

In Chapter 4, we gave an overview of constraints and evolution equations of the Cauchy Einstein field equations (CEFEs). In Chapter 5, we extend this work for the Cauchy Einstein-Maxwell field equations (CEMFEs) by adding charge. We gave the constraints and evolution equations for the EMFEs and obtained solution. There were many motivations for including electric charge in previous models. The first was that it offered a generalisation of previous models, same as the Reissner-Nordstrom is a generalisation from Schwarzschild. It also gives new mathematical and physical information about the nature of such inhomogeneous cosmologies. Moreover, in an FLRW universe the homogeneity of space forbids regions of charged spacetime by definition. There was also relatively little known about the cosmological consequences of electric charge in inhomogeneous models. It gives an answer to a somewhat open question as to what the effects of allowing electric charge in cosmology should be in

general.

An analysis of an inhomogeneous cosmological model that consists of regularly arranged, electrically charged black holes with maximum expansion is presented. We found that the only solution that exist is having zero net charge. This analysis is applied to a cosmological model having eight electrically charged black holes, and we get a simple method of obtaining a charged universe model in which black holes exist in antipodal pairs. Here, each black hole has equal and opposite charge to its antipodal black hole.

We then compared this model to a closed and dust dominated FLRW model with the same total mass. We did this by comparing the scale between the two types of universe at maximum of expansion as a function of the charge to mass ratio of the black holes. We obtained that if the magnitude of the charge on the black holes is increased then the difference between our cosmological model and FLRW is reduced and we found that the largest difference corresponds to the case where there charge is zero i.e. black holes are uncharged. Lastly we calculated the size of the apparent horizons in this initial data which are in fact functions of charge to mass ratio. We also get the result that with the increase in magnitude of the charge of the black holes, the size of the apparent horizon starts decreasing. In the limiting case where the black holes become extremal then the apparent horizons tends to zero radius.

The work presented in thesis can be extended by choosing some other equation of states like quadratic or ploytropic or any other. Among these solutions we can find some physically valid solutions which also satisfy the stability criteria.

In previous models only electric charge is considered in the EMFEs. Another excit-

ing work is adding magnetic charge in the EMFEs along with the electric charge and obtain the new solutions of the EMFEs. It is interesting to find the behaviour of the solutions with magnetic charge, whether theses new solutions satisfy the physical criteria and the stability condition or not. One can also add different equation of states in the EMFEs along with the electric and magnetic charges to find the solutions which are physically valid so that these can be considered as new models for the compact objects with electric and magnetic charges.

Adding the cosmological constant in the CEMFEs and finding new constraints and evolution equations further can be done. Also finding new models for the universe with N charged black holes with angular momentum, are interesting.

References

[1] A. Einstein, *On the Electrodynamics of Moving Bodies*, Annals of Physics, 322, (1905).

[2] C. Misner, K. S. Thorne and J. A. Wheeler, *Gravitation*, W. H. Freeman and Company, (1973).

[3] R. M. Wald, *General Relativity*, The University of Chicago Press, (1984).

[4] G. F. R. Ellis, *Lecture Notes: "Course on General Relativity"*, University of Cape Town, (2009).

[5] D. Feleisch, *A Students Guide to Maxwells Equations*, Cambridge University Press, (2008).

[6] H. Stephani, D. Kramer, M. MacCallum and C. Hoenselaers, *Exact Solutions to Einstein Field Equations*, Cambridge University Press, (2009).

[7] A. Einstein, *Cosmological Considerations in the General Theory of Relativity*, Prussian Academy of Sciences 142, (1917).

[8] E. P. Hubble, *A relation between distance and radial velocity among extra-galactic nebulae*, Proceedings of the National Academy of Sciences USA, 15, (1929).

[9] A. V. Filippenko, and A. G. Riess, *Results from the High-z Supernova Search Team*, Physics Reports, 307, (1998).

[10] D. Goldsmith, *Einstein's Greatest Blunder*, *The Cosmological Constant and Other Fudge Factors in the Physics of the Universe*, Harvard University Press, (1995).

[11] *https://www.nasa.gov/missions/deepspace/f$_d$ark − energy.html*

[12] S. L. Shapiro and S. A. Teukolsky, *Black Holes, White Dwarfs and Neutron Stars: The Physics of Compact Objects*, Wiley-Interscience Publication, (1983).

[13] V. P. Frolov and D. Novikov, *Black Hole Physics: Basic Concepts and New Developments*, Kluwer Academic Publishers, (1998).

[14] K. Schwarzschild, *Uber das Gravitationsfeld eines Masenpunktes nach der Einsteinschen Theorie*, Sitzber Preuss Akad Wiss, 189, (1916).

[15] H. Reissner, *ber die Eigengravitation des elektrischen Feldes nach der Einsteinschen Theorie*, Annalen der Physik (in German), 50, (1916).

[16] R. P. Kerr, *Gravitational Field of a Spinning Mass as an Example of Algebraically Special Metrics*, Physical Review Letters, 11, (1963).

[17] F. Zwicky, *On the Masses of Nebulae and of Clusters of Nebulae*, Astrophysical Journal, 86, (1937).

[18] M. K. Mak and T. Harko, *Anisotropic Stars in General Relativity*, Proceding Royal society London, 459, (2003).

[19] M. K. Mak and T. Harko, *Anisotropic Relativistic Stellar Models*, Annalen Physics, 11, (2003).

[20] S. Thirukkanesh and S. D. Maharaj, *Charged Anisotropic Matter with Linear Equation of State*, Classical and Quantum Gravity, 25, (2008).

[21] T. Feroze, *Exact Solutions of the Einstein-Maxwell Equations with Linear Equation of State*, Canadian Journal of Physics, 90, (2012).

[22] J. M. Sunzu, S. D. Maharaj and S. Ray, *Quark Star Model with Charged Anisotropic Matter*, Astrophysics and Space Science, 354, (2014).

[23] M. Malaver, *Strange Quark Star Model with Quadratic Equation of State*, Frontiers of Mathematics and its Applications, 1, (2014).

[24] T. Feroze and A. A. Siddiqui, *Some Exact Solutions of the Einstein-Maxwell Equations with a Quadratic Equation of State*, Journal of the Korean Physical Society, 65, (2014).

[25] T. Feroze and A. A. Siddiqui, *Charged Anisoptropic Matter with Quadratic Equation of State*, General Relativity and Gravitation, 43, (2011).

[26] S. D. Maharaj and P. M. Takisa, *Regular Models with Quadratic Equation of State*, General Relativity and Gravitation, 44, (2012).

[27] P. M. Takisa, S. D. Maharaj and S. Ray, *Stellar Objects in the Quadratic Regime*, Astrophysics and Space Science, 354, (2014).

[28] R. Shrama and B. S. Ratanpal, *Relativistic Steller Model Admitting a Quadratic Equation of State*, International Journal of Modern Physics D, 22, (2013).

[29] S. D. Maharaj and P. M. Takisa, *Some Charged Polytropic Models*, General Relativity and Gravitation, 45, (2013).

[30] M. Malaver, *Polytropic Stars with Tolman IV Type Potential*, AASCIT Journal of Physics, 1, (2015).

[31] M. Malaver, *Regular Model for a Quark Star with Van der Waals Modified Equations of State*, World Applied Programming, 7, (2013).

[32] S. Thirukkanesh and F. C. Ragel, *Anisotropic Spheres with Van der Waals-type Equation of State*, Pramana Journal of Physics, 83, (2014).

[33] M. Malaver, *Analytical Model for Charged Polytropic Stars with Van der Waals Modified Equations of State*, American Journal of Astronomy and Astrophysics, 1, (2013).

[34] C. B. G. Mclntosh, J. M. Foyster, and A. W. C. Lun, *The classification of the Ricci and Plebanski Tensors in General Relativity using Newman-Penrose Formalism*, Journal of Mathematical Physics, 22, (1980).

[35] Y.K. Gupta and S.K. Maurya, *A class of regular and well behaved relativistic super-dense star models*, Astrophysics Space Science, 332, (2011).

[36] N. Pant, R.N. Mehta, and M.J. Pant, *New class of regular and well behaved exact solutions in general relativity*, Astrophysics Space Science, 330, (2010).

[37] N. Pant, R.N. Mehta, and M.J. Pant, *Well behaved class of charge analogue of Heintzmanns relativistic exact solution*, Astrophysics Space Science, 332, (2011).

[38] L. Herrera, *Cracking of self-gravitating compact objects*, Physics Letters A, 165, (1992).

[39] C. Cattoen, T. Faber, and M. Visser, *Gravastars must have anisotropic pressures*, Classcical Quantum Gravity, 22, (2005).

[40] P. Mazur, E. Mottola, *Gravitational Condensate Stars: An Alternative to Black Holes*, arXiv:gr-qc/0109035, Report number: LA-UR-01-5067 (2001).

[41] P. Mazur, E. Mottola, *Gravitational Vacuum Condensate Stars*, Proceedings of the National Academy of Sciences USA, 101, (2004).

[42] F. S. N. Lobo, *Stable dark energy stars*, Classical Quantum Gravity, 23, (2006).

[43] F. S. N. Lobo, *Phantom energy traversable wormholes*, Physical Review D, 71, (2005).

[44] E. Babichev, V. Dokuchaev and Yu. Eroshenko, *Black hole mass decreasing due to phantom energy accretion*, Physical Review Letters, 93, (2004).

[45] S. S. Yazadjiev, *Exact dark energy star solutions*, Physical Review D, 83, (2011).

[46] F. Piazza, S. Tsujikawa, *Dilatonic ghost condensate as dark energy*, Journal of Cosmology and Astroparticle Physics, 470, (2014).

[47] S. M. Carroll, M. Hoffman, and M. Trodden, *Can the dark energy equation-of-state parameter w be less than -1?*, Physical Review D, 68, (2003).

[48] G. F. R. Ellis, R. Maartens, and M. A. H. MacCallum, *Causality and the speed of sound*, General Relativity and Gravitation, 39, (2007).

[49] G. B. Cook, *Initial data for Numerical Relativity*, Living Review of Realtivity, 3, (2000).

[50] A. Lichnerowicz, *Lintegration des equations de la gravitation relativiste et le probl'eme des n corps.* Journal de Mathmatiques Pures et Appliques, 23, (1944).

[51] T. W. Baumgarte and S. L. Shapiro, *Numerical Relativity: Solving Einstein's Equations on the Computer*, Cambridge University Press, New York, USA, (2010).

[52] J. W. York, *Conformally invariant orthogonal decomposition of symmetric tensors on Riemannian manifolds and the initial-value problem of general relativity*, Journal of Mathematical Physics, 14, (1973).

[53] N. O Murchadha and J. W. York, *Initial-value problem of general relativity. II. Stability of solution of the initial-value equations*, Physical Review D, 10, (1974).

[54] J. A. Wheeler, *The geometrostatic lattice cell*, Foundations of Physics, 13, (1983).

[55] T. Clifton, K. Rosquist and R. Tavakol, *An exact quantification of backreaction in relativistic cosmology*, Physical Review D, 86, (2012).

[56] T. Clifton, *Back-reaction in relativistic cosmology*, International Journal of Modern Physics D, 22, 2013.

[57] T. Buchertn and S. Rasanen, *Backreaction in late-time cosmology*, Annual Review of Nuclear and Particle Science, 62, (2012).

[58] J. Buchert and J. Ehlers, *Lagrangian theory of gravitational instability of Friedman-Lemaitre cosmologies, second-order approach: an improved model for non-linear clustering*, Monthly Notices of the Royal Astronomical Society, 264, (1993).

[59] C. Clarkson, G. Ellis, J. Larena, and O. Umeh, *Does the growth of structure affect our dynamical models of the universe? The averaging, backreaction and fitting problems in cosmology*, Reports on Progress in Physics, 74, (2011).

[60] D. R. Brill and R. W. Lindquist, *Interaction Energy in Geometrostatics*, Physical Review, 131, (1963).

[61] C. W. Misner, *The Method of Images in Geometrostatics*, Annals of Physics, 24, (1963).

[62] Y. Chul-Moon, H. Abe, Y. Takamori, and K. Nakao, *Black Hole universe Construction and Analysis of Initial Data*, Physical Review D, 86, (2012).

[63] E. Bentivegna1 and M. Korzynski, *Evolution of a Family of Expanding Cubic Black-Hole Lattices in Numerical Relativity*, Classical and Quantum Gravity, 30, (2013).

[64] D. Bancel and Y. Choquet-Bruhat, *Existence, Uniqueness, and Local Stability for the Einstein-Maxwell-Boltzman System*, Communications in Mathematical Physics, 33, (1973).

[65] Chul-Moon Yoo, H. Okawa, and K. Nakao, *Black Hole Universe: Time Evolution*, Physical Review Letter, 111, (2013).

[66] E. Bentivegna and M. Korzynski, *Evolution of a Periodic Eight-Black-Hole Lattice in numerical relativity*, Classical and Quantum Gravity, 29, (2012).

[67] J. P. Bruneton and J. Larena, *Dynamics of a Lattice Universe: The dust approximation in cosmology*, Classical and Quantum Gravity, 29, (2012).

[68] T. Clifton, J. Durk, *Exact Initial Data for Black Hole Universes with a Cosmological Constant*, Classical and Quantum Gravity, 34, (2017).

[69] S. D. Majumdar, *A Class of Exact solutions of Einstein's Field Equations*, Physical Review, 72, (1947).

[70] A. Papapetrou, *A Static Solution of the Equations of the Gravitational Field for an Arbitary Charged Distribution*, Proceeding of the Royal Irish Academy, Mamthematical and physical Sciences, 51, (1945-1948).

[71] Gibbons, *The Time Symmetric Initial Value Problem for Black Holes*, Communications in Mathematical Physics, 27, (1972).